

# Neutrino mixing and leptonic CP violation from $S_4$ flavour and generalised CP symmetries

J.T. Penedo,<sup>a</sup> S.T. Petcov<sup>a,b,1</sup> and A.V. Titov<sup>a</sup>

<sup>a</sup>SISSA/INFN,

Via Bonomea 265, 34136 Trieste, Italy

<sup>b</sup>Kavli IPMU (WPI), University of Tokyo,

5-1-5 Kashiwanoha, 277-8583 Kashiwa, Japan

E-mail: [jpenedo@sissa.it](mailto:jpenedo@sissa.it), [petcov@sissa.it](mailto:petcov@sissa.it), [atitov@sissa.it](mailto:atitov@sissa.it)

**ABSTRACT:** We consider a class of models of neutrino mixing with  $S_4$  lepton flavour symmetry combined with a generalised CP symmetry, which are broken to residual  $Z_2$  and  $Z_2 \times H_{\text{CP}}^\nu$  symmetries in the charged lepton and neutrino sectors, respectively,  $H_{\text{CP}}^\nu$  being a remnant CP symmetry of the neutrino Majorana mass term. In this set-up the neutrino mixing angles and CP violation (CPV) phases of the neutrino mixing matrix depend on three real parameters — two angles and a phase. We classify all phenomenologically viable mixing patterns and derive predictions for the Dirac and Majorana CPV phases. Further, we use the results obtained on the neutrino mixing angles and leptonic CPV phases to derive predictions for the effective Majorana mass in neutrinoless double beta decay.

**KEYWORDS:** CP violation, Discrete Symmetries, Neutrino Physics

ARXIV EPRINT: [1705.00309](https://arxiv.org/abs/1705.00309)

---

<sup>1</sup>Also at: Institute of Nuclear Research and Nuclear Energy, Bulgarian Academy of Sciences, 1784 Sofia, Bulgaria.

---

## Contents

<b>1</b>	<b>Introduction</b>	<b>1</b>
<b>2</b>	<b>The framework</b>	<b>4</b>
2.1	The PMNS matrix from $G_e = Z_2$ and $G_\nu = Z_2 \times H_{\text{CP}}^\nu$	5
2.2	Conjugate residual symmetries	8
2.3	Phenomenologically non-viable cases	9
<b>3</b>	<b>Mixing patterns from <math>G_f \times H_{\text{CP}} = S_4 \times H_{\text{CP}}</math> broken to <math>G_e = Z_2</math> and <math>G_\nu = Z_2 \times H_{\text{CP}}^\nu</math></b>	<b>10</b>
3.1	Group $S_4$ and residual symmetries	10
3.2	Explicit forms of the PMNS matrix	12
3.3	Extracting mixing parameters and statistical analysis	14
3.4	Results and discussion	16
<b>4</b>	<b>Neutrinoless double beta decay</b>	<b>39</b>
<b>5</b>	<b>Summary and conclusions</b>	<b>42</b>
<b>A</b>	<b>Symmetry of <math>X_\nu</math></b>	<b>49</b>
<b>B</b>	<b>Conjugate pairs of <math>S_4</math> elements</b>	<b>50</b>
<b>C</b>	<b>Equivalent cases</b>	<b>50</b>
<b>D</b>	<b>Correspondence with earlier results</b>	<b>51</b>

---

## 1 Introduction

Understanding the origin of the pattern of neutrino mixing that emerged from the neutrino oscillation data in the recent years (see, e.g., [1]) is one of the most challenging problems in neutrino physics. It is part of the more general fundamental problem in particle physics of understanding the origins of flavour in the quark and lepton sectors, i.e., of the patterns of quark masses and mixing, and of the charged lepton and neutrino masses and of neutrino mixing.

The idea of extending the Standard Model (SM) with a non-Abelian discrete flavour symmetry has been widely exploited in attempts to make progress towards the understanding the origin(s) of flavour (for reviews on the discrete symmetry approach to the flavour problem see, e.g., [2–4]). In this approach it is assumed that at a certain high-energy scale the theory possesses a flavour symmetry, which is broken at lower energies to residual

symmetries of the charged lepton and neutrino sectors, yielding certain predictions for the values of, and/or correlations between, the low-energy neutrino mixing parameters. In the reference 3-neutrino mixing scheme we are going to consider in what follows (see, e.g., [1]), i) the values of certain pairs of, or of all three, neutrino mixing angles are predicted to be correlated, and/or ii) there is a correlation between the value of the Dirac CP violation (CPV) phase  $\delta$  in the neutrino mixing matrix and the values of the three neutrino mixing angles,<sup>1</sup>  $\theta_{12}$ ,  $\theta_{13}$  and  $\theta_{23}$ , which includes also symmetry dependent fixed parameter(s) (see, e.g., [5–13] and references quoted therein). These correlations are usually referred to as “neutrino mixing sum rules”. As we have already indicated, the sum rules for the Dirac phase  $\delta$ , in particular, depend on the underlying symmetry form of the PMNS matrix [5–9] (see also, e.g., [10–13]), which in turn is determined by the assumed lepton flavour symmetry that typically has to be broken, and by the residual unbroken symmetries in the charged lepton and neutrino sectors (see, e.g., [2–4, 7, 9]). They can be tested experimentally (see, e.g., [6, 10, 14–16]). These tests can provide unique information about the possible existence of a new fundamental symmetry in the lepton sector, which determines the pattern of neutrino mixing [5]. Sufficiently precise experimental data on the neutrino mixing angles and on the Dirac CPV phase can also be used to distinguish between different possible underlying flavour symmetries leading to viable patterns of neutrino mixing.

While in the discrete flavour symmetry approach at least some of the neutrino mixing angles and/or the Dirac phase are determined (directly or indirectly via a sum rule) by the flavour symmetry, the Majorana CPV phases  $\alpha_{21}$  and  $\alpha_{31}$  [17] remain unconstrained. The values of the Majorana CPV phases are instead constrained to lie in certain narrow intervals, or are predicted, in theories which in addition to a flavour symmetry possess at a certain high-energy scale a generalised CP (GCP) symmetry [18]. The GCP symmetry should be implemented in a theory based on a discrete flavour symmetry in a way that is consistent with the flavour symmetry [19, 20]. At low energies the GCP symmetry is broken, in general, to residual CP symmetries of the charged lepton and neutrino sectors.

In the scenarios involving a GCP symmetry, which were most widely explored so far (see, e.g., [19, 21–25]), a non-Abelian flavour symmetry  $G_f$  consistently combined with a GCP symmetry  $H_{CP}$  is broken to residual Abelian symmetries  $G_e = Z_n$ ,  $n > 2$ , or  $Z_m \times Z_k$ ,  $m, k \geq 2$ , and  $G_\nu = Z_2 \times H_{CP}^\nu$  of the charged lepton and neutrino mass terms, respectively.<sup>2</sup> The factor  $H_{CP}^\nu$  in  $G_\nu$  stands for a remnant GCP symmetry of the neutrino mass term. In such a set-up,  $G_e$  fixes completely the form of the unitary matrix  $U_e$  which diagonalises the product  $M_e M_e^\dagger$  and enters into the expression of the PMNS matrix,  $M_e$  being the charged lepton mass matrix (in the charged lepton mass term written in the left-right convention). At the same time,  $G_\nu$  fixes the unitary matrix  $U_\nu$ , diagonalising the neutrino Majorana mass matrix  $M_\nu$  up to a single free real parameter — a rotation angle  $\theta^\nu$ . Given the fact that the PMNS neutrino mixing matrix  $U_{PMNS}$  is given by the product

$$U_{PMNS} = U_e^\dagger U_\nu, \tag{1.1}$$

---

<sup>1</sup>Throughout the present study we use the standard parametrisation of the Pontecorvo, Maki, Nakagawa and Sakata (PMNS) neutrino mixing matrix (see, e.g., [1]).

<sup>2</sup>We note that in refs. [22, 23] the residual symmetry  $G_e$  of the charged lepton mass term is augmented with a remnant CP symmetry  $H_{CP}^e$  as well.

Parameter	Best fit value	$2\sigma$ range	$3\sigma$ range
$\sin^2 \theta_{12}/10^{-1}$	2.97	2.65–3.34	2.50–3.54
$\sin^2 \theta_{13}/10^{-2}$ (NO)	2.15	1.99–2.31	1.90–2.40
$\sin^2 \theta_{13}/10^{-2}$ (IO)	2.16	1.98–2.33	1.90–2.42
$\sin^2 \theta_{23}/10^{-1}$ (NO)	4.25	3.95–4.70	3.81–6.15
$\sin^2 \theta_{23}/10^{-1}$ (IO)	5.89	$3.99\text{--}4.83 \oplus 5.33\text{--}6.21$	3.84–6.36
$\delta/\pi$ (NO)	1.38	1.00–1.90	$0\text{--}0.17 \oplus 0.76\text{--}2$
$\delta/\pi$ (IO)	1.31	0.92–1.88	$0\text{--}0.15 \oplus 0.69\text{--}2$
$\Delta m_{21}^2/10^{-5} \text{ eV}^2$	7.37	7.07–7.73	6.93–7.96
$\Delta m_{31}^2/10^{-3} \text{ eV}^2$ (NO)	2.56	2.49–2.64	2.45–2.69
$\Delta m_{23}^2/10^{-3} \text{ eV}^2$ (IO)	2.54	2.47–2.62	2.42–2.66

**Table 1.** The best fit values,  $2\sigma$  and  $3\sigma$  ranges of the neutrino oscillation parameters obtained in the global analysis of the neutrino oscillation data performed in [26].

all three neutrino mixing angles are expressed in terms of this rotation angle. In this class of models one obtains specific correlations between the values of the three neutrino mixing angles, while the leptonic CPV phases are typically predicted to be exactly 0 or  $\pi$ , or else  $\pi/2$  or  $3\pi/2$ . For example, in the set-up considered in [19] (see also [21]), based on  $G_f \times H_{\text{CP}} = S_4 \times H_{\text{CP}}$  broken to  $G_e = Z_3^T$  and  $G_\nu = Z_2^S \times H_{\text{CP}}^\nu$  with  $H_{\text{CP}}^\nu = \{U, SU\}$ ,<sup>3</sup> the authors find:

$$\sin^2 \theta_{13} = \frac{2}{3} \sin^2 \theta^\nu, \quad \sin^2 \theta_{12} = \frac{1}{2 + \cos 2\theta^\nu} = \frac{1}{3(1 - \sin^2 \theta_{13})}, \quad \sin^2 \theta_{23} = \frac{1}{2}, \quad (1.2)$$

$$|\sin \delta| = 1, \quad \sin \alpha_{21} = \sin \alpha_{31} = 0. \quad (1.3)$$

It follows, in particular, from the results on the neutrino oscillation parameters — best fit values,  $2\sigma$  and  $3\sigma$  allowed ranges — obtained in the latest global fit of neutrino oscillation data [26] and summarised in table 1, to be used in our further analysis,<sup>4</sup> that the predictions quoted in eq. (1.2) for  $\sin^2 \theta_{12}$  and  $\sin^2 \theta_{23}$  lie outside of their respective currently allowed  $2\sigma$  ranges.<sup>5</sup>

Another example of one-parametric models is the extensive study performed in [28], in which the authors have considered two different residual symmetry patterns. The first pattern is the one described above, and the second pattern has  $G_e = Z_2 \times H_{\text{CP}}^e$  and  $G_\nu = Z_2 \times Z_2 \times H_{\text{CP}}^\nu$  as residual symmetries in the charged lepton and neutrino sectors, respectively. The authors have performed an exhaustive scan over discrete groups of order less than 2000, which admit faithful 3-dimensional irreducible representations, and classified phenomenologically viable mixing patterns.

<sup>3</sup> $S, T$  and  $U$  are the generators of  $S_4$  in the basis for its 3-dimensional representation we employ in this work (see subsection 3.2).

<sup>4</sup>The results on the neutrino oscillation parameters obtained in the global fit performed in [27] differ somewhat from, but are compatible at  $1\sigma$  confidence level (C.L.) with, those found in [26] and given in table 1.

<sup>5</sup>We have used the best fit value of  $\sin^2 \theta_{13}$  to obtain the prediction of  $\sin^2 \theta_{12}$  leading to the quoted conclusion. Using the  $2\sigma$  allowed range for  $\sin^2 \theta_{13}$  leads to a minimal value of  $\sin^2 \theta_{12} = 0.340$ , which is above the maximal allowed value of  $\sin^2 \theta_{12}$  at  $2\sigma$  C.L., but inside its  $3\sigma$  range.

Theoretical models based on the approach to neutrino mixing that combines discrete symmetries and GCP invariance, in which the neutrino mixing angles and the leptonic CPV phases are functions of two or three parameters have also been considered in the literature (see, e.g., [29–32]). In these models the residual symmetry  $G_e$  of the charged lepton mass term is typically assumed to be a  $Z_2$  symmetry or to be fully broken. In spite of the larger number of parameters in terms of which the neutrino mixing angles and the leptonic CPV phases are expressed, the values of the CPV phases are still predicted to be correlated with the values of the three neutrino mixing angles. A set-up with  $G_e = Z_2 \times H_{\text{CP}}^e$  and  $G_\nu = Z_2 \times H_{\text{CP}}^\nu$  has been considered in [32]. The resulting PMNS matrix in such a scheme depends on two free real parameters — two angles  $\theta^\nu$  and  $\theta^e$ . The authors have obtained several phenomenologically viable neutrino mixing patterns from  $G_f = S_4$  combined with  $H_{\text{CP}}$ , broken to all possible residual symmetries of the type indicated above. Models allowing for three free parameters have been investigated in [29–31]. In, e.g., [30], the author has considered  $G_f = A_5$  combined with  $H_{\text{CP}}$ , which are broken to  $G_e = Z_2$  and  $G_\nu = Z_2 \times H_{\text{CP}}^\nu$ . In this case, the matrix  $U_e$  depends on an angle  $\theta^e$  and a phase  $\delta^e$ , while the matrix  $U_\nu$  depends on an angle  $\theta^\nu$ . In these two scenarios the leptonic CPV phases possess non-trivial values.

The specific correlations between the values of the three neutrino mixing angles, which characterise the one-parameter models based on  $G_e = Z_n$ ,  $n > 2$ , or  $Z_m \times Z_k$ ,  $m, k \geq 2$ , and  $G_\nu = Z_2 \times H_{\text{CP}}^\nu$ , do not hold in the two- and three-parameter models. In addition, the Dirac CPV phase in the two- and three-parameter models is predicted to have non-trivial values which are correlated with the values of the three neutrino mixing angles and differ from  $0, \pi, \pi/2$  and  $3\pi/2$ , although the deviations from, e.g.,  $3\pi/2$  can be relatively small. The indicated differences between the predictions of the models based on  $G_e = Z_n$ ,  $n > 2$ , or  $Z_m \times Z_k$ ,  $m, k \geq 2$ , and on  $G_e = Z_2$  symmetries make it possible to distinguish between them experimentally by improving the precision on each of the three measured neutrino mixing angles  $\theta_{12}$ ,  $\theta_{23}$  and  $\theta_{13}$ , and by performing a sufficiently precise measurement of the Dirac phase  $\delta$ .

In the present article, we investigate the possible neutrino mixing patterns generated by a  $G_f = S_4$  symmetry combined with an  $H_{\text{CP}}$  symmetry when these symmetries are broken down to  $G_e = Z_2$  and  $G_\nu = Z_2 \times H_{\text{CP}}^\nu$ . In section 2, we describe a general framework for deriving the form of the PMNS matrix, dictated by the chosen residual symmetries. Then, in section 3, we apply this framework to  $G_f = S_4$  combined with  $H_{\text{CP}}$  and obtain all phenomenologically viable mixing patterns. Next, in section 4, using the obtained predictions for the neutrino mixing angles and the Dirac and Majorana CPV phases, we derive predictions for the neutrinoless double beta decay effective Majorana mass. Section 5 contains the conclusions of the present study.

## 2 The framework

We start with a non-Abelian flavour symmetry group  $G_f$ , which admits a faithful irreducible 3-dimensional representation  $\rho$ . The three generations of left-handed (LH) leptons are assigned to this representation. Apart from that, the high-energy theory respects also the GCP symmetry  $H_{\text{CP}}$ , which is implemented consistently along with the flavour symmetry.

At some flavour symmetry breaking scale  $G_f \times H_{\text{CP}}$  gets broken down to residual symmetries  $G_e$  and  $G_\nu$  of the charged lepton and neutrino mass terms, respectively. The residual flavour symmetries are Abelian subgroups of  $G_f$ . The symmetries  $G_e$  and  $G_\nu$  significantly constrain the form of the neutrino mixing matrix  $U_{\text{PMNS}}$ , as we demonstrate below.

## 2.1 The PMNS matrix from $G_e = Z_2$ and $G_\nu = Z_2 \times H_{\text{CP}}^\nu$

We choose  $G_e$  to be a  $Z_2$  symmetry. We will denote it as  $Z_2^{g_e} \equiv \{1, g_e\}$ ,  $g_e^2 = 1$  being an element of  $G_f$  of order two, generating the  $Z_2^{g_e}$  subgroup. The invariance of the charged lepton mass term under  $G_e$  implies

$$\rho(g_e)^\dagger M_e M_e^\dagger \rho(g_e) = M_e M_e^\dagger. \quad (2.1)$$

Below we show how this invariance constrains the form of the unitary matrix  $U_e$ , diagonalising  $M_e M_e^\dagger$ :

$$U_e^\dagger M_e M_e^\dagger U_e = \text{diag}(m_e^2, m_\mu^2, m_\tau^2). \quad (2.2)$$

Lets  $\Omega_e$  be a diagonalising unitary matrix of  $\rho(g_e)$ , such that

$$\Omega_e^\dagger \rho(g_e) \Omega_e = \rho(g_e)^d \equiv \text{diag}(1, -1, -1). \quad (2.3)$$

This result is obtained as follows. The diagonal entries of  $\rho(g_e)^d$  are constrained to be  $\pm 1$ , since this matrix must still furnish a representation of  $Z_2$  and hence its square is the identity. We have assumed that the trace of  $\rho(g_e)$  is  $-1$ , for the relevant elements  $g_e$ , as it is the case for the 3-dimensional representation of  $S_4$  we will consider later on.<sup>6</sup> Note that we can take the order of the eigenvalues of  $\rho(g_e)$  as given in eq. (2.3) without loss of generality, as will become clear later.

Expressing  $\rho(g_e)$  from eq. (2.3) and substituting it in eq. (2.1), we obtain

$$\rho(g_e)^d \Omega_e^\dagger M_e M_e^\dagger \Omega_e \rho(g_e)^d = \Omega_e^\dagger M_e M_e^\dagger \Omega_e. \quad (2.4)$$

This equation implies that  $\Omega_e^\dagger M_e M_e^\dagger \Omega_e$  has the block-diagonal form

$$\begin{pmatrix} \times & 0 & 0 \\ 0 & \times & \times \\ 0 & \times & \times \end{pmatrix}, \quad (2.5)$$

and, since this matrix is hermitian, it can be diagonalised by a unitary matrix with a  $U(2)$  transformation acting on the 2-3 block. In the general case, the  $U(2)$  transformation can be parametrised as follows:

$$\begin{pmatrix} \cos \theta^e & -\sin \theta^e e^{-i\delta^e} \\ \sin \theta^e e^{i\delta^e} & \cos \theta^e \end{pmatrix} \begin{pmatrix} e^{i\beta_1^e} & 0 \\ 0 & e^{i\beta_2^e} \end{pmatrix}. \quad (2.6)$$

---

<sup>6</sup>For the other 3-dimensional irreducible representation of  $S_4$  the trace can be either  $-1$  or  $+1$ , depending on  $g_e$ . Choosing  $+1$  would simply imply a change of sign of  $\rho(g_e)^d$ , which however does not lead to new constraints. The conclusions we reach in what follows are then independent of the choice of 3-dimensional representation.

The diagonal phase matrix is, however, unphysical, since it can be eliminated by rephasing of the charged lepton fields, and we will not keep it in the future. Thus, we arrive to the conclusion that the matrix  $U_e$  diagonalising  $M_e M_e^\dagger$  reads

$$U_e = \Omega_e U_{23}(\theta^e, \delta^e)^\dagger P_e^T, \quad (2.7)$$

with

$$U_{23}(\theta^e, \delta^e) = \begin{pmatrix} 1 & 0 & 0 \\ 0 & \cos \theta^e & \sin \theta^e e^{-i\delta^e} \\ 0 & -\sin \theta^e e^{i\delta^e} & \cos \theta^e \end{pmatrix}, \quad (2.8)$$

and  $P_e$  being one of six permutation matrices, which need to be taken into account, since in the approach under consideration the order of the charged lepton masses is unknown. The six permutation matrices read:

$$P_{123} = \begin{pmatrix} 1 & 0 & 0 \\ 0 & 1 & 0 \\ 0 & 0 & 1 \end{pmatrix}, \quad P_{132} = \begin{pmatrix} 1 & 0 & 0 \\ 0 & 0 & 1 \\ 0 & 1 & 0 \end{pmatrix}, \quad P_{213} = \begin{pmatrix} 0 & 1 & 0 \\ 1 & 0 & 0 \\ 0 & 0 & 1 \end{pmatrix}, \quad (2.9)$$

$$P_{231} = \begin{pmatrix} 0 & 1 & 0 \\ 0 & 0 & 1 \\ 1 & 0 & 0 \end{pmatrix}, \quad P_{312} = \begin{pmatrix} 0 & 0 & 1 \\ 1 & 0 & 0 \\ 0 & 1 & 0 \end{pmatrix}, \quad P_{321} = \begin{pmatrix} 0 & 0 & 1 \\ 0 & 1 & 0 \\ 1 & 0 & 0 \end{pmatrix}. \quad (2.10)$$

Note that the order of indices in  $P_{ijk}$  stands for the order of rows, i.e., when applied from the left to a matrix, it gives the desired order,  $i$ - $j$ - $k$ , of the matrix rows. The same is also true for columns, when  $P_{ijk}$  is applied from the right, except for  $P_{231}$  which leads to the 3-1-2 order of columns and  $P_{312}$  yielding the 2-3-1 order.

In the neutrino sector we have a  $G_\nu = Z_2 \times H_{\text{CP}}^\nu$  residual symmetry. We will denote the  $Z_2$  symmetry of the neutrino mass matrix as  $Z_2^{g_\nu} \equiv \{1, g_\nu\}$ , with  $g_\nu^2 = 1$  being an element of  $G_f$ , generating the  $Z_2^{g_\nu}$  subgroup.  $H_{\text{CP}}^\nu = \{X_\nu\}$  is the set of remnant GCP unitary transformations  $X_\nu$  forming a residual CP symmetry of the neutrino mass matrix.  $H_{\text{CP}}^\nu$  is contained in  $H_{\text{CP}} = \{X\}$  which is the GCP symmetry of the high-energy theory consistently defined along with the flavour symmetry  $G_f$ .<sup>7</sup> The invariance under  $G_\nu$  of the

---

<sup>7</sup>It is worth to comment here on the notation  $H_{\text{CP}}^\nu$  we use. When we write in what follows  $H_{\text{CP}}^\nu = \{X_{\nu 1}, X_{\nu 2}\}$ , we mean a set of GCP transformations ( $X_{\nu 1}$  and  $X_{\nu 2}$ ) compatible with the residual flavour  $Z_2^{g_\nu}$  symmetry (see eq. (2.13)). However, when writing  $G_\nu = Z_2^{g_\nu} \times H_{\text{CP}}^\nu$ ,  $H_{\text{CP}}^\nu$  is intended to be a group generated by  $X_{\nu 1}$ . Namely, following appendix B in [19],  $H_{\text{CP}}^\nu$  is isomorphic to  $\{\mathcal{I}, \mathcal{X}_{\nu 1}\}$ , where  $\mathcal{I}$  is the unit matrix and

$$\mathcal{X}_{\nu 1} = \begin{pmatrix} 0 & X_{\nu 1} \\ X_{\nu 1}^* & 0 \end{pmatrix},$$

both of them acting on  $(\varphi, \varphi^*)^T$ . Then,  $Z_2^{g_\nu}$  is isomorphic to  $\{\mathcal{I}, \mathcal{G}_\nu\}$ , where

$$\mathcal{G}_\nu = \begin{pmatrix} \rho(g_\nu) & 0 \\ 0 & \rho^*(g_\nu) \end{pmatrix}$$

acts again on  $(\varphi, \varphi^*)^T$ . Finally, it is not difficult to convince oneself that the full residual symmetry group  $G_\nu$  is given by a direct product  $Z_2^{g_\nu} \times H_{\text{CP}}^\nu$ , and the second GCP transformation  $X_{\nu 2} = \rho(g_\nu) X_{\nu 1}$  is contained in it. The same logic applies to the notation  $H_{\text{CP}}$ , and, as has been shown in appendix B of [19], the full symmetry group is a semi-direct product  $G_f \rtimes H_{\text{CP}}$ . Note that these notations are widely used in the literature.

neutrino mass matrix implies that the following two equations hold:

$$\rho(g_\nu)^T M_\nu \rho(g_\nu) = M_\nu, \quad (2.11)$$

$$X_\nu^T M_\nu X_\nu = M_\nu^*. \quad (2.12)$$

In addition, the consistency condition between  $Z_2^{g_\nu}$  and  $H_{\text{CP}}^\nu$  has to be respected:

$$X_\nu \rho^*(g_\nu) X_\nu^{-1} = \rho(g_\nu). \quad (2.13)$$

To derive the form of the unitary matrix  $U_\nu$  diagonalising the neutrino Majorana mass matrix  $M_\nu$  as

$$U_\nu^T M_\nu U_\nu = \text{diag}(m_1, m_2, m_3), \quad (2.14)$$

$m_j > 0$  being the neutrino masses, we will follow the method presented in [32].

Lets  $\Omega_{\nu 1}$  be a diagonalising unitary matrix of  $\rho(g_\nu)$ , such that

$$\Omega_{\nu 1}^\dagger \rho(g_\nu) \Omega_{\nu 1} = \rho(g_\nu)^d \equiv \text{diag}(1, -1, -1). \quad (2.15)$$

Expressing  $\rho(g_\nu)$  from this equation and substituting it in the consistency condition, eq. (2.13), we find

$$\rho(g_\nu)^d \Omega_{\nu 1}^\dagger X_\nu \Omega_{\nu 1}^* \rho(g_\nu)^d = \Omega_{\nu 1}^\dagger X_\nu \Omega_{\nu 1}^*, \quad (2.16)$$

meaning that  $\Omega_{\nu 1}^\dagger X_\nu \Omega_{\nu 1}^*$  is a block-diagonal matrix, having the form of eq. (2.5). Moreover, this matrix is symmetric, since the GCP transformations  $X_\nu$  have to be symmetric in order for all the three neutrino masses to be different [19, 21], as is required by the data. In appendix A we provide a proof of this. Being a complex (unitary) symmetric matrix, it is diagonalised by a unitary matrix  $\Omega_{\nu 2}$  via the transformation:

$$\Omega_{\nu 2}^\dagger (\Omega_{\nu 1}^\dagger X_\nu \Omega_{\nu 1}^*) \Omega_{\nu 2} = (\Omega_{\nu 1}^\dagger X_\nu \Omega_{\nu 1}^*)^d. \quad (2.17)$$

The matrix  $(\Omega_{\nu 1}^\dagger X_\nu \Omega_{\nu 1}^*)^d$  is, in general, a diagonal phase matrix. However, we can choose  $(\Omega_{\nu 1}^\dagger X_\nu \Omega_{\nu 1}^*)^d = \text{diag}(1, 1, 1)$  as the phases of  $(\Omega_{\nu 1}^\dagger X_\nu \Omega_{\nu 1}^*)^d$  can be moved to the matrix  $\Omega_{\nu 2}$ . With this choice we obtain the Takagi factorisation of the  $X_\nu$  (valid for unitary symmetric matrices):

$$X_\nu = \Omega_\nu \Omega_\nu^T, \quad (2.18)$$

with  $\Omega_\nu = \Omega_{\nu 1} \Omega_{\nu 2}$ .

Since, as we have noticed earlier,  $\Omega_{\nu 1}^\dagger X_\nu \Omega_{\nu 1}^*$  has the form of eq. (2.5), the matrix  $\Omega_{\nu 2}$  can be chosen without loss of generality to have the form of eq. (2.5) with a unitary  $2 \times 2$  matrix in the 2-3 block. This implies that the matrix  $\Omega_\nu = \Omega_{\nu 1} \Omega_{\nu 2}$  also diagonalises  $\rho(g_\nu)$ . Indeed,

$$\Omega_\nu^\dagger \rho(g_\nu) \Omega_\nu = \Omega_{\nu 2}^\dagger \rho(g_\nu)^d \Omega_{\nu 2} = \rho(g_\nu)^d, \quad (2.19)$$

where we have used eq. (2.15).

We substitute next  $X_\nu$  from eq. (2.18) in the GCP invariance condition of the neutrino mass matrix, eq. (2.12), and find that the matrix  $\Omega_\nu^T M_\nu \Omega_\nu$  is real. Furthermore, this is a symmetric matrix, since the neutrino Majorana mass matrix  $M_\nu$  is symmetric. A real



symmetric matrix can be diagonalised by a real orthogonal transformation. Employing eqs. (2.19) and (2.11), we have

$$\rho(g_\nu)^d \Omega_\nu^T M_\nu \Omega_\nu \rho(g_\nu)^d = \Omega_\nu^T M_\nu \Omega_\nu, \quad (2.20)$$

implying that  $\Omega_\nu^T M_\nu \Omega_\nu$  is a block-diagonal matrix as in eq. (2.5). Thus, the required orthogonal transformation is a rotation in the 2-3 plane on an angle  $\theta^\nu$ :

$$R_{23}(\theta^\nu) = \begin{pmatrix} 1 & 0 & 0 \\ 0 & \cos \theta^\nu & \sin \theta^\nu \\ 0 & -\sin \theta^\nu & \cos \theta^\nu \end{pmatrix}. \quad (2.21)$$

Finally, the matrix  $U_\nu$  diagonalising  $M_\nu$  reads

$$U_\nu = \Omega_\nu R_{23}(\theta^\nu) P_\nu Q_\nu, \quad (2.22)$$

where  $P_\nu$  is one of the six permutation matrices, which accounts for different order of  $m_j$ , and the matrix  $Q_\nu$  renders them positive. Without loss of generality  $Q_\nu$  can be parametrised as follows:

$$Q_\nu = \text{diag}(1, i^{k_1}, i^{k_2}), \quad \text{with } k_{1,2} = 0, 1. \quad (2.23)$$

Assembling together the results for  $U_e$  and  $U_\nu$ , eqs. (2.7) and (2.22), we obtain for the form of the PMNS matrix:

$$U_{\text{PMNS}} = P_e U_{23}(\theta^e, \delta^e) \Omega_e^\dagger \Omega_\nu R_{23}(\theta^\nu) P_\nu Q_\nu. \quad (2.24)$$

Thus, in the approach we are following the PMNS matrix depends on three free real parameters<sup>8</sup> — the two angles  $\theta^e$  and  $\theta^\nu$  and the phase  $\delta^e$ . One of the elements of the PMNS matrix is fixed to be a constant by the employed residual symmetries. We note finally that, since  $R_{23}(\theta^\nu + \pi) = R_{23}(\theta^\nu) \text{diag}(1, -1, -1)$ , where the diagonal matrix can be absorbed into  $Q_\nu$ , and  $U_{23}(\theta^e + \pi, \delta^e) = \text{diag}(1, -1, -1) U_{23}(\theta^e, \delta^e)$ , where the diagonal matrix contributes to the unphysical charged lepton phases, it is sufficient to consider  $\theta^e$  and  $\theta^\nu$  in the interval  $[0, \pi)$ .

## 2.2 Conjugate residual symmetries

In this subsection we briefly recall why the residual symmetries  $G'_e$  and  $G'_\nu$  conjugate to  $G_e$  and  $G_\nu$ , respectively, under the same element of the flavour symmetry group  $G_f$  lead to the same PMNS matrix (see, e.g., [19, 22]). Two pairs of residual symmetries  $\{Z_2^{g_e}, Z_2^{g_\nu}\}$  and  $\{Z_2^{g'_e}, Z_2^{g'_\nu}\}$  are conjugate to each other under  $h \in G_f$  if

$$h g_e h^{-1} = g'_e \quad \text{and} \quad h g_\nu h^{-1} = g'_\nu. \quad (2.25)$$

---

<sup>8</sup>It should be noted that the matrix  $\Omega_{\nu 2}$  in eq. (2.17) with  $(\Omega_{\nu 1}^\dagger X_\nu \Omega_{\nu 1}^*)^d = \text{diag}(1, 1, 1)$ , and thus the matrix  $\Omega_\nu = \Omega_{\nu 1} \Omega_{\nu 2}$  in eq. (2.18), is determined up to a multiplication by an orthogonal matrix  $O$  on the right. The matrix  $\Omega_{\nu 2} O$  must be unitary since it diagonalises a complex symmetric matrix, which implies that  $O$  must be unitary in addition of being orthogonal, and therefore must be a real matrix. Equation (2.19) restricts further this real orthogonal matrix  $O$  to have the form of a real rotation in the 2-3 plane, which can be “absorbed” in the  $R_{23}(\theta^\nu)$  matrix in eq. (2.24).

At the representation level this means

$$\rho(h) \rho(g_e) \rho(h)^\dagger = \rho(g'_e) \quad \text{and} \quad \rho(h) \rho(g_\nu) \rho(h)^\dagger = \rho(g'_\nu). \quad (2.26)$$

Substituting  $\rho(g_e)$  and  $\rho(g_\nu)$  from these equalities to eqs. (2.1) and (2.11), respectively, we obtain

$$\rho(g'_e)^\dagger M'_e M_e^\dagger \rho(g'_e) = M'_e M_e^\dagger \quad \text{and} \quad \rho(g'_\nu)^T M'_\nu \rho(g'_\nu) = M'_\nu, \quad (2.27)$$

where the primed mass matrices are related to the original ones as

$$M'_e M_e^\dagger = \rho(h) M_e M_e^\dagger \rho(h)^\dagger \quad \text{and} \quad M'_\nu = \rho(h)^* M_\nu \rho(h)^\dagger. \quad (2.28)$$

As can be understood from eq. (2.12) (or eq. (2.13)), the matrix  $M'_\nu$  will respect a remnant CP symmetry  $H'_{\text{CP}} = \{X'_\nu\}$ , which is related to  $H_{\text{CP}} = \{X_\nu\}$  as follows:

$$X'_\nu = \rho(h) X_\nu \rho(h)^T. \quad (2.29)$$

Obviously, the unitary transformations  $U'_e$  and  $U'_\nu$  diagonalising the primed mass matrices are given by

$$U'_e = \rho(h) U_e \quad \text{and} \quad U'_\nu = \rho(h) U_\nu, \quad (2.30)$$

thus yielding

$$U'_{\text{PMNS}} = U_e^\dagger U'_\nu = U_e^\dagger \rho(h) U_\nu = U_{\text{PMNS}}. \quad (2.31)$$

### 2.3 Phenomenologically non-viable cases

Here we demonstrate that at least two types of residual symmetries  $\{G_e, G_\nu\} = \{Z_2^{g_e}, Z_2^{g_\nu} \times H'_{\text{CP}}\}$ , characterised by certain  $g_e$  and  $g_\nu$ , cannot lead to phenomenologically viable form of the PMNS matrix.

- **Type I:**  $g_e = g_\nu$ . In this case, we can choose  $\Omega_e = \Omega_\nu P$ , with  $P_{123}$  or  $P_{132}$ . Then, eq. (2.24) yields

$$U_{\text{PMNS}} = P_e U_{23}(\theta^e, \delta^e) P R_{23}(\theta^\nu) P_\nu Q_\nu. \quad (2.32)$$

This means that up to permutations of the rows and columns  $U_{\text{PMNS}}$  has the form of eq. (2.5), i.e., contains four zero entries, which are ruled out by neutrino oscillation data [26, 27].

- **Type II:**  $g_e, g_\nu \in Z_2 \times Z_2 \subset G_f$ . Now we consider two different order two elements  $g_e \neq g_\nu$ , which belong to the same  $Z_2 \times Z_2 = \{1, g_e, g_\nu, g_e g_\nu\}$  subgroup of  $G_f$ . In this case, since  $g_e$  and  $g_\nu$  commute, there exists a unitary matrix simultaneously diagonalising both  $\rho(g_e)$  and  $\rho(g_\nu)$ . Note, however, that the order of eigenvalues in the resulting diagonal matrices will be different. Namely, lets  $\Omega_{\nu 1}$  be a diagonalising matrix of  $\rho(g_\nu)$  and  $\rho(g_e)$ , and lets  $\Omega_{\nu 1}$  diagonalise  $\rho(g_\nu)$  as in eq. (2.15). Then,  $\Omega_{\nu 1}^\dagger \rho(g_e) \Omega_{\nu 1}$  can yield either  $\text{diag}(-1, 1, -1)$  or  $\text{diag}(-1, -1, 1)$ , but not  $\text{diag}(1, -1, -1)$ . Hence,  $\Omega_e$  diagonalising  $\rho(g_e)$  as in eq. (2.3), must read

$$\Omega_e = \Omega_{\nu 1} P, \quad \text{with} \quad P = P_{213} \text{ or } P_{312} \quad \text{if} \quad \Omega_{\nu 1}^\dagger \rho(g_e) \Omega_{\nu 1} = \text{diag}(-1, 1, -1), \quad (2.33)$$

$$\text{and} \quad P = P_{231} \text{ or } P_{321} \quad \text{if} \quad \Omega_{\nu 1}^\dagger \rho(g_e) \Omega_{\nu 1} = \text{diag}(-1, -1, 1). \quad (2.34)$$

Taking into account that  $\Omega_\nu = \Omega_{\nu 1} \Omega_{\nu 2}$ , with  $\Omega_{\nu 2}$  of the block-diagonal form given in eq. (2.5), we obtain

$$U_{\text{PMNS}} = P_e U_{23}(\theta^e, \delta^e) P^T \Omega_{\nu 2} R_{23}(\theta^\nu) P_\nu Q_\nu, \quad (2.35)$$

where  $P^T \Omega_{\nu 2}$ , depending on  $P$ , can take one of the following forms:

$$\begin{pmatrix} 0 & \times & \times \\ \times & 0 & 0 \\ 0 & \times & \times \end{pmatrix} \quad \text{or} \quad \begin{pmatrix} 0 & \times & \times \\ 0 & \times & \times \\ \times & 0 & 0 \end{pmatrix}. \quad (2.36)$$

As a consequence,  $U_{\text{PMNS}}$  up to permutations of the rows and columns has the form

$$\begin{pmatrix} 0 & \times & \times \\ \times & \times & \times \\ \times & \times & \times \end{pmatrix}, \quad (2.37)$$

containing one zero element, which is ruled out by the data.

### 3 Mixing patterns from $G_f \rtimes H_{\text{CP}} = S_4 \rtimes H_{\text{CP}}$ broken to $G_e = Z_2$ and $G_\nu = Z_2 \times H'_{\text{CP}}$

#### 3.1 Group $S_4$ and residual symmetries

$S_4$  is the symmetric group of permutations of four objects. This group is isomorphic to the group of rotational symmetries of the cube.  $S_4$  can be defined in terms of three generators  $S$ ,  $T$  and  $U$ , satisfying [33]

$$S^2 = T^3 = U^2 = (ST)^3 = (SU)^2 = (TU)^2 = (STU)^4 = 1. \quad (3.1)$$

From 24 elements of the group there are nine elements of order two, which belong to two of five conjugacy classes of  $S_4$  (see, e.g., [21]):

$$3C_2 : \{S, TST^2, T^2ST\}, \quad (3.2)$$

$$6C'_2 : \{U, TU, SU, T^2U, STSU, ST^2SU\}. \quad (3.3)$$

Each of these nine elements generates a corresponding  $Z_2$  subgroup of  $S_4$ . Each subgroup can be the residual symmetry of  $M_e M_e^\dagger$ , and, combined with compatible CP transformations, yield the residual symmetry of  $M_\nu$ . Hence, we have 81 possible pairs of only residual flavour symmetries (taking into account remnant CP symmetries increases the number of possibilities). Many of them, however, being conjugate to each other, will lead to the same form of the PMNS matrix, as explained in subsection 2.2. Thus, we first identify the pairs of elements  $\{g_e, g_\nu\}$ , which are not related by the similarity transformation given in eq. (2.25). We find nine distinct cases for which  $\{g_e, g_\nu\}$  can be chosen as

$$\{S, S\}, \quad \{U, U\}, \quad \{T^2ST, S\}, \quad \{S, U\}, \quad \{U, S\}, \quad \{SU, U\}, \quad (3.4)$$

$$\{S, TU\}, \quad \{TU, S\}, \quad \{TU, U\}. \quad (3.5)$$

The pair  $\{S, S\}$  is obviously conjugate to  $\{TST^2, TST^2\}$  and  $\{T^2ST, T^2ST\}$ , while  $\{U, U\}$  is conjugate to  $\{g_e, g_\nu\}$  with  $g_e = g_\nu$  being one of the remaining five elements from conjugacy class  $6C'_2$  given in eq. (3.3). The pairs  $\{T^2ST, S\}$ ,  $\{S, U\}$ ,  $\{U, S\}$  and  $\{SU, U\}$  are conjugate to five pairs each, and  $\{S, TU\}$  and  $\{TU, S\}$  to eleven pairs each. Finally,  $\{TU, U\}$  is conjugate to 23 pairs. As it should be, the total number of pairs yields 81. The complete lists of pairs of elements which are conjugate to each of these nine pairs are given in appendix B.

The cases in eq. (3.4) do not lead to phenomenologically viable results. The first two of them belong to the cases of Type I (see subsection 2.3). The remaining four belong to Type II, since  $S_4$  contains  $Z_2^S \times Z_2^{TST^2} = \{1, S, TST^2, T^2ST\}$  and  $Z_2^S \times Z_2^U = \{1, S, U, SU\}$  subgroups (see, e.g., [34]). Thus, we are left with three cases in eq. (3.5).

We have chosen  $g_\nu$  in such a way that it is  $S, U$  or  $TU$  for all the cases in eq. (3.5). Now we need to identify the remnant CP transformations  $X_\nu$  compatible with each of these three elements. It is known that the GCP symmetry  $H_{\text{CP}} = \{X\}$  compatible with  $G_f = S_4$  is of the same form of  $G_f$  itself [20], i.e.,

$$X = \rho(g), \quad g \in S_4. \tag{3.6}$$

Thus, to find  $X_\nu$  compatible with  $g_\nu$  of interest, we need to select those  $X = \rho(g)$ , which i) satisfy the consistency condition in eq. (2.13) and ii) are symmetric in order to avoid partially degenerate neutrino mass spectrum, as was noted earlier. The result reads:<sup>9</sup>

$$X_\nu = 1, (S), U, (SU), TST^2U, (T^2STU) \quad \text{for } g_\nu = S; \tag{3.7}$$

$$X_\nu = 1, (U), S, (SU) \quad \text{for } g_\nu = U; \tag{3.8}$$

$$X_\nu = U, (T), STS, (T^2STU) \quad \text{for } g_\nu = TU. \tag{3.9}$$

A GCP transformation in parentheses appears automatically to be a remnant CP symmetry of  $M_\nu$ , if  $X_\nu$  which precedes this in the list is a remnant CP symmetry. This is a consequence of eqs. (2.11) and (2.12), which imply that if  $X_\nu$  is a residual CP symmetry of  $M_\nu$ , then  $\rho(g_\nu)X_\nu$  is a residual CP symmetry as well. Therefore, we have three sets of remnant CP transformations compatible with  $Z_2^S$ , namely,  $H_{\text{CP}}^\nu = \{1, S\}$ ,  $\{U, SU\}$  and  $\{TST^2U, T^2STU\}$ , two sets compatible with  $Z_2^U$ , which are  $H_{\text{CP}}^\nu = \{1, U\}$  and  $\{S, SU\}$ , and two sets consistent with  $Z_2^{TU}$ , which read  $H_{\text{CP}}^\nu = \{U, T\}$  and  $\{STS, T^2STU\}$ . Taking them into account, we end up with seven possible pairs of residual symmetries  $\{G_e, G_\nu\} = \{Z_2^{g_e}, Z_2^{g_\nu} \times H_{\text{CP}}^\nu\}$ , with  $\{g_e, g_\nu\}$  as in eq. (3.5). In what follows, we will consider them case by case and classify all phenomenologically viable mixing patterns they lead to.

Before starting, however, let us recall the current knowledge on the absolute values of the PMNS matrix elements, which we will use in what follows. The  $3\sigma$  ranges of the absolute values of the PMNS matrix elements read [35]

$$|U_{\text{PMNS}}|_{3\sigma} = \begin{pmatrix} 0.796 \rightarrow 0.855 & 0.497 \rightarrow 0.587 & 0.140 \rightarrow 0.153 \\ 0.245 \rightarrow 0.513 & 0.543 \rightarrow 0.709 & 0.614 \rightarrow 0.768 \\ 0.244 \rightarrow 0.510 & 0.456 \rightarrow 0.642 & 0.624 \rightarrow 0.776 \end{pmatrix} \tag{3.10}$$

---

<sup>9</sup>For notation simplicity we will not write the representation symbol  $\rho$ , keeping in mind that  $X_\nu = g$  meas  $X_\nu = \rho(g)$  with  $g \in G_f$ .

for the neutrino mass spectrum with normal ordering (NO), and

$$|U_{\text{PMNS}}|_{3\sigma} = \begin{pmatrix} 0.796 \rightarrow 0.855 & 0.497 \rightarrow 0.587 & 0.140 \rightarrow 0.153 \\ 0.223 \rightarrow 0.503 & 0.452 \rightarrow 0.703 & 0.614 \rightarrow 0.783 \\ 0.257 \rightarrow 0.526 & 0.464 \rightarrow 0.712 & 0.605 \rightarrow 0.775 \end{pmatrix} \quad (3.11)$$

for the neutrino mass spectrum with inverted ordering (IO). The ranges in eqs. (3.10) and (3.11) differ a little from the results obtained in [27].

### 3.2 Explicit forms of the PMNS matrix

First, we present an explicit example of constructing the PMNS matrix in the case of  $g_e = S$ ,  $g_\nu = TU$  and  $H_{\text{CP}}^\nu = \{U, T\}$ , which is the first case out of the seven potentially viable cases indicated above. We will work in the basis for  $S_4$  from [36], in which the matrices for the generators  $S$ ,  $T$  and  $U$  in the 3-dimensional representation read

$$S = \frac{1}{3} \begin{pmatrix} -1 & 2 & 2 \\ 2 & -1 & 2 \\ 2 & 2 & -1 \end{pmatrix}, \quad T = \begin{pmatrix} 1 & 0 & 0 \\ 0 & \omega^2 & 0 \\ 0 & 0 & \omega \end{pmatrix} \quad \text{and} \quad U = - \begin{pmatrix} 1 & 0 & 0 \\ 0 & 0 & 1 \\ 0 & 1 & 0 \end{pmatrix}, \quad (3.12)$$

where  $\omega = e^{2\pi i/3}$ . For simplicity we use the same notation ( $S$ ,  $T$  and  $U$ ) for the generators and their 3-dimensional representation matrices. We will follow the procedure described in subsection 2.1. The matrix  $\Omega_e$  which diagonalises  $\rho(g_e) = S$  (see eq. (2.3)) is given by

$$\Omega_e = \frac{1}{\sqrt{6}} \begin{pmatrix} \sqrt{2} & -\sqrt{3} & -1 \\ \sqrt{2} & 0 & 2 \\ \sqrt{2} & \sqrt{3} & -1 \end{pmatrix}. \quad (3.13)$$

The matrix  $\Omega_\nu$ , such that  $\Omega_\nu \Omega_\nu^T = U$  (see eq. (2.18)), reads

$$\Omega_\nu = \frac{1}{\sqrt{2}} \begin{pmatrix} 0 & 0 & \sqrt{2}i \\ e^{\frac{2\pi i}{3}} & -e^{\frac{i\pi}{6}} & 0 \\ e^{\frac{i\pi}{3}} & e^{-\frac{i\pi}{6}} & 0 \end{pmatrix}. \quad (3.14)$$

Using the master formula in eq. (2.24), we obtain that up to permutations of the rows and columns  $U_{\text{PMNS}}$  has the form

$$\begin{pmatrix} \frac{i}{\sqrt{2}} & \times & \times \\ \times & \times & \times \\ \times & \times & \times \end{pmatrix}, \quad (3.15)$$

where “ $\times$ ” entries are functions of the free parameters  $\theta^\nu$ ,  $\theta^e$  and  $\delta^e$ . Taking into account the current data, eqs. (3.10) and (3.11), the fixed element with the absolute value of  $1/\sqrt{2} \approx 0.707$  can be  $(U_{\text{PMNS}})_{\mu 2}$ ,  $(U_{\text{PMNS}})_{\mu 3}$ ,  $(U_{\text{PMNS}})_{\tau 2}$  or  $(U_{\text{PMNS}})_{\tau 3}$ . Note that  $|(U_{\text{PMNS}})_{\tau 2}| = 0.707$  is outside the  $3\sigma$  range in the case of the NO neutrino mass spectrum, while  $|(U_{\text{PMNS}})_{\mu 2}| = 0.707$  is at the border of the  $3\sigma$  allowed ranges for both the NO and IO spectra.

Let us consider as an example the first possibility, i.e.,  $P_e = P_\nu = P_{213}$ , leading to  $|(U_{\text{PMNS}})_{\mu 2}| = 1/\sqrt{2}$ . In this case the mixing angles of the standard parametrisation of the PMNS matrix are related to the free parameters  $\theta^\nu$ ,  $\theta^e$  and  $\delta^e$  as follows:

$$\begin{aligned} \sin^2 \theta_{13} = |(U_{\text{PMNS}})_{e3}|^2 = \frac{1}{24} & \left[ \cos 2\theta^\nu \left( \sin 2\theta^e \left( 3 \sin \delta^e + 4\sqrt{3} \cos \delta^e \right) + 4 \cos 2\theta^e - 1 \right) \right. \\ & \left. + \sqrt{2} \sin 2\theta^\nu \left( \sin 2\theta^e \left( \sqrt{3} \cos \delta^e - 6 \sin \delta^e \right) + \cos 2\theta^e + 2 \right) - 3 \sin \delta^e \sin 2\theta^e + 9 \right], \end{aligned} \quad (3.16)$$

$$\sin^2 \theta_{23} = \frac{|(U_{\text{PMNS}})_{\mu 3}|^2}{1 - |(U_{\text{PMNS}})_{e3}|^2} = \frac{3 - 2\sqrt{2} \sin 2\theta^\nu + \cos 2\theta^\nu}{12 \cos^2 \theta_{13}}, \quad (3.17)$$

$$\sin^2 \theta_{12} = \frac{|(U_{\text{PMNS}})_{e2}|^2}{1 - |(U_{\text{PMNS}})_{e3}|^2} = \frac{1 + \sin \delta^e \sin 2\theta^e}{4 \cos^2 \theta_{13}}. \quad (3.18)$$

Moreover, from  $|(U_{\text{PMNS}})_{\mu 2}| = 1/\sqrt{2}$  we obtain a sum rule for  $\cos \delta$ :

$$\cos \delta = \frac{2 \cos^2 \theta_{12} \cos^2 \theta_{23} + 2 \sin^2 \theta_{12} \sin^2 \theta_{23} \sin^2 \theta_{13} - 1}{\sin 2\theta_{12} \sin 2\theta_{23} \sin \theta_{13}}. \quad (3.19)$$

Let us comment now on the following issue. Once one of the elements of the PMNS matrix is fixed to be a constant, we still have four possible configurations, namely, a permutation of two remaining columns, a permutation of two remaining rows and both of them. For instance, in the case considered above, except for  $P_e = P_\nu = P_{213}$ , we can have a fixed  $(U_{\text{PMNS}})_{\mu 2}$  with  $(P_e, P_\nu) = (P_{213}, P_{231})$ ,  $(P_{312}, P_{213})$  and  $(P_{312}, P_{231})$ . These combinations of the permutation matrices will not lead, however, to different mixing patterns by virtue of the following relations:

$$R_{23}(\theta^\nu) P_{231} = R_{23}(\theta^\nu + \pi/2) P_{213} \text{diag}(-1, 1, 1), \quad (3.20)$$

$$P_{312} U_{23}(\theta^e, \delta^e) = \text{diag}\left(e^{i\delta^e}, 1, -e^{-i\delta^e}\right) P_{213} U_{23}(\theta^e + \pi/2, \delta^e). \quad (3.21)$$

Indeed, e.g., in the case of  $(P_e, P_\nu) = (P_{312}, P_{231})$ , defining  $\hat{\theta}^\nu = \theta^\nu + \pi/2$ ,  $\hat{\theta}^e = \theta^e + \pi/2$  and absorbing the matrix  $\text{diag}(-1, 1, 1)$  in the matrix  $Q_\nu$ , we obtain the same PMNS matrix as in the case of  $(P_e, P_\nu) = (P_{213}, P_{213})$ :

$$U_{\text{PMNS}} = P_{213} U_{23}(\hat{\theta}^e, \delta^e) \Omega_e^\dagger \Omega_\nu R_{23}(\hat{\theta}^\nu) P_{213} Q_\nu. \quad (3.22)$$

The phases in the matrix  $\text{diag}(e^{i\delta^e}, 1, -e^{-i\delta^e})$  are unphysical, and we have disregarded them.

We list in table 2 the matrices  $\Omega_e$  and  $\Omega_\nu$  for all seven phenomenologically viable pairs of residual symmetries  $\{G_e, G_\nu\} = \{Z_2^{g_e}, Z_2^{g_\nu} \times H_{\text{CP}}^\nu\}$ . It turns out, however, that four of these seven pairs, namely,  $\{G_e, G_\nu\} = \{Z_2^S, Z_2^{TU} \times H_{\text{CP}}^\nu\}$  with  $H_{\text{CP}}^\nu = \{U, T\}$  and  $\{STS, T^2STU\}$ , and  $\{G_e, G_\nu\} = \{Z_2^{TU}, Z_2^S \times H_{\text{CP}}^\nu\}$  with  $H_{\text{CP}}^\nu = \{U, SU\}$  and  $\{TST^2U, T^2STU\}$ , lead to the same predictions for the mixing parameters. We demonstrate this in appendix C.

$g_e$	$\Omega_e$	$g_\nu$	$H_{\text{CP}}^\nu$	$\Omega_\nu$
$S$	$\frac{1}{\sqrt{6}} \begin{pmatrix} \sqrt{2} & -\sqrt{3} & -1 \\ \sqrt{2} & 0 & 2 \\ \sqrt{2} & \sqrt{3} & -1 \end{pmatrix}$	$TU$	$\{U, T\}$	$\frac{1}{\sqrt{2}} \begin{pmatrix} 0 & 0 & \sqrt{2}i \\ e^{\frac{2\pi i}{3}} & -e^{\frac{i\pi}{6}} & 0 \\ e^{\frac{i\pi}{3}} & e^{-\frac{i\pi}{6}} & 0 \end{pmatrix}$
			$\{STS, T^2STU\}$	$\frac{1}{\sqrt{6}} \begin{pmatrix} 0 & 2i & \sqrt{2} \\ \sqrt{3}e^{\frac{i\pi}{6}} & e^{\frac{i\pi}{6}} & -\sqrt{2}e^{-\frac{i\pi}{3}} \\ \sqrt{3}e^{-\frac{i\pi}{6}} & -e^{-\frac{i\pi}{6}} & -\sqrt{2}e^{\frac{i\pi}{3}} \end{pmatrix}$
$TU$	$\frac{1}{\sqrt{2}} \begin{pmatrix} 0 & 0 & \sqrt{2} \\ e^{\frac{i\pi}{3}} & e^{-\frac{2\pi i}{3}} & 0 \\ 1 & 1 & 0 \end{pmatrix}$	$S$	$\{1, S\}$	$\frac{1}{\sqrt{6}} \begin{pmatrix} \sqrt{2} & -\sqrt{3} & -1 \\ \sqrt{2} & 0 & 2 \\ \sqrt{2} & \sqrt{3} & -1 \end{pmatrix}$
			$\{U, SU\}$	$\frac{i}{\sqrt{6}} \begin{pmatrix} \sqrt{2} & -2 & 0 \\ \sqrt{2} & 1 & -\sqrt{3}i \\ \sqrt{2} & 1 & \sqrt{3}i \end{pmatrix}$
			$\{TST^2U, T^2STU\}$	$\frac{1}{\sqrt{3}} \begin{pmatrix} 1 & i & 1 \\ 1 & e^{-\frac{i\pi}{6}} & -e^{-\frac{i\pi}{3}} \\ 1 & -e^{\frac{i\pi}{6}} & -e^{\frac{i\pi}{3}} \end{pmatrix}$
		$U$	$\{1, U\}$	$\frac{1}{\sqrt{2}} \begin{pmatrix} 0 & 0 & \sqrt{2} \\ -1 & 1 & 0 \\ 1 & 1 & 0 \end{pmatrix}$
			$\{S, SU\}$	$-\frac{i}{\sqrt{6}} \begin{pmatrix} 0 & \sqrt{2}i & -2 \\ \sqrt{3} & \sqrt{2}i & 1 \\ -\sqrt{3} & \sqrt{2}i & 1 \end{pmatrix}$

**Table 2.** The matrices  $\Omega_e$  and  $\Omega_\nu$  dictated by the residual symmetries  $G_e = Z_2^{g_e}$  and  $G_\nu = Z_2^{g_\nu} \times H_{\text{CP}}^\nu$  for all seven phenomenologically viable pairs of  $G_e$  and  $G_\nu$ . For each pair  $H_{\text{CP}}^\nu = \{X_{\nu 1}, X_{\nu 2}\}$  of remnant GCP transformations, the given matrix  $\Omega_\nu$  provides the Takagi factorisation of the first element, i.e.,  $X_{\nu 1} = \Omega_\nu \Omega_\nu^T$ .<sup>10</sup>

### 3.3 Extracting mixing parameters and statistical analysis

In this subsection we perform a statistical analysis of the predictions for the neutrino mixing angles and CPV phases for each of the four distinctive sets of the residual flavour and CP

<sup>10</sup>  $X_{\nu 2}$  is instead factorised as  $X_{\nu 2} = \tilde{\Omega}_\nu \tilde{\Omega}_\nu^T$ , with  $\tilde{\Omega}_\nu = \Omega_\nu \text{diag}(1, i, i)$ , as follows from  $X_{\nu 2} = \rho(g_\nu) X_{\nu 1} = \Omega_\nu \Omega_\nu^\dagger \rho(g_\nu) \Omega_\nu \Omega_\nu^T = \Omega_\nu \rho(g_\nu)^d \Omega_\nu^T$ , with  $\rho(g_\nu)^d$  defined in eq. (2.15).

symmetries, which are  $\{G_e, G_\nu\} = \{Z_2^{TU}, Z_2^S \times H_{\text{CP}}^\nu\}$  with  $H_{\text{CP}}^\nu = \{1, S\}$  and  $\{U, SU\}$ , and  $\{G_e, G_\nu\} = \{Z_2^{TU}, Z_2^U \times H_{\text{CP}}^\nu\}$  with  $H_{\text{CP}}^\nu = \{1, U\}$  and  $\{S, SU\}$ . This allows us to derive predictions for the three neutrino mixing angles and the three leptonic CPV phases, which, in many of the cases analysed in the present study is impossible to obtain purely analytically.

Once a pair of residual symmetries and the permutation matrices  $P_e$  and  $P_\nu$  are specified, we have the expressions for  $\sin^2 \theta_{ij}$  in terms of  $\theta^\nu$ ,  $\theta^e$  and  $\delta^e$  of the type of eqs. (3.16)–(3.18). Moreover, employing a sum rule for  $\cos \delta$  analogous to that in eq. (3.19) and computing the rephasing invariant

$$J_{\text{CP}} = \text{Im} \{ (U_{\text{PMNS}})_{e1}^* (U_{\text{PMNS}})_{\mu 3}^* (U_{\text{PMNS}})_{e3} (U_{\text{PMNS}})_{\mu 1} \}, \quad (3.23)$$

which determines the magnitude of CPV effects in neutrino oscillations [37] and which in the standard parametrisation of the PMNS matrix is proportional to  $\sin \delta$ ,

$$J_{\text{CP}} = \frac{1}{8} \sin 2\theta_{12} \sin 2\theta_{23} \sin 2\theta_{13} \cos \theta_{13} \sin \delta, \quad (3.24)$$

we know the value of  $\delta$  for any  $\theta^\nu$ ,  $\theta^e$  and  $\delta^e$ . Similarly, making use of the two charged lepton rephasing invariants,<sup>11</sup> associated with the Majorana phases [38–41],

$$I_1 = \text{Im} \{ (U_{\text{PMNS}})_{e1}^* (U_{\text{PMNS}})_{e2} \} \quad \text{and} \quad I_2 = \text{Im} \{ (U_{\text{PMNS}})_{e1}^* (U_{\text{PMNS}})_{e3} \}, \quad (3.25)$$

and the corresponding real parts

$$R_1 = \text{Re} \{ (U_{\text{PMNS}})_{e1}^* (U_{\text{PMNS}})_{e2} \} \quad \text{and} \quad R_2 = \text{Re} \{ (U_{\text{PMNS}})_{e1}^* (U_{\text{PMNS}})_{e3} \}, \quad (3.26)$$

which in the standard parametrisation of the PMNS matrix read:

$$I_1 = \sin \theta_{12} \cos \theta_{12} \cos^2 \theta_{13} \sin(\alpha_{21}/2), \quad I_2 = \cos \theta_{12} \sin \theta_{13} \cos \theta_{13} \sin(\alpha_{31}/2 - \delta), \quad (3.27)$$

$$R_1 = \sin \theta_{12} \cos \theta_{12} \cos^2 \theta_{13} \cos(\alpha_{21}/2), \quad R_2 = \cos \theta_{12} \sin \theta_{13} \cos \theta_{13} \cos(\alpha_{31}/2 - \delta), \quad (3.28)$$

we also obtain the values of  $\alpha_{21}$  and  $\alpha_{31}$  for any  $\theta^\nu$ ,  $\theta^e$  and  $\delta^e$ .

Further, we scan randomly over  $\theta^\nu \in [0, \pi)$ ,  $\theta^e \in [0, \pi)$  and  $\delta^e \in [0, 2\pi)$  and calculate the values of  $\sin^2 \theta_{ij}$  and the CPV phases. We require  $\sin^2 \theta_{ij}$  to lie in the corresponding  $3\sigma$  ranges given in table 1. The obtained values of  $\sin^2 \theta_{ij}$  and  $\delta$  can be characterised by a certain value of the  $\chi^2$  function constructed as follows:

$$\chi^2(\vec{x}) = \sum_{i=1}^4 \chi_i^2(x_i), \quad (3.29)$$

where  $\vec{x} = \{x_i\} = (\sin^2 \theta_{12}, \sin^2 \theta_{13}, \sin^2 \theta_{23}, \delta)$  and  $\chi_i^2$  are one-dimensional projections for NO and IO taken from [26].<sup>12</sup> Thus, we have a list of points  $(\sin^2 \theta_{12}, \sin^2 \theta_{13}, \sin^2 \theta_{23}, \delta)$ ,

<sup>11</sup>In their general form, when one keeps explicit the unphysical phases  $\xi_j$  in the Majorana condition  $C \bar{\nu}_j^T = \xi_j \nu_j$ ,  $j = 1, 2, 3$ , the rephasing invariants related to the Majorana phases involve  $\xi_j$  and are invariant under phase transformations of both the charged lepton and neutrino fields (see, for example, eqs. (22)–(28) in [38]). We have set  $\xi_j = 1$ .

<sup>12</sup>We note that according to the latest global oscillation data, there is an overall preference for NO over IO of  $\Delta\chi_{\text{IO-NO}}^2 \approx 3.6$ . Nevertheless, we take a conservative approach and treat both orderings on an equal footing. A discussion on this issue can be found in [26].



$\alpha_{21}, \alpha_{31}, \chi^2$ ). To see the restrictions on the mixing parameters imposed by flavour and CP symmetries we consider all 15 different pairs  $(a, b)$  of the mixing parameters. For each pair we divide the plane  $(a, b)$  into bins and find a minimum of the  $\chi^2$  function in each bin. We present results in terms of heat maps with colour representing a minimal value of  $\chi^2$  in each bin. The results obtained in each case are discussed in the following subsection.

### 3.4 Results and discussion

In this subsection we systematically go through all different potentially viable cases and summarise their particular features. All these cases can be divided in four groups corresponding to a particular pair of residual symmetries  $\{G_e, G_\nu\}$ .

In each case we concentrate on results for the ordering for which a better compatibility with the global data is attained. Note that results for NO and IO differ only i) due to the fact that the  $3\sigma$  ranges of  $\sin^2 \theta_{13}$  and  $\sin^2 \theta_{23}$  depend slightly on the ordering and ii) in the respective  $\chi^2$  landscapes. Moreover, we present numerical results for the Majorana phases obtained for  $k_1 = k_2 = 0$ , where  $k_1$  and  $k_2$  are defined in eq. (2.23). However, one should keep in mind that all four  $(k_1, k_2)$  pairs, where  $k_i = 0, 1$ , are allowed. Whenever  $k_{1(2)} = 1$ , the predicted range for  $\alpha_{21(31)}$  shifts by  $\pi$ . The values of the  $k_i$  are important for the predictions of the neutrinoless double beta decay effective Majorana mass (see, e.g., [38, 42–44]), which we obtain in section 4.

**Group A:**  $\{G_e, G_\nu\} = \{Z_2^{TU}, Z_2^S \times H_{\text{CP}}^\nu\}$  with  $H_{\text{CP}}^\nu = \{\mathbf{1}, \mathbf{S}\}$ . Using the corresponding matrices  $\Omega_e$  and  $\Omega_\nu$  from table 2 and the master formula for the PMNS matrix in eq. (2.24), we find the following form of the PMNS matrix (up to permutations of rows and columns and the phases in the matrix  $Q_\nu$ ):

$$U_{\text{PMNS}}^A = \frac{1}{2\sqrt{3}} \begin{pmatrix} \sqrt{6} e^{-\frac{i\pi}{6}} & \sqrt{3} e^{i\theta^\nu} & \sqrt{3} e^{-i\theta^\nu} \\ \sqrt{2} c^e e^{\frac{i\pi}{3}} + 2 s^e e^{-i\delta^e} & a_1(\theta^\nu, \theta^e, \delta^e) & a_2(\theta^\nu, \theta^e, \delta^e) \\ 2 c^e - \sqrt{2} s^e e^{\frac{i\pi}{3}} e^{i\delta^e} & a_3(\theta^\nu, \theta^e, \delta^e) & a_4(\theta^\nu, \theta^e, \delta^e) \end{pmatrix}, \quad (3.30)$$

with  $c^e \equiv \cos \theta^e$ ,  $s^e \equiv \sin \theta^e$ ,  $c^\nu \equiv \cos \theta^\nu$ ,  $s^\nu \equiv \sin \theta^\nu$  and

$$a_1(\theta^\nu, \theta^e, \delta^e) = \left[ \sqrt{3} c^\nu + (2 - i\sqrt{3}) s^\nu \right] c^e + \sqrt{2} (s^\nu - \sqrt{3} c^\nu) s^e e^{-i\delta^e}, \quad (3.31)$$

$$a_2(\theta^\nu, \theta^e, \delta^e) = \left[ \sqrt{3} s^\nu - (2 - i\sqrt{3}) c^\nu \right] c^e - \sqrt{2} (c^\nu + \sqrt{3} s^\nu) s^e e^{-i\delta^e}, \quad (3.32)$$

$$a_3(\theta^\nu, \theta^e, \delta^e) = \sqrt{2} (s^\nu - \sqrt{3} c^\nu) c^e - \left[ \sqrt{3} c^\nu + (2 - i\sqrt{3}) s^\nu \right] s^e e^{i\delta^e}, \quad (3.33)$$

$$a_4(\theta^\nu, \theta^e, \delta^e) = -\sqrt{2} (c^\nu + \sqrt{3} s^\nu) c^e - \left[ \sqrt{3} s^\nu - (2 - i\sqrt{3}) c^\nu \right] s^e e^{i\delta^e}. \quad (3.34)$$

From eq. (3.30), we see that the absolute values of the elements of the first row are fixed. Namely, the modulus of the first element is equal to  $1/\sqrt{2}$ , while the moduli of the second and third elements equal  $1/2$ . Taking into account the current knowledge of the mixing parameters, eqs. (3.10) and (3.11), this implies that there are only two potentially viable cases: i) with  $|(U_{\text{PMNS}})_{\mu 1}| = |(U_{\text{PMNS}})_{\mu 2}| = 1/2$  and  $|(U_{\text{PMNS}})_{\mu 3}| = 1/\sqrt{2}$ , and ii) with  $|(U_{\text{PMNS}})_{\tau 1}| = |(U_{\text{PMNS}})_{\tau 2}| = 1/2$  and  $|(U_{\text{PMNS}})_{\tau 3}| = 1/\sqrt{2}$ .

- **Case A1:**  $|(U_{\text{PMNS}})_{\mu 1}| = |(U_{\text{PMNS}})_{\mu 2}| = 1/2$ ,  $|(U_{\text{PMNS}})_{\mu 3}| = 1/\sqrt{2}$  ( $P_e = P_{213}$ ,  $P_\nu = P_{321}$ ). In this case we obtain

$$\sin^2 \theta_{23} = \frac{1}{2(1 - \sin^2 \theta_{13})} \tag{3.35}$$

$$= \frac{1}{2}(1 + \sin^2 \theta_{13}) + \mathcal{O}(\sin^4 \theta_{13}) . \tag{3.36}$$

This means that only a narrow interval  $\sin^2 \theta_{23} \in [0.510, 0.512]$  is allowed using the  $3\sigma$  region for  $\sin^2 \theta_{13}$ . From the equality  $|(U_{\text{PMNS}})_{\mu 1}| = 1/2$ , which we find to hold in this case, it follows that  $\cos \delta$  satisfies the following sum rule:

$$\cos \delta = \frac{1 - 4 \sin^2 \theta_{12} \cos^2 \theta_{23} - 4 \cos^2 \theta_{12} \sin^2 \theta_{23} \sin^2 \theta_{13}}{2 \sin 2\theta_{12} \sin 2\theta_{23} \sin \theta_{13}} , \tag{3.37}$$

where the mixing angles in addition are correlated among themselves. We find that  $\sin^2 \theta_{13}$  is constrained to lie in the interval  $(0.0213, 0.0240(2)]$  for NO (IO) and, hence,  $\sin^2 \theta_{23}$  in  $[0.5109, 0.5123(4)]$ . This range of values of  $\sin^2 \theta_{23}$  is not compatible with its current  $2\sigma$  range. Moreover,  $\sin^2 \theta_{12}$  is found to be between approximately 0.345 and 0.354, which is outside its current  $2\sigma$  range as well. What concerns the CPV phases, the predicted values of  $\delta$  are distributed around 0, namely,  $\delta \in [-0.11\pi, 0.11\pi]$ , of  $\alpha_{21}$  around  $\pi$ ,  $\alpha_{21} \in (0.93\pi, 1.07\pi)$ , while the values of  $\alpha_{31}$  fill the whole range, i.e.,  $\alpha_{31} \in [0, 2\pi)$ . These numbers, presented for the NO spectrum, remain practically unchanged for the IO spectrum. However, the global minimum  $\chi_{\text{min}}^2$  of the  $\chi^2$  function, defined in eq. (3.29), yields approximately 22 (19) for NO (IO), which implies that this case is disfavoured by the global data at more than  $4\sigma$ .

- **Case A2:**  $|(U_{\text{PMNS}})_{\tau 1}| = |(U_{\text{PMNS}})_{\tau 2}| = 1/2$ ,  $|(U_{\text{PMNS}})_{\tau 3}| = 1/\sqrt{2}$  ( $P_e = P_\nu = P_{321}$ ). This case shares the predicted ranges for  $\sin^2 \theta_{12}$ ,  $\sin^2 \theta_{13}$ ,  $\alpha_{21}$  and  $\alpha_{31}$  with case A1, but differs in the predictions for  $\sin^2 \theta_{23}$  and  $\delta$ . Again, there is a correlation between  $\sin^2 \theta_{13}$  and  $\sin^2 \theta_{23}$ :

$$\sin^2 \theta_{23} = \frac{1 - 2 \sin^2 \theta_{13}}{2(1 - \sin^2 \theta_{13})} \tag{3.38}$$

$$= \frac{1}{2}(1 - \sin^2 \theta_{13}) + \mathcal{O}(\sin^4 \theta_{13}) , \tag{3.39}$$

which, in particular, implies that  $\sin^2 \theta_{23} \in [0.4877(6), 0.4891]$ , which is not compatible with its present  $2\sigma$  range. We also find that  $|(U_{\text{PMNS}})_{\tau 1}| = 1/2$ . This equality leads to the following sum rule:

$$\cos \delta = \frac{4 \sin^2 \theta_{12} \sin^2 \theta_{23} + 4 \cos^2 \theta_{12} \cos^2 \theta_{23} \sin^2 \theta_{13} - 1}{2 \sin 2\theta_{12} \sin 2\theta_{23} \sin \theta_{13}} . \tag{3.40}$$

It is worth noting that we should always keep in mind the correlations between the mixing angles in expressions of this type. The values of  $\delta$  in this case lie around  $\pi$ , in the interval  $[0.89\pi, 1.11\pi]$ . As in the previous case, the global minimum of  $\chi^2$  is somewhat large,  $\chi_{\text{min}}^2 \approx 18.5$  (15) for NO (IO), meaning that this case is also disfavoured.

**Group B:**  $\{G_e, G_\nu\} = \{Z_2^{TU}, Z_2^S \times H_{\text{CP}}^\nu\}$  with  $H_{\text{CP}}^\nu = \{U, SU\}$ . For this choice of the residual symmetries, the PMNS matrix reads (up to permutations of rows and columns and the phases in the matrix  $Q_\nu$ ):

$$U_{\text{PMNS}}^{\text{B}} = \frac{1}{2\sqrt{3}} \begin{pmatrix} \sqrt{6} e^{\frac{i\pi}{3}} & \sqrt{3}(c^\nu + s^\nu) e^{\frac{i\pi}{3}} & \sqrt{3}(s^\nu - c^\nu) e^{\frac{i\pi}{3}} \\ -\sqrt{2} c^e e^{-\frac{i\pi}{6}} + 2i s^e e^{-i\delta^e} & b_1(\theta^\nu, \theta^e, \delta^e) & b_2(\theta^\nu, \theta^e, \delta^e) \\ 2i c^e + \sqrt{2} s^e e^{-\frac{i\pi}{6}} e^{i\delta^e} & b_3(\theta^\nu, \theta^e, \delta^e) & b_4(\theta^\nu, \theta^e, \delta^e) \end{pmatrix}, \quad (3.41)$$

with

$$b_1(\theta^\nu, \theta^e, \delta^e) = (3s^\nu - c^\nu) c^e e^{-\frac{i\pi}{6}} - 2\sqrt{2} i c^\nu s^e e^{-i\delta^e}, \quad (3.42)$$

$$b_2(\theta^\nu, \theta^e, \delta^e) = -(3c^\nu + s^\nu) c^e e^{-\frac{i\pi}{6}} - 2\sqrt{2} i s^\nu s^e e^{-i\delta^e}, \quad (3.43)$$

$$b_3(\theta^\nu, \theta^e, \delta^e) = -2\sqrt{2} i c^\nu c^e - (3s^\nu - c^\nu) s^e e^{-\frac{i\pi}{6}} e^{i\delta^e}, \quad (3.44)$$

$$b_4(\theta^\nu, \theta^e, \delta^e) = -2\sqrt{2} i s^\nu c^e + (3c^\nu + s^\nu) s^e e^{-\frac{i\pi}{6}} e^{i\delta^e}. \quad (3.45)$$

Equation (3.41) implies that the absolute value of one element of the PMNS matrix is predicted to be  $1/\sqrt{2}$ . Thus, we have four potentially viable cases.

- **Case B1:**  $|(U_{\text{PMNS}})_{\mu 2}| = 1/\sqrt{2}$  ( $P_e = P_\nu = P_{213}$ ). Note that from eqs. (3.10) and (3.11) it follows that this magnitude of the fixed element is inside its  $3\sigma$  range for NO, but slightly outside the corresponding range for IO. Hence, we will focus on the results for NO. The characteristic feature of this case is the following sum rule for  $\cos \delta$ :

$$\cos \delta = \frac{2 \cos^2 \theta_{12} \cos^2 \theta_{23} + 2 \sin^2 \theta_{12} \sin^2 \theta_{23} \sin^2 \theta_{13} - 1}{\sin 2\theta_{12} \sin 2\theta_{23} \sin \theta_{13}}, \quad (3.46)$$

which arises from the equality of  $|(U_{\text{PMNS}})_{\mu 2}|$  to  $1/\sqrt{2}$ . The pair correlations between the mixing parameters in this case are summarised in figure 1. The colour palette corresponds to values of  $\chi^2$  for NO. As can be seen, while all values of  $\sin^2 \theta_{13}$  in its  $3\sigma$  range are allowed, the parameters  $\sin^2 \theta_{12}$  and  $\sin^2 \theta_{23}$  are found to lie in  $[0.250, 0.308]$  and  $[0.381, 0.425)$  intervals, respectively. The predicted values of  $\delta$  span the range  $[0.68\pi, 1.32\pi]$ . Thus, CPV effects in neutrino oscillations due to the phase  $\delta$  can be suppressed. The Majorana phases instead are distributed in relatively narrow regions around 0, so the magnitude of the neutrinoless double beta decay effective Majorana mass (see section 4 and, e.g., [38, 42–44]) is predicted (for  $k_1 = k_2 = 0$ ) to have a value close to the maximal possible for the NO spectrum. Namely,  $\alpha_{21} \in [-0.16\pi, 0.16\pi]$  and  $\alpha_{31} \in (-0.13\pi, 0.13\pi)$ . In addition,  $\delta$  is strongly correlated with  $\alpha_{21}$  and  $\alpha_{31}$ , which in turn exhibit a strong correlation between themselves. Finally,  $\chi_{\text{min}}^2 \approx 7$  for both NO and IO, i.e., this case is compatible with the global data at less than  $3\sigma$ .<sup>13</sup>

<sup>13</sup>The apparent contradiction between the obtained value of  $\chi_{\text{min}}^2 \approx 7$ , which suggests compatibility also for IO, and the expectation of  $\chi_{\text{min}}^2 \gtrsim 9$ , according to eq. (3.11), arises from the way we construct the  $\chi^2$  function (see eq. (3.29)), which does not explicitly include covariances between the oscillation parameters.

- **Case B2:**  $|(U_{\text{PMNS}})_{\tau 2}| = 1/\sqrt{2}$  ( $P_e = P_{321}$ ,  $P_\nu = P_{213}$ ). Note that this value of  $|(U_{\text{PMNS}})_{\tau 2}|$  is compatible at  $3\sigma$  with the global data in the case of IO spectrum, but not in the case of NO spectrum, as can be seen from eqs. (3.10) and (3.11). Thus, below we present results for the IO spectrum only. As in case B1, the whole  $3\sigma$  range for  $\sin^2 \theta_{13}$  is allowed. The obtained ranges of values of  $\alpha_{21}$  and  $\alpha_{31}$  are the same of the preceding case. The range for  $\sin^2 \theta_{12}$  differs somewhat from that obtained in case B1, and it reads  $\sin^2 \theta_{12} \in [0.250, 0.328]$ .<sup>14</sup> The predictions for  $\sin^2 \theta_{23}$  and  $\delta$  are different. Now the following sum rule, derived from  $|(U_{\text{PMNS}})_{\tau 2}| = 1/\sqrt{2}$ , holds:

$$\cos \delta = \frac{1 - 2 \cos^2 \theta_{12} \sin^2 \theta_{23} - 2 \sin^2 \theta_{12} \cos^2 \theta_{23} \sin^2 \theta_{13}}{\sin 2\theta_{12} \sin 2\theta_{23} \sin \theta_{13}}. \quad (3.47)$$

The values of  $\delta$  are concentrated in  $[-0.38\pi, 0.38\pi]$ . For  $\sin^2 \theta_{23}$  we find the range  $(0.575, 0.636]$ . The correlations between the phases are of the same type as in case B1. We summarise the results in figure 2. Finally,  $\chi_{\text{min}}^2 \approx 6$  in the case of IO and  $\chi_{\text{min}}^2 \approx 12.5$  for NO, which reflects incompatibility of this case at more than  $3\sigma$  for the NO spectrum. This occurs mainly due to the predicted values of  $\sin^2 \theta_{23}$ , which are outside its current  $2\sigma$  range for NO.

- **Case B3:**  $|(U_{\text{PMNS}})_{\mu 3}| = 1/\sqrt{2}$  ( $P_e = P_{213}$ ,  $P_\nu = P_{321}$ ). Since  $|(U_{\text{PMNS}})_{\mu 3}| = 1/\sqrt{2}$ , the angles  $\theta_{13}$  and  $\theta_{23}$  are correlated as in case A1, i.e., according to eq. (3.35). For IO this leads to  $\sin^2 \theta_{23} \in [0.5097, 0.5124]$  due to the fact that the whole  $3\sigma$  range of  $\sin^2 \theta_{13}$  is found to be allowed, as can be seen from figure 3. Note that this range is outside the current  $2\sigma$  range of  $\sin^2 \theta_{23}$ . In addition, we find that the whole  $3\sigma$  range of the values of  $\sin^2 \theta_{12}$  can be reproduced. In contrast to case A1,  $|(U_{\text{PMNS}})_{\mu 1}|$  does not equal  $1/2$ , but depends on  $\theta^\nu$  in the following way:

$$|(U_{\text{PMNS}})_{\mu 1}|^2 = \frac{1 - \sin 2\theta^\nu}{4}. \quad (3.48)$$

From this equation we find

$$\cos \delta = \frac{1 - 4 \sin^2 \theta_{12} \cos^2 \theta_{23} - 4 \cos^2 \theta_{12} \sin^2 \theta_{23} \sin^2 \theta_{13} - \sin 2\theta^\nu}{2 \sin 2\theta_{12} \sin 2\theta_{23} \sin \theta_{13}}, \quad (3.49)$$

i.e.,  $\cos \delta$  depends on  $\theta^\nu$  explicitly (not only via  $\theta_{12}$ ,  $\theta_{23}$  and  $\theta_{13}$ ). With this relation, any value of  $\delta$  between 0 and  $2\pi$  is allowed (see figure 3). The Majorana phases, however, are constrained to lie around 0 in the following intervals:  $\alpha_{21} \in [-0.23\pi, 0.23\pi]$  and  $\alpha_{31} \in (-0.18\pi, 0.18\pi)$ . Moreover, both phases  $\alpha_{21}$  and  $\alpha_{31}$  are correlated in one and the same peculiar way with the phase  $\delta$ . The correlation between  $\alpha_{21}$  and  $\alpha_{31}$  is similar to those in cases B1 and B2 (cf. figures 1 and 2). Due to the predicted values of  $\sin^2 \theta_{23}$ , which belong to the upper octant, IO is preferred over NO, the corresponding  $\chi_{\text{min}}^2$  being approximately 5 and 8.5.

---

<sup>14</sup>This difference is related to the fact that the current  $3\sigma$  range of  $\sin^2 \theta_{23}$  for IO, which reads  $[0.384, 0.636]$ , is not symmetric with respect to 0.5. The asymmetry of 0.02 translates to increase of the allowed range of  $\sin^2 \theta_{12}$  by approximately 0.02. This can be better understood from the top right plots in figures 1 and 2.

- **Case B4:**  $|(U_{\text{PMNS}})_{\tau 3}| = 1/\sqrt{2}$  ( $P_e = P_\nu = P_{321}$ ). The predicted ranges of all the mixing parameters are the same of case B3, except for  $\sin^2 \theta_{23}$ , which respects the relation in eq. (3.38), and thus belongs to  $[0.4876, 0.4903]$  in the case of IO spectrum. As in the previous case, this interval falls outside the  $2\sigma$  range of  $\sin^2 \theta_{23}$ . The results obtained in this case for the IO spectrum are presented in figure 4. Similarly to the preceding case, we find

$$|(U_{\text{PMNS}})_{\tau 1}|^2 = \frac{1 - \sin 2\theta^\nu}{4}, \quad (3.50)$$

which leads to

$$\cos \delta = \frac{\sin 2\theta^\nu + 4 \sin^2 \theta_{12} \sin^2 \theta_{23} + 4 \cos^2 \theta_{12} \cos^2 \theta_{23} \sin^2 \theta_{13} - 1}{2 \sin 2\theta_{12} \sin 2\theta_{23} \sin \theta_{13}}. \quad (3.51)$$

The correlation between the Majorana phases is similar to that in the previous case. Also in this case,  $\chi_{\min}^2 \approx 4.5$  for IO is lower than that of approximately 6.5 for NO, the reason being again the predicted range of  $\sin^2 \theta_{23}$ .

**Group C:**  $\{G_e, G_\nu\} = \{Z_2^{TU}, Z_2^U \times H_{\text{CP}}^\nu\}$  with  $H_{\text{CP}}^\nu = \{\mathbf{1}, \mathbf{U}\}$ . Using the corresponding matrices  $\Omega_e$  and  $\Omega_\nu$  given in table 2 and eq. (2.24), we obtain the following form of the PMNS matrix (up to permutations of rows and columns and the phases in the matrix  $Q_\nu$ ):

$$U_{\text{PMNS}}^{\text{C}} = \frac{1}{2} \begin{pmatrix} e^{i\frac{\pi}{3}} & \sqrt{3} c^\nu e^{-\frac{i\pi}{6}} & \sqrt{3} s^\nu e^{-\frac{i\pi}{6}} \\ \sqrt{3} c^e e^{-\frac{i\pi}{6}} & c^\nu c^e e^{\frac{i\pi}{3}} - 2 s^\nu s^e e^{-i\delta^e} & s^\nu c^e e^{\frac{i\pi}{3}} + 2 c^\nu s^e e^{-i\delta^e} \\ -\sqrt{3} s^e e^{-\frac{i\pi}{6}} e^{i\delta^e} & -2 s^\nu c^e - c^\nu s^e e^{\frac{i\pi}{3}} e^{i\delta^e} & 2 c^\nu c^e - s^\nu s^e e^{\frac{i\pi}{3}} e^{i\delta^e} \end{pmatrix}. \quad (3.52)$$

Thus, this pair of residual symmetries leads the absolute value of the fixed element to be  $1/2$ . Taking into account the current uncertainties in the values of the neutrino mixing parameters, eqs. (3.10) and (3.11), we have to consider five potentially viable cases corresponding to  $(U_{\text{PMNS}})_{e2}$ ,  $(U_{\text{PMNS}})_{\mu 1}$ ,  $(U_{\text{PMNS}})_{\tau 1}$ ,  $(U_{\text{PMNS}})_{\mu 2}$  or  $(U_{\text{PMNS}})_{\tau 2}$  being the fixed element.

- **Case C1:**  $|(U_{\text{PMNS}})_{e2}| = 1/2$  ( $P_e = P_{123}$ ,  $P_\nu = P_{213}$ ). Fixing  $(U_{\text{PMNS}})_{e2}$  leads to the following relation between  $\sin^2 \theta_{13}$  and  $\sin^2 \theta_{12}$ :

$$\sin^2 \theta_{12} = \frac{1}{4(1 - \sin^2 \theta_{13})} \quad (3.53)$$

$$= \frac{1}{4} (1 + \sin^2 \theta_{13}) + \mathcal{O}(\sin^4 \theta_{13}). \quad (3.54)$$

Since this case allows for the whole  $3\sigma$  range of  $\sin^2 \theta_{13}$  (see figure 5), we find  $\sin^2 \theta_{12} \in (0.2548, 0.2562)$ . Note that this narrow interval is outside the current  $2\sigma$  range of  $\sin^2 \theta_{12}$ . At the same time, this case reproduces the whole  $3\sigma$  range of the values of  $\sin^2 \theta_{23}$ . From

$$|(U_{\text{PMNS}})_{\mu 2}|^2 = \frac{3 \cos^2 \theta^e}{4}, \quad (3.55)$$

we obtain

$$\cos \delta = \frac{4 \cos^2 \theta_{12} \cos^2 \theta_{23} + 4 \sin^2 \theta_{12} \sin^2 \theta_{23} \sin^2 \theta_{13} - 3 \cos^2 \theta^e}{2 \sin 2\theta_{12} \sin 2\theta_{23} \sin \theta_{13}}, \quad (3.56)$$

i.e.,  $\cos \delta$  explicitly depends on  $\theta^e$ , and eventually this relation does not constrain  $\delta$ . Instead the Majorana phase  $\alpha_{21}$  is predicted to be exactly  $\pi$  (exactly 0) for  $k_1 = 0$  ( $k_1 = 1$ ). While the second Majorana phase  $\alpha_{31}$  itself remains unconstrained, the difference  $\alpha_{31} - 2\delta = 0$  ( $\pi$ ) for  $k_2 = 0$  ( $k_2 = 1$ ), i.e., we have a strong linear correlation between  $\delta$  and  $\alpha_{31}$  (see figure 5). The reason for these trivial values of  $\alpha_{21}$  and  $\alpha_{31} - 2\delta$  is the following. In the standard parametrisation of the PMNS matrix,  $\alpha_{21}$  and the combination  $(\alpha_{31} - 2\delta)$  may be extracted from the phases of the first row of the PMNS matrix, as can be seen from eqs. (3.25)–(3.28). In case C1, none of the phases of the first row elements of the PMNS matrix depend (mod  $\pi$ ) on the free parameters  $\theta^\nu$ ,  $\theta^e$  and  $\delta^e$ . Namely, the phases of  $(U_{\text{PMNS}})_{e1}$ ,  $(U_{\text{PMNS}})_{e2}$  and  $(U_{\text{PMNS}})_{e3}$  are fixed (mod  $\pi$  and up to a global phase) to be  $-\pi/6$ ,  $\pi/3$  and  $-\pi/6$ , respectively. Notice that only in groups B and C the relative phases of the first row can be predicted (mod  $\pi$ ) to be independent of  $\theta^\nu$ ,  $\theta^e$  and  $\delta^e$ . Furthermore, case C1 stands out since it is, out of these relevant cases, the only one which survives the constraints on the magnitudes of the PMNS matrix elements given in eqs. (3.10) and (3.11). Finally,  $\chi_{\text{min}}^2 \approx 7$  for both mass orderings.

- **Case C2:**  $|(U_{\text{PMNS}})_{\mu 1}| = 1/2$  ( $P_e = P_{213}$ ,  $P_\nu = P_{123}$ ). The correlations between the mixing parameters obtained in this case for NO are summarised in figure 6 (the results for IO are very similar). This case accounts for the whole  $3\sigma$  range of  $\sin^2 \theta_{13}$ , but constrains the values of the two other angles. Namely, we find  $\sin^2 \theta_{12} \in [0.285, 0.354]$  and  $\sin^2 \theta_{23} \in [0.381, 0.524]$ . This case enjoys the sum rule for  $\cos \delta$  given in eq. (3.37), since  $|(U_{\text{PMNS}})_{\mu 1}| = 1/2$  as it was also in case A1. As a consequence, we find  $\delta$  to be constrained:  $\delta \in (-0.38\pi, 0.38\pi)$ . Both Majorana phases are distributed in relatively narrow intervals around  $\pi$ :  $\alpha_{21} \in (0.85\pi, 1.15\pi)$  and  $\alpha_{31} \in [0.91\pi, 1.09\pi]$ . The phase  $\delta$  is correlated with each of the two Majorana phases in a similar way. The latter in turn are correlated linearly between themselves. Overall, NO is slightly preferred over IO in this case. The corresponding values of  $\chi_{\text{min}}^2$  read 4.5 and 5.5, respectively.
- **Case C3:**  $|(U_{\text{PMNS}})_{\tau 1}| = 1/2$  ( $P_e = P_{321}$ ,  $P_\nu = P_{123}$ ). This case shares some of the predictions of case C2. Namely, the whole  $3\sigma$  range of  $\sin^2 \theta_{13}$  is allowed, and the ranges of  $\alpha_{21}$  and  $\alpha_{31}$  are the same as in the preceding case, as can be seen from figure 7, in which we present the results for the IO neutrino mass spectrum. The interval of values of  $\sin^2 \theta_{12}$  differs somewhat from that of case C2 and reads  $\sin^2 \theta_{12} \in [0.279, 0.354]$ . The predictions for  $\sin^2 \theta_{23}$  and  $\delta$ , however, are very different from those of case C2. The allowed values of  $\sin^2 \theta_{23}$  are concentrated mostly in the upper octant,  $\sin^2 \theta_{23} \in [0.475, 0.636]$ . The sum rule for  $\cos \delta$  in eq. (3.40) is valid in this case, since  $|(U_{\text{PMNS}})_{\tau 1}| = 1/2$ , and we find the values of  $\delta$  to be symmetrically distributed around  $\pi$  in the interval  $[0.60\pi, 1.40\pi]$ . The pairwise correlations between the CPV phases are of the same type as in case C2 (taking into account an approximate shift of  $\delta$  by  $\pi$ , as suggested by figures 6 and 7). Due to the predicted range of  $\sin^2 \theta_{23}$ , this case is favoured by the data for IO, for which  $\chi_{\text{min}}^2 \approx 1.5$ , while for NO we find  $\chi_{\text{min}}^2 \approx 8.5$ .

- **Case C4:**  $|(U_{\text{PMNS}})_{\mu 2}| = 1/2$  ( $P_e = P_\nu = P_{213}$ ). From eqs. (3.10) and (3.11) it follows that the value of  $|(U_{\text{PMNS}})_{\mu 2}| = 1/2$  is allowed at  $3\sigma$  only for IO. Thus, below we present results obtained in the IO case. In the case under consideration there are no constraints on the ranges of  $\sin^2 \theta_{12}$  and  $\sin^2 \theta_{13}$ . The atmospheric angle is, in turn, found to lie in the upper octant,  $\sin^2 \theta_{23} \in (0.505, 0.636]$ . As can be seen in figure 8,  $\delta \in [-0.54\pi, 0.54\pi]$ , which is a consequence of the following correlation between  $\cos \delta$  and the mixing angles:

$$\cos \delta = \frac{4 \cos^2 \theta_{12} \cos^2 \theta_{23} + 4 \sin^2 \theta_{12} \sin^2 \theta_{23} \sin^2 \theta_{13} - 1}{2 \sin 2\theta_{12} \sin 2\theta_{23} \sin \theta_{13}}, \quad (3.57)$$

obtained from  $|(U_{\text{PMNS}})_{\mu 2}| = 1/2$ . There is also a peculiar correlation between  $\sin^2 \theta_{23}$  and  $\delta$ . The phases  $\alpha_{21} \in [0.73\pi, 1.27\pi]$  and  $\alpha_{31} \in [-0.18\pi, 0.18\pi]$ . The values of all the three phases are highly correlated among themselves. The predicted values of  $\sin^2 \theta_{23}$  in the upper octant lead to  $\chi_{\min}^2 \approx 8.5$  for NO (see footnote 13), which is bigger than that of  $\chi_{\min}^2 \approx 2$  for IO.

- **Case C5:**  $|(U_{\text{PMNS}})_{\tau 2}| = 1/2$  ( $P_e = P_{321}$ ,  $P_\nu = P_{213}$ ). The last case of this group, analogously to case C4, does not constrain the ranges of  $\sin^2 \theta_{12}$  and  $\sin^2 \theta_{13}$ . Moreover, it leads to almost the same allowed ranges of  $\alpha_{21}$  and  $\alpha_{31}$  as in the previous case,  $\alpha_{21} \in (0.74\pi, 1.26\pi)$  and  $\alpha_{31} \in [-0.16\pi, 0.16\pi]$ . The differences are in predictions for  $\sin^2 \theta_{23}$  and  $\delta$ . Now the atmospheric angle lies in the lower octant, namely, for NO we find  $\sin^2 \theta_{23} \in [0.381, 0.494]$ . The condition  $|(U_{\text{PMNS}})_{\tau 2}| = 1/2$  gives rise to the following sum rule:

$$\cos \delta = \frac{1 - 4 \cos^2 \theta_{12} \sin^2 \theta_{23} - 4 \sin^2 \theta_{12} \cos^2 \theta_{23} \sin^2 \theta_{13}}{2 \sin 2\theta_{12} \sin 2\theta_{23} \sin \theta_{13}}. \quad (3.58)$$

The allowed values of  $\delta$  span the range  $[0.51\pi, 1.49\pi]$ . The correlations between the mixing parameters in this case are summarised in figure 9. Finally, we have  $\chi_{\min}^2 \approx 0.5$  for both NO and IO.

**Group D:**  $\{G_e, G_\nu\} = \{Z_2^{TU}, Z_2^U \times H_{\text{CP}}^\nu\}$  with  $H_{\text{CP}}^\nu = \{S, SU\}$ . For this last group of cases, we find that the PMNS matrix takes the following form (up to permutations of rows and columns and the phases in the matrix  $Q_\nu$ ):

$$U_{\text{PMNS}}^{\text{D}} = \frac{1}{2\sqrt{3}} \begin{pmatrix} -\sqrt{3} e^{-\frac{i\pi}{6}} & \sqrt{3} (\sqrt{2} c^\nu + i s^\nu) e^{-\frac{i\pi}{6}} & \sqrt{3} (\sqrt{2} s^\nu - i c^\nu) e^{-\frac{i\pi}{6}} \\ 3 c^e e^{\frac{i\pi}{3}} & d_1(\theta^\nu, \theta^e, \delta^e) & d_2(\theta^\nu, \theta^e, \delta^e) \\ -3 s^e e^{\frac{i\pi}{3}} e^{i\delta^e} & d_3(\theta^\nu, \theta^e, \delta^e) & d_4(\theta^\nu, \theta^e, \delta^e) \end{pmatrix}, \quad (3.59)$$

where

$$d_1(\theta^\nu, \theta^e, \delta^e) = (\sqrt{2} c^\nu + i s^\nu) c^e e^{\frac{i\pi}{3}} + 2 (c^\nu - i\sqrt{2} s^\nu) s^e e^{-i\delta^e}, \quad (3.60)$$

$$d_2(\theta^\nu, \theta^e, \delta^e) = (\sqrt{2} s^\nu - i c^\nu) c^e e^{\frac{i\pi}{3}} + 2 (s^\nu + i\sqrt{2} c^\nu) s^e e^{-i\delta^e}, \quad (3.61)$$

$$d_3(\theta^\nu, \theta^e, \delta^e) = 2 (c^\nu - i\sqrt{2} s^\nu) c^e - (\sqrt{2} c^\nu + i s^\nu) s^e e^{\frac{i\pi}{3}} e^{i\delta^e}, \quad (3.62)$$

$$d_4(\theta^\nu, \theta^e, \delta^e) = 2 (s^\nu + i\sqrt{2} c^\nu) c^e - (\sqrt{2} s^\nu - i c^\nu) s^e e^{\frac{i\pi}{3}} e^{i\delta^e}. \quad (3.63)$$

Therefore, the absolute value of the fixed element of the neutrino mixing matrix yields  $1/2$ . Thus, we have again five potentially viable cases.

- **Case D1:**  $|(U_{\text{PMNS}})_{e2}| = 1/2$  ( $P_e = P_{123}$ ,  $P_\nu = P_{213}$ ). In this case we find

$$\sin^2 \theta_{13} = \frac{3 - \cos 2\theta^\nu}{8}, \quad (3.64)$$

which implies that  $\sin^2 \theta_{13}$  can have values between  $1/4$  and  $1/2$ . Thus, this case is ruled out.

- **Case D2:**  $|(U_{\text{PMNS}})_{\mu 1}| = 1/2$  ( $P_e = P_{213}$ ,  $P_\nu = P_{123}$ ). This case allows for the whole  $3\sigma$  range of  $\sin^2 \theta_{13}$  and, in the case of NO, for the following ranges of  $\sin^2 \theta_{12}$  and  $\sin^2 \theta_{23}$ :  $\sin^2 \theta_{12} \in [0.284, 0.354]$  and  $\sin^2 \theta_{23} \in [0.381, 0.512]$ . The sum rule for  $\cos \delta$  in eq. (3.37) holds, since  $|(U_{\text{PMNS}})_{\mu 1}| = 1/2$ . We find  $\delta \in [-0.37\pi, 0.37\pi]$ . What concerns the Majorana phases,  $\alpha_{21}$  spans a relatively broad interval  $[0.25\pi, 1.75\pi]$ , while  $\alpha_{31} \in [-0.48\pi, 0.48\pi]$ . There are very particular correlations between  $\alpha_{21(31)}$  and all the other mixing parameters in this case, as can be seen in figure 10, in which we summarise the results for NO. Finally,  $\chi_{\min}^2 \approx 4.5$  for NO, and it is slightly higher,  $\chi_{\min}^2 \approx 5.5$ , for IO.
- **Case D3:**  $|(U_{\text{PMNS}})_{\tau 1}| = 1/2$  ( $P_e = P_{321}$ ,  $P_\nu = P_{123}$ ). As in the previous case, the whole  $3\sigma$  range of  $\sin^2 \theta_{13}$  gets reproduced. The allowed ranges of  $\sin^2 \theta_{12}$ ,  $\alpha_{21}$  and  $\alpha_{31}$  are very similar to those of case D2. Namely, in the case of IO spectrum we have  $\sin^2 \theta_{12} \in [0.279, 0.354]$ ,  $\alpha_{21} \in [0.21\pi, 1.79\pi]$  and  $\alpha_{31} \in (-0.53\pi, 0.53\pi)$ . Instead, the values of  $\sin^2 \theta_{23}$  occupy mostly the upper octant,  $\sin^2 \theta_{23} \in [0.488, 0.636]$ . The sum rule in eq. (3.40), which holds in this case since  $|(U_{\text{PMNS}})_{\tau 1}| = 1/2$ , leads to the values of  $\delta$  distributed around  $\pi$  in a rather broad range of  $(0.59\pi, 1.41\pi)$ . The correlations between the Majorana phases and  $\delta$  are as in the previous case, but again with an approximate shift of  $\delta$  by  $\pi$  (see figure 11). The minimal value  $\chi_{\min}^2 \approx 1.5$  in the IO case, while for the NO spectrum we get approximately 8.5. This difference is due to the allowed values of  $\sin^2 \theta_{23}$ .
- **Case D4:**  $|(U_{\text{PMNS}})_{\mu 2}| = 1/2$  ( $P_e = P_\nu = P_{213}$ ). This case can account only for a part of the  $3\sigma$  range of  $\sin^2 \theta_{13}$ , namely,  $\sin^2 \theta_{13} \in [0.0214, 0.0240(2)]$  for NO (IO) spectrum. The constraints on two other angles are more severe. We find that only a narrow region of the values of  $\sin^2 \theta_{23}$ , which falls outside its present  $2\sigma$  range, is allowed, namely,  $\sin^2 \theta_{23} \in [0.505, 0.512]$ . For the solar mixing angle we have  $\sin^2 \theta_{12} \in [0.345, 0.354]$ , which is also outside the current  $2\sigma$  range of this parameter. The sum rule in eq. (3.57), which is also valid in this case, constrains  $\delta$  to lie in a narrow interval around 0:  $\delta \in [-0.11\pi, 0.11\pi]$ . The Majorana phases instead are distributed in narrow intervals around  $\pi$ . Namely,  $\alpha_{21} \in (0.83\pi, 1.17\pi)$  and  $\alpha_{31} \in [0.92\pi, 1.08\pi]$ . However, the global minimum of  $\chi^2$  is somewhat large in this case for both NO and IO orderings. Namely, we find  $\chi_{\min}^2 \approx 22$  (19) for NO (IO), i.e., this case is disfavoured at more than  $4\sigma$  by the current global data.



- **Case D5:**  $|(U_{\text{PMNS}})_{\tau 2}| = 1/2$  ( $P_e = P_{321}$ ,  $P_\nu = P_{213}$ ). This last case shares the predicted ranges for  $\sin^2 \theta_{12}$ ,  $\sin^2 \theta_{13}$ ,  $\alpha_{21}$  and  $\alpha_{31}$  with case D4. Therefore, this case is also not compatible with the  $2\sigma$  range of the values of  $\sin^2 \theta_{12}$ . For  $\sin^2 \theta_{23}$  instead we find the narrow interval in the lower octant,  $\sin^2 \theta_{23} \in [0.488, 0.495]$ , which lies outside the  $2\sigma$  range of  $\sin^2 \theta_{23}$ . We find  $\cos \delta$  to satisfy the sum rule in eq. (3.58), which in this case gives us the values of  $\delta$  in a narrow interval around  $\pi$ ,  $\delta \in [0.89\pi, 1.11\pi]$ . Thus, all the three CPV phases are concentrated in narrow ranges around  $\pi$ . Finally, we find  $\chi_{\text{min}}^2 \approx 18.5$  (15) for NO (IO), which implies that this case is also disfavoured by the latest global neutrino oscillation data.

The PMNS matrix in case A2 is related with that in case A1 by the permutation matrix  $P_{312}$  as  $U_{\text{PMNS}}^{\text{A2}} = P_{312} U_{\text{PMNS}}^{\text{A1}}$ . Given that  $P_{312} = P_{132} P_{321}$ , one can see that these matrices are related by  $\mu - \tau$  interchange, after an unphysical exchange of the first and third rows of  $U_{\text{PMNS}}^{\text{A1}}$  has been performed (which amounts to a redefinition of the free parameter  $\theta^e$ , as shown in eq. (3.21)). The same also holds for the following pairs of cases: (B1, B2), (B3, B4), (C2, C3), (C4, C5), (D2, D3) and (D4, D5). As can be seen from the discussion above and figures 1–4 and 6–11, cases inside a pair share some qualitative features. Namely, i) the predicted ranges of  $\sin^2 \theta_{12}$ ,  $\sin^2 \theta_{13}$ ,  $\alpha_{21}$  and  $\alpha_{31}$  are approximately the same; ii) the predicted range of  $\sin^2 \theta_{23}$  gets approximately reflected around  $1/2$ , i.e.,  $\sin^2 \theta_{23} \rightarrow 1 - \sin^2 \theta_{23}$ ; iii) the predicted range of the CPV phase  $\delta$  experiences an approximate shift by  $\pi$ , i.e.,  $\delta \rightarrow \delta + \pi$ .

In tables 3 and 4 we summarise the predicted ranges of the mixing parameters obtained in all the phenomenologically viable cases discussed above. The corresponding best fit values together with  $\chi_{\text{min}}^2$  are presented in tables 5 and 6. Finally, in table 7 we show whether the cases compatible with the  $3\sigma$  ranges of the three mixing angles are also compatible with their corresponding  $2\sigma$  ranges.

The results shown in tables 3–6 allow to assess the possibilities to critically test the predictions of the viable cases of the model and to distinguish between them. We recall that the current  $1\sigma$  uncertainties on the measured values of  $\sin^2 \theta_{12}$ ,  $\sin^2 \theta_{13}$  and  $\sin^2 \theta_{23}$  are [26] 5.8%, 4.0% and 9.6%, respectively. These uncertainties are foreseen to be further reduced by the currently active and/or future planned experiments. The Daya Bay collaboration plans to determine  $\sin^2 \theta_{13}$  with  $1\sigma$  uncertainty of 3% [45]. The uncertainties on  $\sin^2 \theta_{12}$  and  $\sin^2 \theta_{23}$  are planned to be reduced significantly. The parameter  $\sin^2 \theta_{12}$  is foreseen to be measured with  $1\sigma$  relative error of 0.7% in the JUNO experiment [46, 47]. In the proposed upgrading of the currently taking data T2K experiment [48, 49], for example,  $\theta_{23}$  is estimated to be determined with a  $1\sigma$  error of  $1.7^\circ$ ,  $0.5^\circ$  and  $0.7^\circ$  if the best fit value of  $\sin^2 \theta_{23} = 0.50$ ,  $0.43$  and  $0.60$ , respectively. This implies that for these three values of  $\sin^2 \theta_{23}$  the absolute  $1\sigma$  error would be 0.0297, 0.0086 and 0.0120. This error on  $\sin^2 \theta_{23}$  will be further reduced in the future planned T2HK [50] and DUNE [51–53] experiments. If  $\delta = 3\pi/2$ , the CP-conserving case of  $\sin \delta = 0$  would be disfavoured for the NO mass spectrum in the same experiment at least at  $3\sigma$  C.L. Higher precision measurements of  $\delta$  are planned to be performed in the T2HK and DUNE experiments.

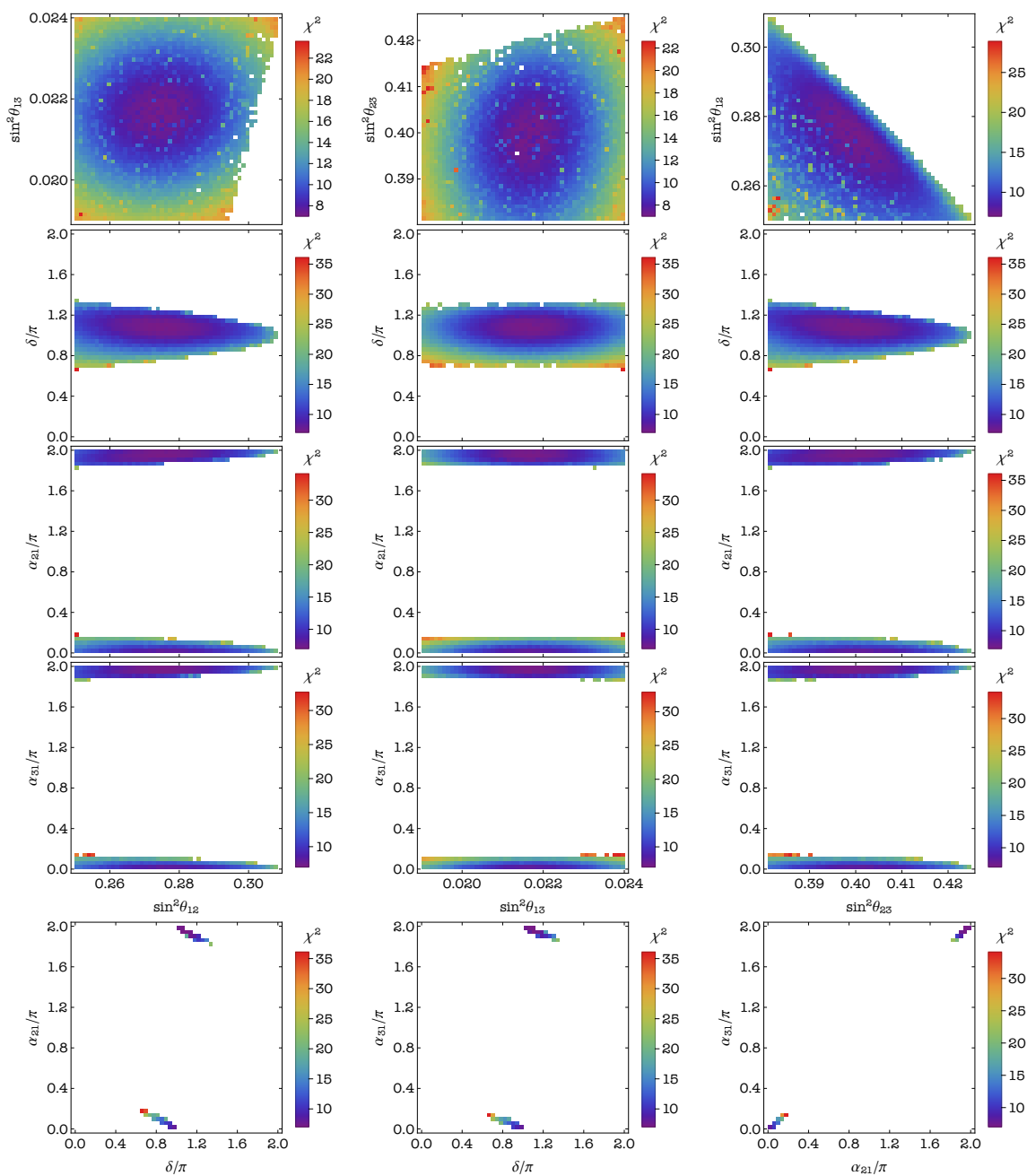


**Figure 1.** Correlations between the neutrino mixing parameters in case B1. The values of all the three mixing angles are required to lie in their respective  $3\sigma$  ranges. Colour represents values of  $\chi^2$  for the NO neutrino mass spectrum.

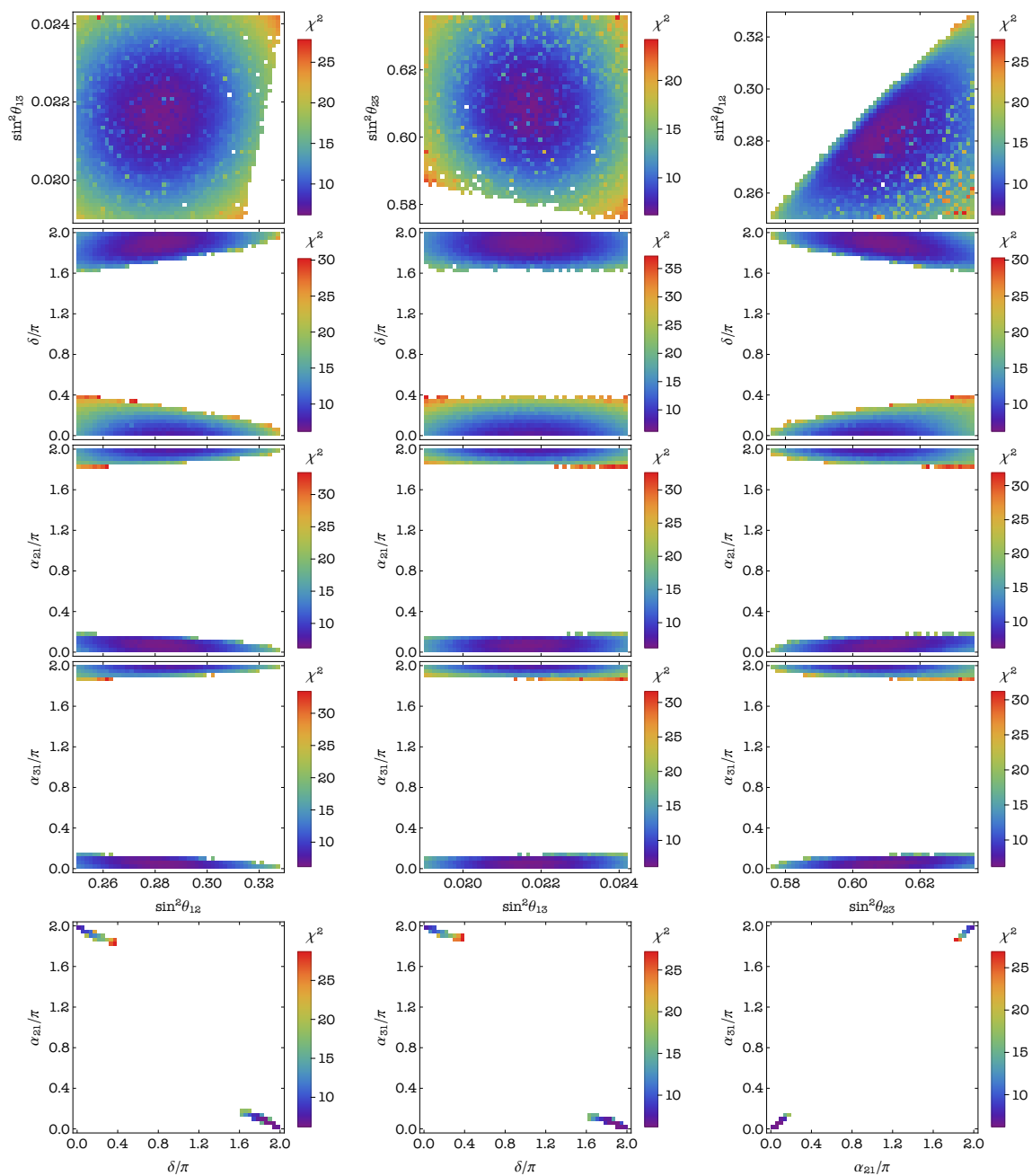


**Figure 2.** Correlations between the neutrino mixing parameters in case B2. The values of all the three mixing angles are required to lie in their respective  $3\sigma$  ranges. Colour represents values of  $\chi^2$  for the IO neutrino mass spectrum.

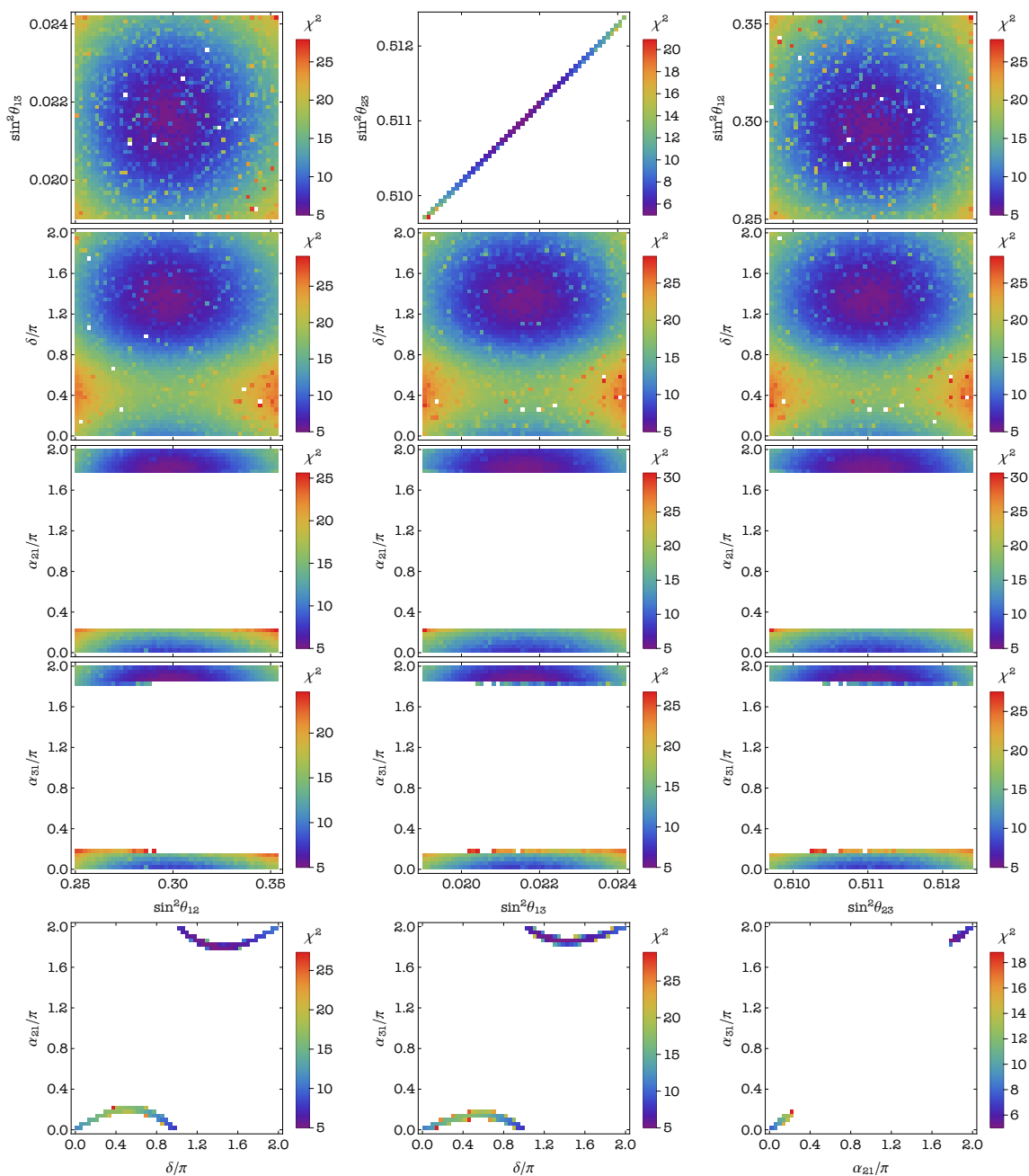


**Figure 3.** Correlations between the neutrino mixing parameters in case B3. The values of all the three mixing angles are required to lie in their respective  $3\sigma$  ranges. Colour represents values of  $\chi^2$  for the IO neutrino mass spectrum. Note that this case is not compatible with the  $2\sigma$  range of  $\sin^2 \theta_{23}$ .

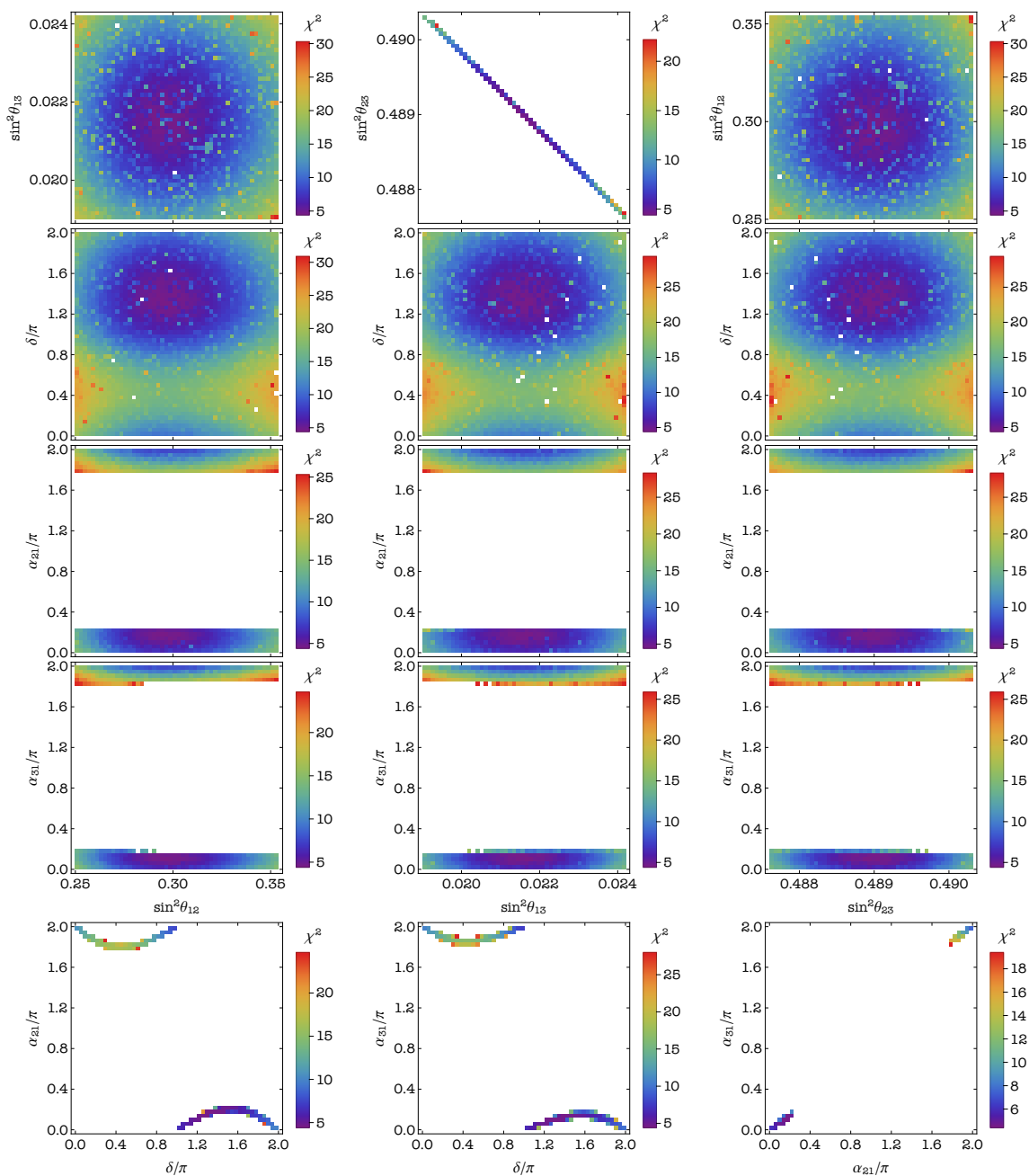


**Figure 4.** Correlations between the neutrino mixing parameters in case B4. The values of all the three mixing angles are required to lie in their respective  $3\sigma$  ranges. Colour represents values of  $\chi^2$  for the IO neutrino mass spectrum. Note that this case is not compatible with the  $2\sigma$  range of  $\sin^2 \theta_{23}$ .

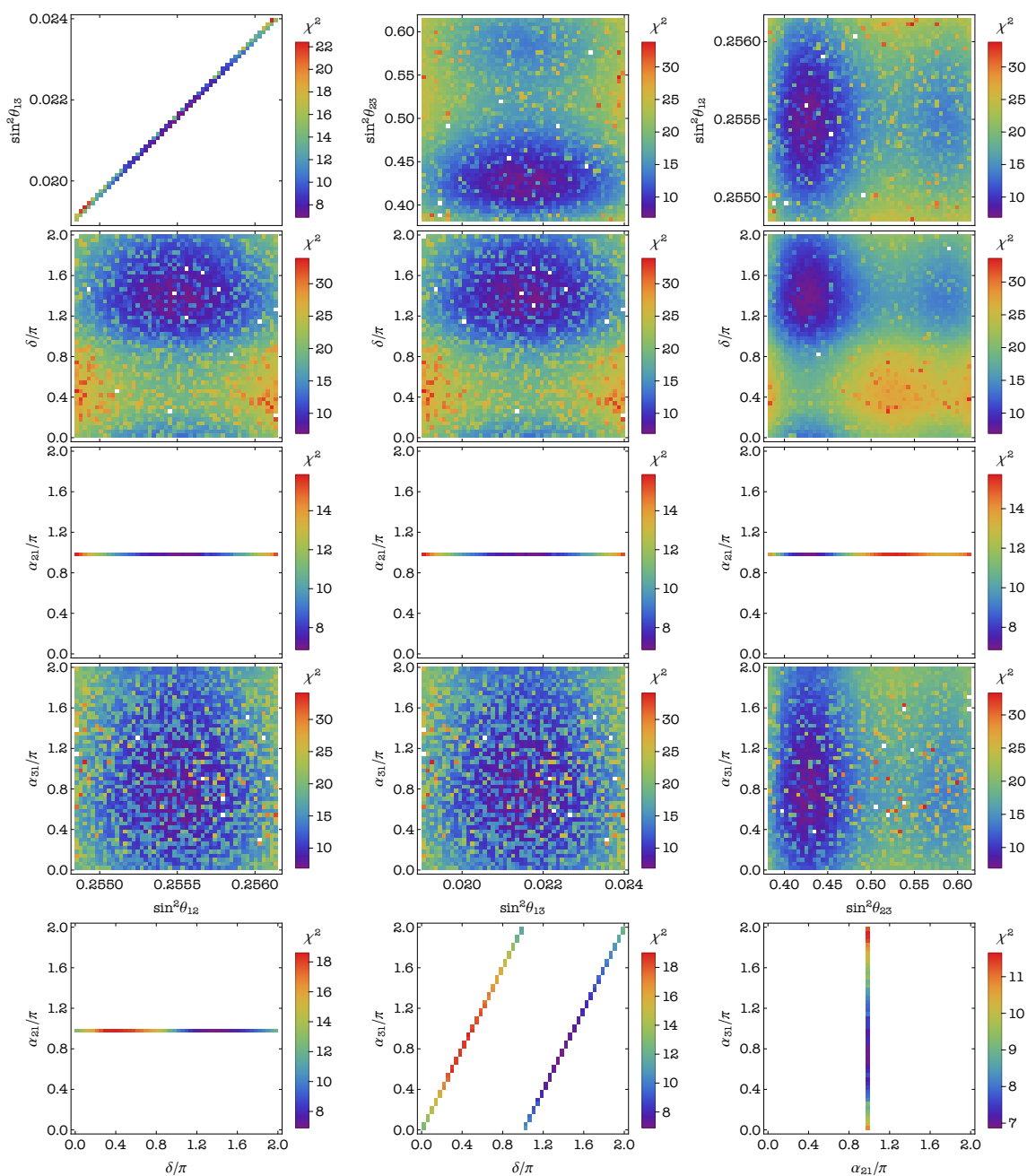


**Figure 5.** Correlations between the neutrino mixing parameters in case C1. The values of all the three mixing angles are required to lie in their respective  $3\sigma$  ranges. Colour represents values of  $\chi^2$  for the NO neutrino mass spectrum. Note that this case is not compatible with the  $2\sigma$  range of  $\sin^2\theta_{12}$ .

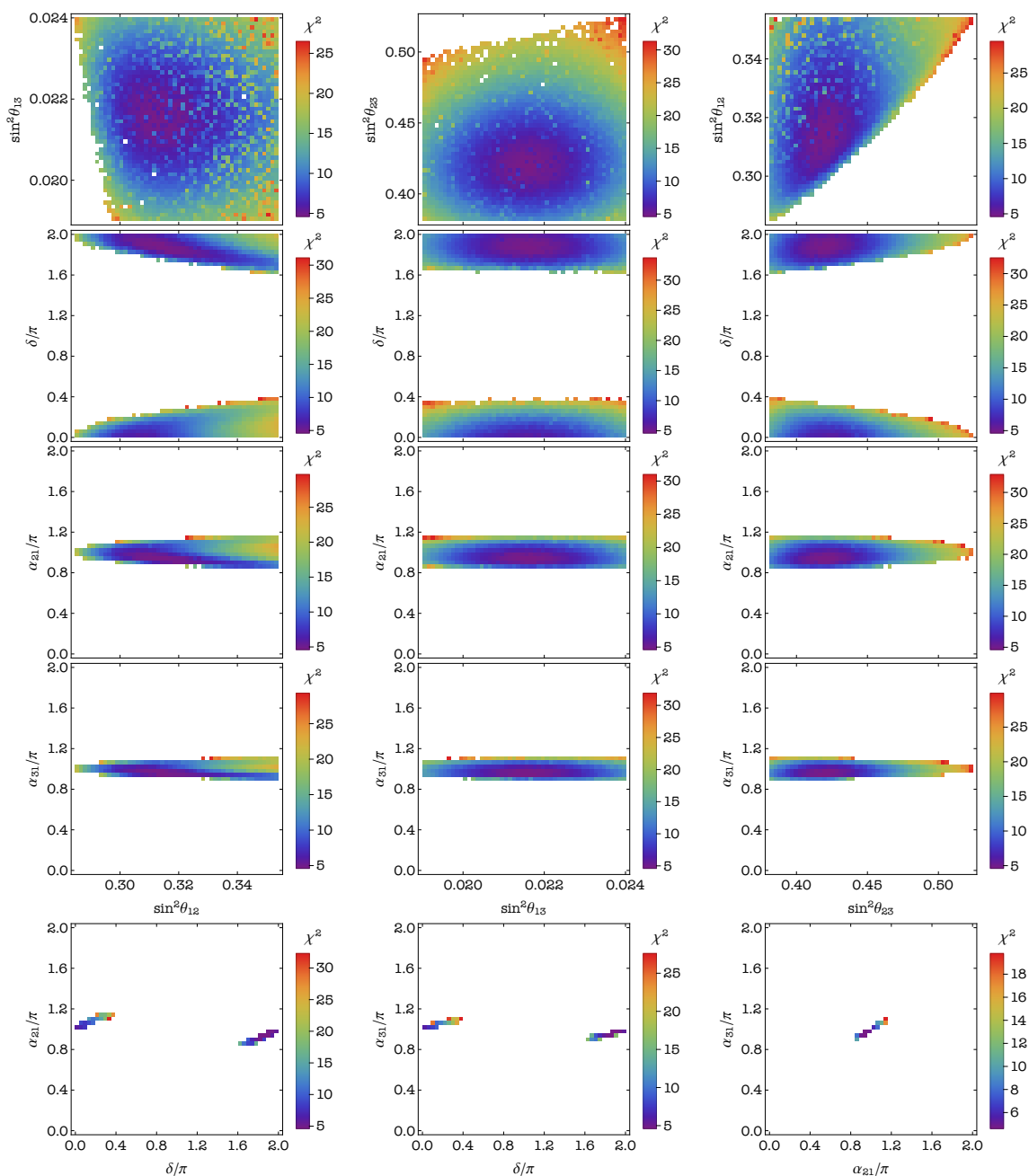


**Figure 6.** Correlations between the neutrino mixing parameters in case C2. The values of all the three mixing angles are required to lie in their respective  $3\sigma$  ranges. Colour represents values of  $\chi^2$  for the NO neutrino mass spectrum.

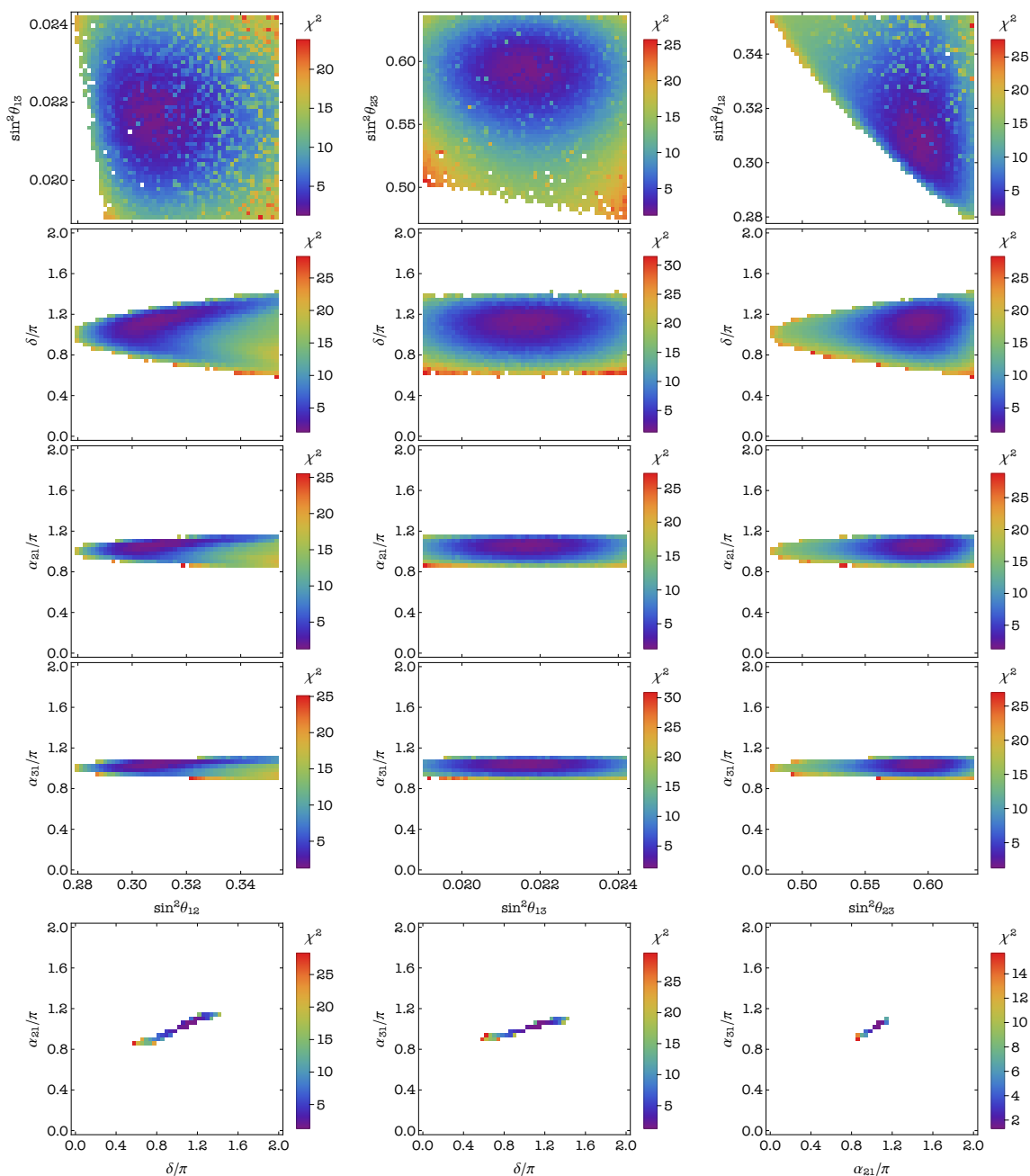


**Figure 7.** Correlations between the neutrino mixing parameters in case C3. The values of all the three mixing angles are required to lie in their respective  $3\sigma$  ranges. Colour represents values of  $\chi^2$  for the IO neutrino mass spectrum.



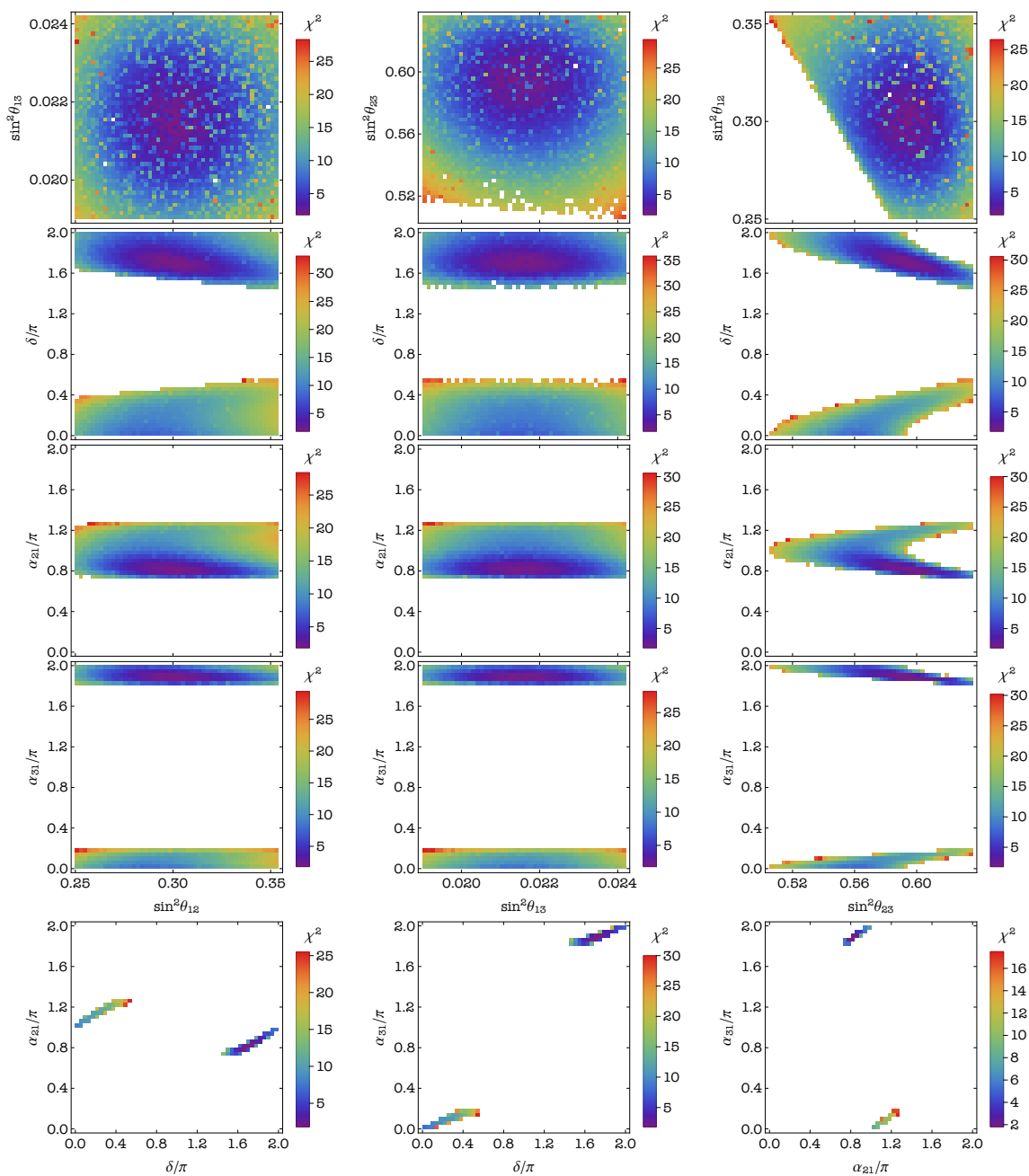


**Figure 8.** Correlations between the neutrino mixing parameters in case C4. The values of all the three mixing angles are required to lie in their respective  $3\sigma$  ranges. Colour represents values of  $\chi^2$  for the IO neutrino mass spectrum.

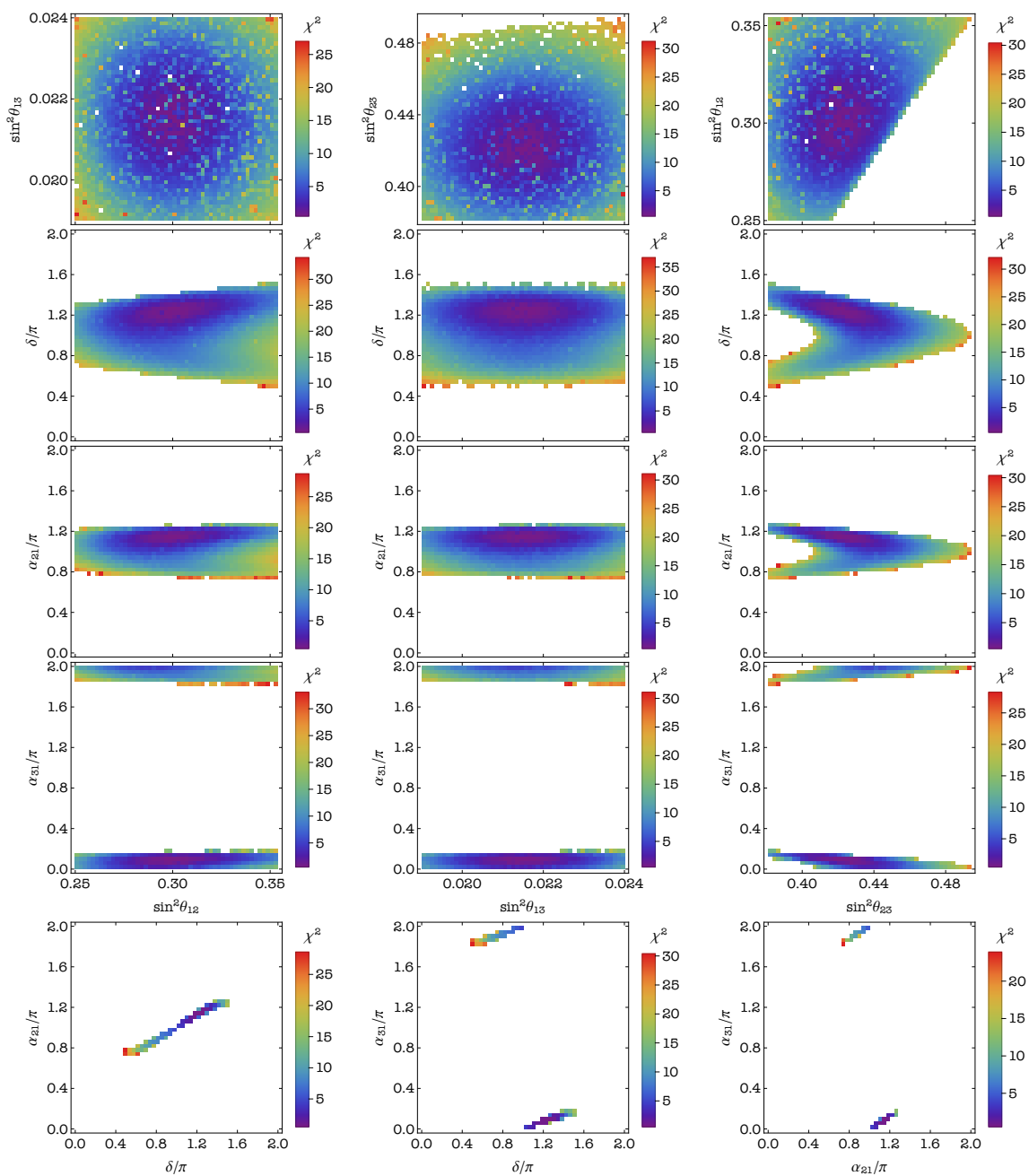


**Figure 9.** Correlations between the neutrino mixing parameters in case C5. The values of all the three mixing angles are required to lie in their respective  $3\sigma$  ranges. Colour represents values of  $\chi^2$  for the NO neutrino mass spectrum.

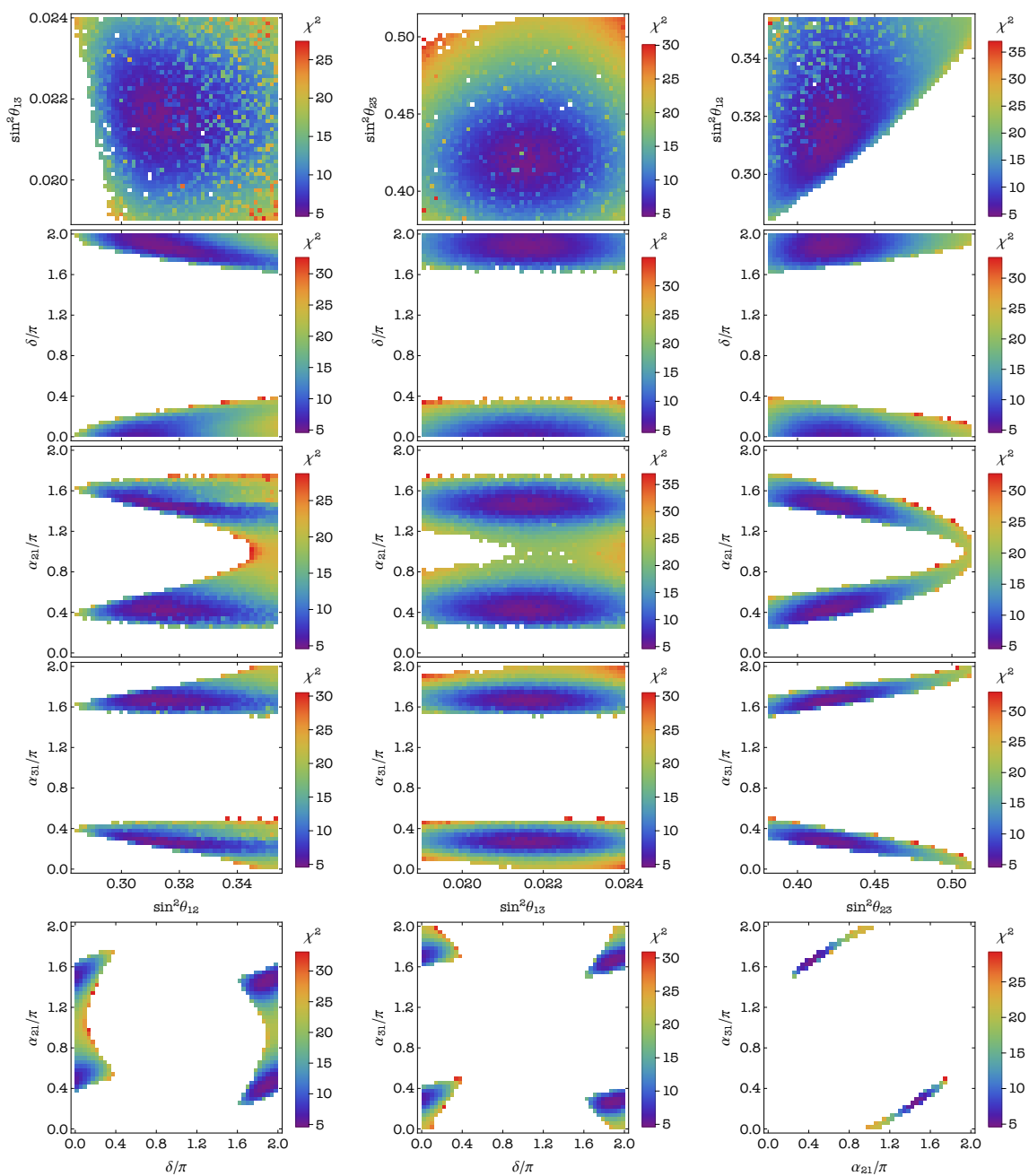


**Figure 10.** Correlations between the neutrino mixing parameters in case D2. The values of all the three mixing angles are required to lie in their respective  $3\sigma$  ranges. Colour represents values of  $\chi^2$  for the NO neutrino mass spectrum.

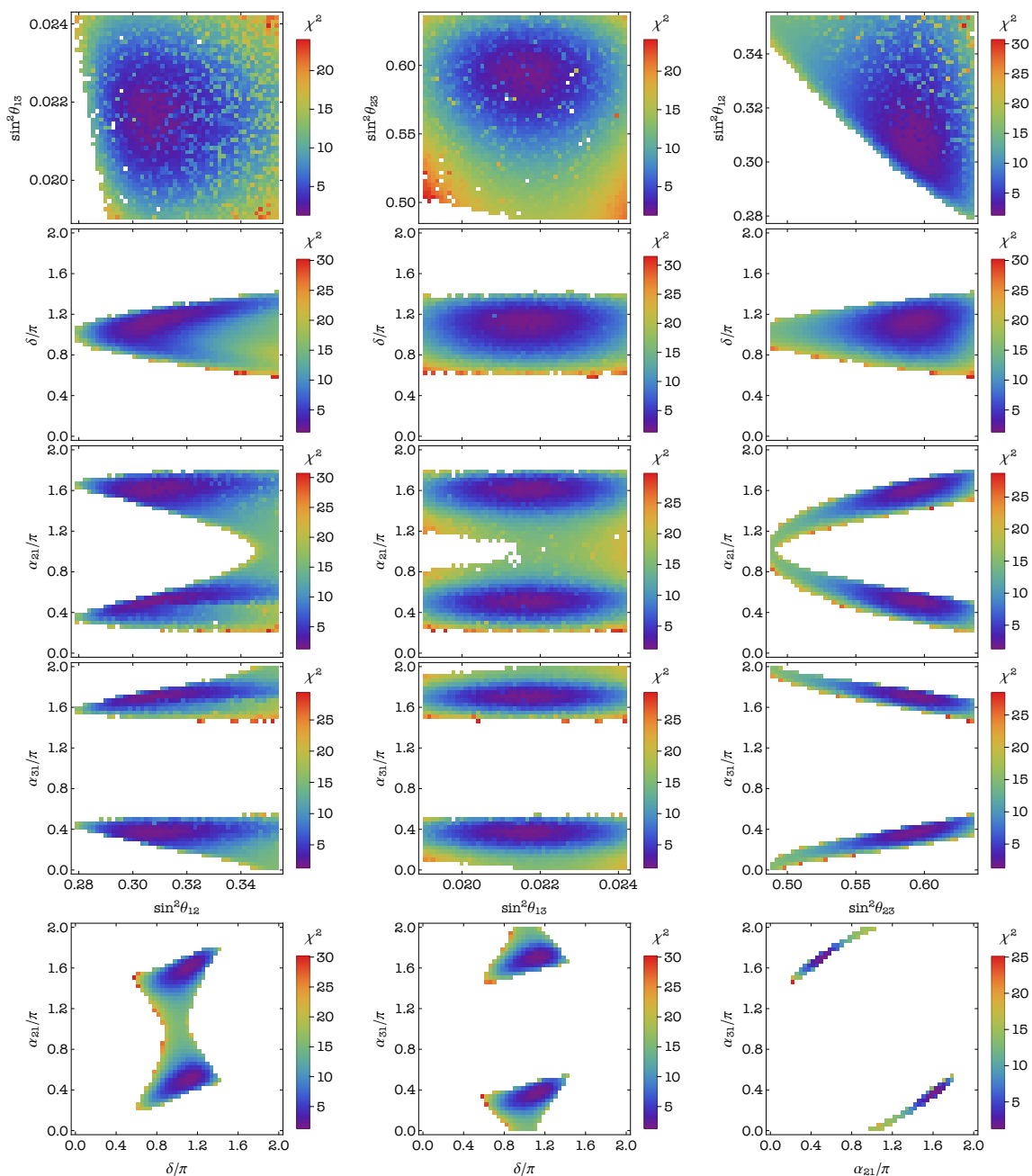


**Figure 11.** Correlations between the neutrino mixing parameters in case D3. The values of all the three mixing angles are required to lie in their respective  $3\sigma$  ranges. Colour represents values of  $\chi^2$  for the IO neutrino mass spectrum.

We turn now to the possibilities to discriminate experimentally between the different cases listed in tables 3–6 using the prospective data on  $\sin^2 \theta_{12}$ ,  $\sin^2 \theta_{13}$ ,  $\sin^2 \theta_{23}$  and  $\delta$ . The first thing to notice is that the predicted ranges for  $\sin^2 \theta_{12}$ ,  $\sin^2 \theta_{13}$ ,  $\sin^2 \theta_{23}$  and  $\delta$  in cases A1 and A2 practically coincide with the predictions respectively in cases D4 and D5. However, cases A1, D4 and cases A2, D5 are strongly disfavoured by the current data: for the NO (IO) neutrino mass spectrum A1 and D4 are disfavoured at  $4.7\sigma$  ( $4.4\sigma$ ), while A2 and D5 are disfavoured at  $4.3\sigma$  ( $3.9\sigma$ ). In all these cases  $\sin^2 \theta_{12}$ , in particular, is predicted to lie in the interval (0.345,0.354) compatible with the current  $3\sigma$  range and, given the current best fit value of  $\sin^2 \theta_{12}$  and prospective JUNO precision on  $\sin^2 \theta_{12}$ , it is very probable that future more precise data on  $\sin^2 \theta_{12}$  will rule out completely these scenarios. We will not discuss them further in this subsection.

It follows also from tables 5 and 6 that the combined results on the best fit values of  $\sin^2 \theta_{12}$ ,  $\sin^2 \theta_{23}$  and  $\delta$  we have obtained in the different viable cases (excluding A1, A2, D4 and D5) differ significantly. Assuming, for example, that the experimentally determined best fit values of  $\sin^2 \theta_{12}$  and  $\sin^2 \theta_{23}$  will coincide with those found by us for a given viable case, it is not difficult to convince oneself inspecting tables 5 and 6 that the cited prospective  $1\sigma$  errors on  $\sin^2 \theta_{12}$  and  $\sin^2 \theta_{23}$  will allow to discriminate between the different viable cases identified in our study. More specifically, considering as an example only the case of NO neutrino mass spectrum, the prospective high precision measurement of  $\sin^2 \theta_{12}$  will allow to discriminate between case C1 and all other cases B1–B4, C2–C5, D2 and D3. The same measurement will make it possible to distinguish i) between case B1 and all the other cases except B2, ii) between case B2 and all the other cases except B1, B3 and B4, and similarly iii) between case B3 and all the other cases except B2, B4, C4 and C5. However, the differences between the best fit values of  $\sin^2 \theta_{23}$  in cases B1, B2 and B3 (or B4) are sufficiently large, which would permit to distinguish between these three cases if  $\sin^2 \theta_{23}$  were measured with the prospective precision. It follows from table 5, however, that it would be very challenging to discriminate between cases B3 and B4: it will require extremely high precision measurement of  $\sin^2 \theta_{23}$ . These two cases would be ruled out, however, if the experimentally determined best fit value of  $\sin^2 \theta_{23}$  differs significantly from the results for  $\sin^2 \theta_{23}$ , namely, 0.511 and 0.489, we have obtained for  $\sin^2 \theta_{23}$  in the B3 and B4 cases.

In the remaining cases C2–C5 and D2–D3, the results we have obtained for  $\sin^2 \theta_{12}$ , as table 6 shows, are very similar. However, the predictions for the pair  $\sin^2 \theta_{23}$  and  $\delta$  differ significantly in cases C2 or D2, and C3 or D3. The cases within each pair would be ruled out if the experimentally determined values of  $\sin^2 \theta_{23}$  and  $\delta$  differ significantly from the predicted best fit values.

Thus, the planned future high precision measurements of  $\sin^2 \theta_{12}$  and  $\sin^2 \theta_{23}$ , together with more precise data on the Dirac phase  $\delta$ , will make it possible to critically test the predictions of the cases listed in tables 3–6. A comprehensive analysis of the possibilities to distinguish between the different viable cases found in our work in the considered  $S_4$  model can only be done when more precise data first of all on  $\sin^2 \theta_{12}$  and  $\sin^2 \theta_{23}$ , and then on  $\delta$ , will be available.

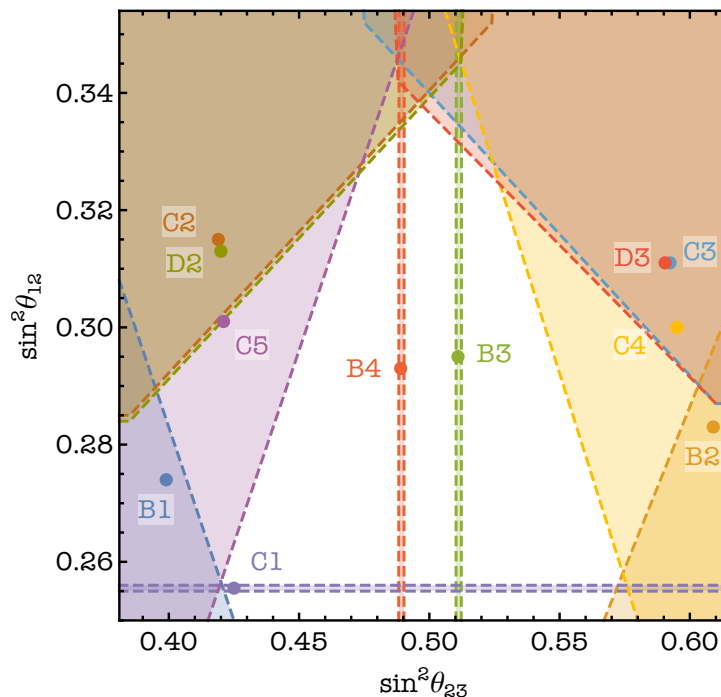


**Figure 12.** Summary of the predicted allowed regions in the  $(\sin^2 \theta_{23}, \sin^2 \theta_{12})$  plane and the corresponding best fit points in cases B1–B4, C1–C5, D2 and D3 for the NO neutrino mass spectrum. The values of all the three mixing angles are required to lie in their respective current  $3\sigma$  ranges.

We schematically summarise in figure 12 the predicted  $3\sigma$  allowed regions in the plane  $(\sin^2 \theta_{23}, \sin^2 \theta_{12})$  for all currently viable cases from figures 1–11. In this figure we also present the best fit point in each case used in the preceding discussion. When future more precise data on  $\sin^2 \theta_{23}$  and  $\sin^2 \theta_{12}$  become available, the experimentally allowed region in the  $(\sin^2 \theta_{23}, \sin^2 \theta_{12})$  plane will shrink, and only a limited number of cases, if any, will remain viable. It will be possible to distinguish further between some or all of the remaining viable cases with a high precision measurement of  $\delta$ .

Finally, we note that the sum rules for  $\sin^2 \theta_{23}$  ( $\sin^2 \theta_{12}$  in case C1) and/or  $\cos \delta$  obtained in the present study follow from those derived in [7] for certain values of the parameters  $\sin^2 \theta_{ij}^o$ , fixed by  $G_f = S_4$  and the residual  $Z_2^{g_e}$  and  $Z_2^{g_\nu}$  flavour symmetries, and the additional constraints provided by the GCP symmetry  $H_{\text{CP}}^\nu$ . Note that in [7] only flavour symmetry, without imposing a GCP symmetry, has been considered. As we have seen in subsection 2.1, a GCP symmetry does not allow for a free phase  $\delta^\nu$  coming from the neutrino sector, which is present otherwise. This, in turn, leads to the fact that in certain cases the parameter  $\sin \hat{\theta}_{ij}^\nu$  (see eq. (213) in [7]), which is free in [7], gets fixed by the GCP symmetry. Thus, we find additional correlations between  $\theta_{ij}$  and between  $\theta_{ij}$  and  $\cos \delta$  in these cases. We provide the correspondence between the phenomenologically viable cases of the present study and the cases considered in [7] in appendix D.

$H_{\text{CP}}^\nu$	Case (p.f.e.)	$\frac{\sin^2 \theta_{12}}{10^{-1}}$	$\frac{\sin^2 \theta_{13}}{10^{-1}}$	$\frac{\sin^2 \theta_{23}}{10^{-1}}$	$\delta/\pi$	$\alpha_{21}/\pi$ (mod 1)	$\alpha_{31}/\pi$ (mod 1)
$\{1, S\}$	A1	3.45–3.54	2.13–2.40	5.11–5.12	$0-0.11 \oplus 1.89-2$	$0-0.07 \oplus 0.93-1$	0–1
	( $\mu 3$ )	3.44–3.54	2.13–2.42	5.11–5.12	$0-0.12 \oplus 1.88-2$	$0-0.07 \oplus 0.93-1$	0–1
	A2	3.45–3.54	2.13–2.40	4.88–4.89	0.89–1.11	$0-0.07 \oplus 0.93-1$	0–1
	( $\tau 3$ )	3.44–3.54	2.13–2.42	4.88–4.89	0.88–1.12	$0-0.07 \oplus 0.93-1$	0–1
$\{U, SU\}$	B1	2.50–3.08	Full $3\sigma$	3.81–4.25	0.68–1.32	$0-0.16 \oplus 0.84-1$	$0-0.13 \oplus 0.88-1$
	( $\mu 2$ )	2.50–3.06	Full $3\sigma$	3.84–4.25	0.69–1.31	$0-0.16 \oplus 0.84-1$	$0-0.12 \oplus 0.88-1$
	B2	2.50–3.03	Full $3\sigma$	5.76–6.15	$0-0.30 \oplus 1.70-2$	$0-0.16 \oplus 0.84-1$	$0-0.12 \oplus 0.88-1$
	( $\tau 2$ )	2.50–3.28	Full $3\sigma$	5.76–6.36	$0-0.38 \oplus 1.61-2$	$0-0.17 \oplus 0.83-1$	$0-0.13 \oplus 0.87-1$
	B3	Full $3\sigma$	Full $3\sigma$	5.10–5.12	0–2	$0-0.23 \oplus 0.77-1$	$0-0.18 \oplus 0.83-1$
	( $\mu 3$ )	Full $3\sigma$	Full $3\sigma$	5.10–5.12	0–2	$0-0.23 \oplus 0.77-1$	$0-0.18 \oplus 0.82-1$
	B4	Full $3\sigma$	Full $3\sigma$	4.88–4.90	0–2	$0-0.23 \oplus 0.77-1$	$0-0.17 \oplus 0.83-1$
	( $\tau 3$ )	Full $3\sigma$	Full $3\sigma$	4.88–4.90	0–2	$0-0.23 \oplus 0.77-1$	$0-0.18 \oplus 0.82-1$

**Table 3.** Ranges of the mixing parameters for the viable cases, i.e., those cases for which the predicted values of all the three mixing angles lie inside their respective  $3\sigma$  allowed ranges. The cases presented here correspond to  $G_e = Z_2^{g_e}$  and  $G_\nu = Z_2^{g_\nu} \times H_{\text{CP}}^\nu$  with  $\{g_e, g_\nu\} = \{TU, S\}$ , for which the magnitude of the fixed element is  $1/\sqrt{2}$  (p.f.e. denotes its position in  $U_{\text{PMNS}}$ ). For each case, the upper and lower rows refer to NO and IO, respectively.

$H_{\text{CP}}^\nu$	Case (p.f.e.)	$\frac{\sin^2 \theta_{12}}{10^{-1}}$	$\frac{\sin^2 \theta_{13}}{10^{-1}}$	$\frac{\sin^2 \theta_{23}}{10^{-1}}$	$\delta/\pi$	$\alpha_{21}/\pi$ (mod 1)	$\alpha_{31}/\pi$ (mod 1)
$\{1, U\}$	C1	2.55–2.56	Full $3\sigma$	Full $3\sigma$	0–2	0 (exactly)	0–1
	( $\epsilon 2$ )	2.55–2.56	Full $3\sigma$	Full $3\sigma$	0–2	0 (exactly)	0–1
	C2	2.85–3.54	Full $3\sigma$	3.81–5.24	$0-0.38 \oplus 1.62-2$	$0-0.15 \oplus 0.85-1$	$0-0.09 \oplus 0.91-1$
	( $\mu 1$ )	2.86–3.54	Full $3\sigma$	3.84–5.25	$0-0.37 \oplus 1.63-2$	$0-0.15 \oplus 0.85-1$	$0-0.09 \oplus 0.91-1$
	C3	2.87–3.54	Full $3\sigma$	4.75–6.15	0.63–1.37	$0-0.15 \oplus 0.86-1$	$0-0.09 \oplus 0.91-1$
	( $\tau 1$ )	2.79–3.54	Full $3\sigma$	4.75–6.36	0.60–1.40	$0-0.15 \oplus 0.85-1$	$0-0.09 \oplus 0.91-1$
	C4	Full $3\sigma$	Full $3\sigma$	5.06–6.15	$0-0.48 \oplus 1.52-2$	$0-0.25 \oplus 0.75-1$	$0-0.16 \oplus 0.84-1$
	( $\mu 2$ )	Full $3\sigma$	Full $3\sigma$	5.05–6.36	$0-0.54 \oplus 1.45-2$	$0-0.27 \oplus 0.73-1$	$0-0.18 \oplus 0.82-1$
$\{S, SU\}$	C5	Full $3\sigma$	Full $3\sigma$	3.81–4.94	0.51–1.49	$0-0.26 \oplus 0.74-1$	$0-0.17 \oplus 0.84-1$
	( $\tau 2$ )	Full $3\sigma$	Full $3\sigma$	3.84–4.94	0.52–1.48	$0-0.25 \oplus 0.74-1$	$0-0.16 \oplus 0.84-1$
	D2	2.84–3.54	Full $3\sigma$	3.81–5.12	$0-0.38 \oplus 1.63-2$	0–1	$0-0.48 \oplus 0.52-1$
	( $\mu 1$ )	2.85–3.54	Full $3\sigma$	3.84–5.12	$0-0.37 \oplus 1.63-2$	0–1	$0-0.48 \oplus 0.52-1$
	D3	2.87–3.54	Full $3\sigma$	4.88–6.15	0.63–1.37	0–1	$0-0.47 \oplus 0.52-1$
	( $\tau 1$ )	2.79–3.54	Full $3\sigma$	4.88–6.36	0.59–1.41	0–1	0–1
	D4	3.45–3.54	2.14–2.40	5.05–5.12	$0-0.11 \oplus 1.89-2$	$0-0.16 \oplus 0.83-1$	$0-0.08 \oplus 0.92-1$
	( $\mu 2$ )	3.45–3.54	2.14–2.42	5.05–5.12	$0-0.11 \oplus 1.89-2$	$0-0.17 \oplus 0.83-1$	$0-0.08 \oplus 0.91-1$
D5	3.45–3.54	2.13–2.40	4.88–4.95	0.89–1.11	$0-0.16 \oplus 0.83-1$	$0-0.08 \oplus 0.92-1$	
( $\tau 2$ )	3.45–3.54	2.13–2.42	4.88–4.95	0.88–1.11	$0-0.17 \oplus 0.83-1$	$0-0.09 \oplus 0.91-1$	

**Table 4.** The same as in table 3, but for  $G_e = Z_2^{g_e}$  and  $G_\nu = Z_2^{g_\nu} \times H_{\text{CP}}^\nu$  with  $\{g_e, g_\nu\} = \{TU, U\}$ . In this case the magnitude of the fixed element is  $1/2$ .

$H_{\text{CP}}^\nu$	Case (p.f.e.)	$\frac{\sin^2 \theta_{12}}{10^{-1}}$	$\frac{\sin^2 \theta_{13}}{10^{-2}}$	$\frac{\sin^2 \theta_{23}}{10^{-1}}$	$\delta/\pi$	$\alpha_{21}/\pi$ (mod 1)	$\alpha_{31}/\pi$ (mod 1)	$\chi_{\text{min}}^2$
$\{1, S\}$	A1	3.54	2.18	5.11	1.96	0.97	0.43	22.0
	( $\mu 3$ )	3.53	2.19	5.11	1.95	0.97	0.89	19.0
	A2	3.54	2.18	4.89	1.05	0.03	0.01	18.5
	( $\tau 3$ )	3.53	2.20	4.89	1.04	0.02	0.67	15.0
$\{U, SU\}$	B1	2.74	2.17	3.99	1.09	0.94	0.96	7.0
	( $\mu 2$ )	2.75	2.18	4.01	1.07	0.96	0.97	7.0
	B2	2.83	2.17	6.09	1.89	0.07	0.05	12.5
	( $\tau 2$ )	2.83	2.17	6.09	1.89	0.07	0.05	6.0
	B3	2.95	2.15	5.11	1.36	0.80	0.85	8.5
	( $\mu 3$ )	2.95	2.15	5.11	1.36	0.80	0.85	5.0
	B4	2.93	2.16	4.89	1.38	0.19	0.13	6.5
	( $\tau 3$ )	2.97	2.16	4.89	1.31	0.16	0.11	4.5

**Table 5.** Best fit values of the mixing parameters and the corresponding value of the  $\chi^2$  function,  $\chi_{\text{min}}^2$ , for the viable cases, i.e., those cases for which the predicted values of all the three mixing angles lie inside their respective  $3\sigma$  allowed ranges. The cases presented here correspond to  $G_e = Z_2^{g_e}$  and  $G_\nu = Z_2^{g_\nu} \times H_{\text{CP}}^\nu$  with  $\{g_e, g_\nu\} = \{TU, S\}$ , for which the magnitude of the fixed element is  $1/\sqrt{2}$  (p.f.e. denotes its position in  $U_{\text{PMNS}}$ ). For each case, the upper and lower rows refer to NO and IO, respectively.

#### 4 Neutrinoless double beta decay

As we have seen, in the class of models investigated in the present article the Dirac and Majorana CPV phases,  $\delta$  and  $\alpha_{21}$ ,  $\alpha_{31}$ , are (statistically) predicted to lie in specific, in most cases relatively narrow, intervals and their values are strongly correlated. The only exception is case C1, in which the exact predictions  $\alpha_{21} = 0$  or  $\pi$  and  $(\alpha_{31} - \delta) = 0$  or  $\pi$  hold.

These results make it possible to derive predictions for the absolute value of the neutrinoless double beta  $((\beta\beta)_{0\nu})$  decay effective Majorana mass,  $\langle m \rangle$  (see, e.g., refs. [1, 42–44]), as a function of the lightest neutrino mass. As is well known, information about  $|\langle m \rangle|$  is provided by the experiments on  $(\beta\beta)_{0\nu}$ -decay of even-even nuclei  $^{48}\text{Ca}$ ,  $^{76}\text{Ge}$ ,  $^{82}\text{Se}$ ,  $^{100}\text{Mo}$ ,  $^{116}\text{Cd}$ ,  $^{130}\text{Te}$ ,  $^{136}\text{Xe}$ ,  $^{150}\text{Nd}$ , etc.,  $(A, Z) \rightarrow (A, Z+2) + e^- + e^-$ , in which the total lepton charge changes by two units, and through the observation of which the possible Majorana nature of massive neutrinos can be revealed. If the light neutrinos with definite mass  $\nu_j$  are Majorana fermions, their exchange between two neutrons of the initial nucleus  $(A, Z)$  can trigger the process of  $(\beta\beta)_{0\nu}$ -decay. In this case the  $(\beta\beta)_{0\nu}$ -decay amplitude has the following general form (see, e.g., refs. [42–44]):  $A((\beta\beta)_{0\nu}) = G_{\text{F}}^2 \langle m \rangle M(A, Z)$ , with  $G_{\text{F}}$ ,  $\langle m \rangle$  and  $M(A, Z)$  being respectively the Fermi constant, the  $(\beta\beta)_{0\nu}$ -decay effective Majorana mass and the nuclear matrix element (NME) of the process. All the dependence of  $A((\beta\beta)_{0\nu})$  on the neutrino mixing parameters is contained in  $\langle m \rangle$ . The current best



$H_{\text{CP}}^\nu$	Case (p.f.e.)	$\frac{\sin^2 \theta_{12}}{10^{-1}}$	$\frac{\sin^2 \theta_{13}}{10^{-2}}$	$\frac{\sin^2 \theta_{23}}{10^{-1}}$	$\delta/\pi$	$\alpha_{21}/\pi$ (mod 1)	$\alpha_{31}/\pi$ (mod 1)	$\chi_{\text{min}}^2$
$\{1, U\}$	C1	2.56	2.16	4.25	1.32	0	0.64	7.0
	(e2)	2.56	2.16	5.85	1.36	0	0.73	7.0
	C2	3.15	2.16	4.19	1.86	0.93	0.96	4.5
	( $\mu$ 1)	3.14	2.16	4.24	1.88	0.94	0.96	5.5
	C3	3.11	2.16	5.92	1.15	0.07	0.05	8.5
	( $\tau$ 1)	3.08	2.17	5.93	1.13	0.06	0.04	1.5
	C4	3.00	2.14	5.95	1.69	0.81	0.88	8.5
	( $\mu$ 2)	3.00	2.14	5.95	1.69	0.81	0.88	2.0
	C5	3.01	2.15	4.21	1.25	0.15	0.10	0.5
	( $\tau$ 2)	2.99	2.17	4.26	1.22	0.13	0.09	0.5
$\{S, SU\}$	D2	3.13	2.15	4.20	1.88	0.43	0.65	4.5
	( $\mu$ 1)	3.15	2.17	4.23	1.87	0.43	0.66	5.5
	D3	3.11	2.17	5.91	1.14	0.61	0.38	8.5
	( $\tau$ 1)	3.06	2.16	5.96	1.12	0.50	0.69	1.5
	D4	3.54	2.18	5.11	1.96	0.97	0.98	22.0
	( $\mu$ 2)	3.53	2.20	5.11	1.95	0.97	0.98	19.0
	D5	3.54	2.19	4.89	1.05	0.03	0.02	18.5
	( $\tau$ 2)	3.53	2.19	4.89	1.04	0.03	0.01	15.0

**Table 6.** The same as in table 5, but for  $G_e = Z_2^{g_e}$  and  $G_\nu = Z_2^{g_\nu} \times H_{\text{CP}}^\nu$  with  $\{g_e, g_\nu\} = \{TU, U\}$ . In this case the magnitude of the fixed element is 1/2.

		A1	A2	B1	B2	B3	B4	C1	C2	C3	C4	C5	D2	D3	D4	D5
$3\sigma$	NO	✓	✓	✓	✓	✓	✓	✓	✓	✓	✓	✓	✓	✓	✓	✓
	IO	✓	✓	✓	✓	✓	✓	✓	✓	✓	✓	✓	✓	✓	✓	✓
$2\sigma$	NO	✗	✗	✓	✗	✗	✗	✗	✓	✗	✗	✓	✓	✗	✗	✗
	IO	✗	✗	✓	✓	✗	✗	✗	✓	✓	✓	✓	✓	✓	✗	✗

**Table 7.** Compatibility of the cases under consideration with the  $3\sigma$  and  $2\sigma$  experimentally allowed ranges of the three neutrino mixing angles for both types of the neutrino mass spectrum.

limits on  $|\langle m \rangle|$  have been obtained by the KamLAND-Zen [54] and GERDA Phase II [55] experiments searching for  $(\beta\beta)_{0\nu}$ -decay of  $^{136}\text{Xe}$  and  $^{76}\text{Ge}$ , respectively:

$$|\langle m \rangle| < (0.061 - 0.165) \text{ eV} [54] \quad \text{and} \quad |\langle m \rangle| < (0.15 - 0.33) \text{ eV} [55], \quad (4.1)$$

both at 90% C.L., where the intervals reflect the estimated uncertainties in the relevant NMEs used to extract the limits on  $|\langle m \rangle|$  from the experimentally obtained lower bounds

on the  $^{136}\text{Xe}$  and  $^{76}\text{Ge}$   $(\beta\beta)_{0\nu}$ -decay half-lives (for a review of the limits on  $|\langle m \rangle|$  obtained in other  $(\beta\beta)_{0\nu}$ -decay experiments and a detailed discussion of the NME calculations for  $(\beta\beta)_{0\nu}$ -decay and their uncertainties see, e.g., [56]). It is important to note that a large number of experiments of a new generation aims at a sensitivity to  $|\langle m \rangle| \sim (0.01 - 0.05)$  eV, which will allow to probe the whole range of the predictions for  $|\langle m \rangle|$  in the case of IO neutrino mass spectrum [57, 58] (see, e.g., [56, 59] for reviews of the currently running and future planned  $(\beta\beta)_{0\nu}$ -decay experiments and their prospective sensitivities).

The predictions for  $|\langle m \rangle|$  (see, e.g., [38, 42–44]),

$$|\langle m \rangle| = \left| \sum_{i=1}^3 m_i U_{ei}^2 \right| = \left| m_1 \cos^2 \theta_{12} \cos^2 \theta_{13} + m_2 \sin^2 \theta_{12} \cos^2 \theta_{13} e^{i\alpha_{21}} + m_3 \sin^2 \theta_{13} e^{i(\alpha_{31} - 2\delta)} \right|, \quad (4.2)$$

$m_{1,2,3}$  being the light Majorana neutrino masses, depend on the values of the Majorana phase  $\alpha_{21}$  and on the Majorana-Dirac phase difference  $(\alpha_{31} - 2\delta)$ . For the normal hierarchical (NH), inverted hierarchical (IH) and quasi-degenerate (QD), neutrino mass spectra  $|\langle m \rangle|$  is given by (see, e.g., [1, 60]):

$$|\langle m \rangle| \cong \left| \sqrt{\Delta m_{21}^2} \sin^2 \theta_{12} \cos^2 \theta_{13} e^{i\alpha_{21}} + \sqrt{\Delta m_{31}^2} \sin^2 \theta_{13} e^{i(\alpha_{31} - 2\delta)} \right| \quad (\text{NH}), \quad (4.3)$$

$$|\langle m \rangle| \cong \sqrt{\Delta m_{23}^2} \cos^2 \theta_{13} \left| \cos^2 \theta_{12} + \sin^2 \theta_{12} e^{i\alpha_{21}} \right| \quad (\text{IH}), \quad (4.4)$$

$$|\langle m \rangle| \cong m_0 \left| \cos^2 \theta_{12} + \sin^2 \theta_{12} e^{i\alpha_{21}} \right| \quad (\text{QD}), \quad (4.5)$$

where  $m_0 \cong m_{1,2,3}$ . We recall that the NH spectrum corresponds to  $m_1 \ll m_2 < m_3$ , and thus,  $m_2 = (m_1^2 + \Delta m_{21}^2)^{\frac{1}{2}} \cong (\Delta m_{21}^2)^{\frac{1}{2}} \cong 8.6 \times 10^{-3}$  eV,  $m_3 = (m_2^2 + \Delta m_{31}^2)^{\frac{1}{2}} \cong (\Delta m_{31}^2)^{\frac{1}{2}} \cong 0.0506$  eV. The IH spectrum corresponds to  $m_3 \ll m_1 < m_2$ , and therefore,  $m_1 = (m_3^2 + \Delta m_{23}^2 - \Delta m_{21}^2)^{\frac{1}{2}} \cong (\Delta m_{23}^2 - \Delta m_{21}^2)^{\frac{1}{2}} \cong 0.0497$  eV,  $m_2 = (m_3^2 + \Delta m_{23}^2)^{\frac{1}{2}} \cong (\Delta m_{23}^2)^{\frac{1}{2}} \cong 0.0504$  eV. In the case of QD spectrum we have:  $m_1 \cong m_2 \cong m_3 \cong m_0$ ,  $m_j^2 \gg \Delta m_{31(23)}^2$ ,  $m_0 \gtrsim 0.10$  eV. In eqs. (4.3) and (4.4) we have assumed that the contributions respectively  $\propto m_1$  and  $\propto m_3$  are negligible, while in eq. (4.5) we have neglected corrections  $\propto \sin^2 \theta_{13}$ ,<sup>15</sup> and  $\propto \Delta m_{31(23)}^2/m_0^2$ . Clearly, the values of the phases  $(\alpha_{31} - \alpha_{21} - 2\delta)$  and  $\alpha_{21}$  determine the ranges of possible values of  $|\langle m \rangle|$  in the cases of NH and IH (QD) spectra, respectively. Using the  $3\sigma$  ranges of the allowed values of the neutrino oscillation parameters from table 1, we find that:

- i)  $0.79 \times 10^{-3}$  eV  $\lesssim |\langle m \rangle| \lesssim 4.33 \times 10^{-3}$  eV in the case of NH spectrum;
- ii)  $\sqrt{\Delta m_{23}^2} \cos^2 \theta_{13} \cos 2\theta_{12} \lesssim |\langle m \rangle| \lesssim \sqrt{\Delta m_{23}^2} \cos^2 \theta_{13}$ , or  $1.4 \times 10^{-2}$  eV  $\lesssim |\langle m \rangle| \lesssim 5.1 \times 10^{-2}$  eV in the case of IH spectrum;
- iii)  $m_0 \cos 2\theta_{12} \lesssim |\langle m \rangle| \lesssim m_0$ , or  $2.9 \times 10^{-2}$  eV  $\lesssim |\langle m \rangle| \lesssim m_0$  eV,  $m_0 \gtrsim 0.10$  eV, in the case of QD spectrum, where we have used the fact that at  $3\sigma$  C.L.,  $\cos 2\theta_{12} \geq 0.29$ .

<sup>15</sup>The term  $\propto \sin^2 \theta_{13}$  gives a subleading contribution because even in the case of  $\alpha_{21} = \pi$ , when the leading term  $\propto (\cos^2 \theta_{12} - \sin^2 \theta_{12})$  has a minimal value,  $\sin^2 \theta_{13} \ll \cos 2\theta_{12}$  since  $\sin^2 \theta_{13} \leq 0.0242$  while  $\cos 2\theta_{12} \geq 0.29$  at  $3\sigma$ .

In what follows, we obtain predictions for  $|\langle m \rangle|$  using the phenomenologically viable neutrino mixing patterns found in subsection 3.4. In figures 13–16 we present  $|\langle m \rangle|$  as a function of the lightest neutrino mass  $m_{\min}$  ( $m_{\min} = m_1$  for the NO spectrum and  $m_{\min} = m_3$  for the IO spectrum) in cases B1–B4, C1–C3, C4 and C5, and D2 and D3. The solid and dashed lines limit the found allowed regions of  $|\langle m \rangle|$  calculated using the predicted ranges for  $\theta_{12}$ ,  $\theta_{13}$ ,  $\alpha_{21}$ ,  $(\alpha_{31} - 2\delta)$ . In the left panels we require the predicted values of  $\sin^2 \theta_{12}$ ,  $\sin^2 \theta_{13}$  and  $\sin^2 \theta_{23}$  to lie in their corresponding experimentally allowed  $3\sigma$  intervals, while in the right panels we require them to be inside the corresponding  $2\sigma$  ranges. The mass squared differences  $\Delta m_{21}^2$  and  $\Delta m_{31(23)}^2$  in the case of NO (IO) spectrum are varied in their appropriate ranges given in table 1. The light-blue (light-red) areas in the left and right panels are obtained varying the neutrino oscillation parameters  $\theta_{12}$ ,  $\theta_{13}$ ,  $\Delta m_{21}^2$  and  $\Delta m_{31(23)}^2$  in their full  $3\sigma$  and  $2\sigma$  NO (IO) ranges, respectively, and varying the phases  $\alpha_{21}$  and  $(\alpha_{31} - 2\delta)$  in the interval  $[0, 2\pi)$ . The horizontal brown and grey bands indicate the current most stringent upper limits on  $|\langle m \rangle|$ , given in eq. (4.1), set by KamLAND-Zen and GERDA Phase II, respectively. The vertical grey line represents the prospective upper limit on  $m_{\min} \lesssim 0.2 \text{ eV}$  from the KATRIN experiment [61].

Several comments are in order. Firstly, for given values of  $(k_1, k_2)$  and a given ordering we find  $|\langle m \rangle|$  to be inside of a band, which occupies a certain part of the allowed parameter space. Secondly, we note that most cases are compatible with both  $3\sigma$  and  $2\sigma$  ranges of all the mixing angles for both neutrino mass orderings (see table 7). There are several exceptions. Namely, cases B2, C3, C4 and D3, in which, due to the correlations imposed by the employed symmetry, the predictions for  $\sin^2 \theta_{23}$  for the NO spectrum are not compatible with its  $2\sigma$  allowed range (see tables 3 and 4). Moreover, there is incompatibility for both orderings of cases B3 and B4 with the allowed  $2\sigma$  ranges of  $\sin^2 \theta_{23}$  (see table 3), and of case C1 with the  $2\sigma$  range of  $\sin^2 \theta_{12}$  (see table 4). Thirdly, the predictions for  $|\langle m \rangle|$  compatible with the  $3\sigma$  ranges of all the mixing angles are almost the same for the following pairs of cases: (B1, B2), (B3, B4), (C2, C3), (C4, C5) and (D2, D3). As discussed at the end of subsection 3.4, the cases in each pair share some qualitative features, in particular, the allowed ranges of  $\theta_{12}$ ,  $\theta_{13}$ ,  $\alpha_{21}$  and  $(\alpha_{31} - 2\delta)$  are approximately equal. We note also that case C1 stands out by having relatively narrow bands for  $|\langle m \rangle|$  due to the predicted values of  $\alpha_{21} = k_1 \pi$  and  $(\alpha_{31} - 2\delta) = k_2 \pi$ . Finally, the results shown in figures 13–16 and derived using the predictions for the CPV phases and the mixing angles  $\theta_{12}$  and  $\theta_{13}$  in the case when the predicted values of all the three mixing angles  $\theta_{12}$ ,  $\theta_{13}$  and  $\theta_{23}$  are compatible with their respective  $3\sigma$  experimentally allowed ranges, can be obtained analytically in the limiting cases of NH, IH and QD spectra using eqs. (4.3)–(4.5), the values of  $\Delta m_{21}^2$  and  $\Delta m_{31(23)}^2$  quoted in table 1 and the results on  $\sin^2 \theta_{12}$ ,  $\sin^2 \theta_{13}$ ,  $\delta$ ,  $\alpha_{21}$  and  $\alpha_{31}$  given in tables 3 and 4.

## 5 Summary and conclusions

In the present article we have derived predictions for the 3-neutrino (lepton) mixing and leptonic Dirac and Majorana CP violation in a class of models based on  $S_4$  lepton flavour symmetry combined with a generalised CP (GCP) symmetry  $H_{\text{CP}}$ , which are broken to

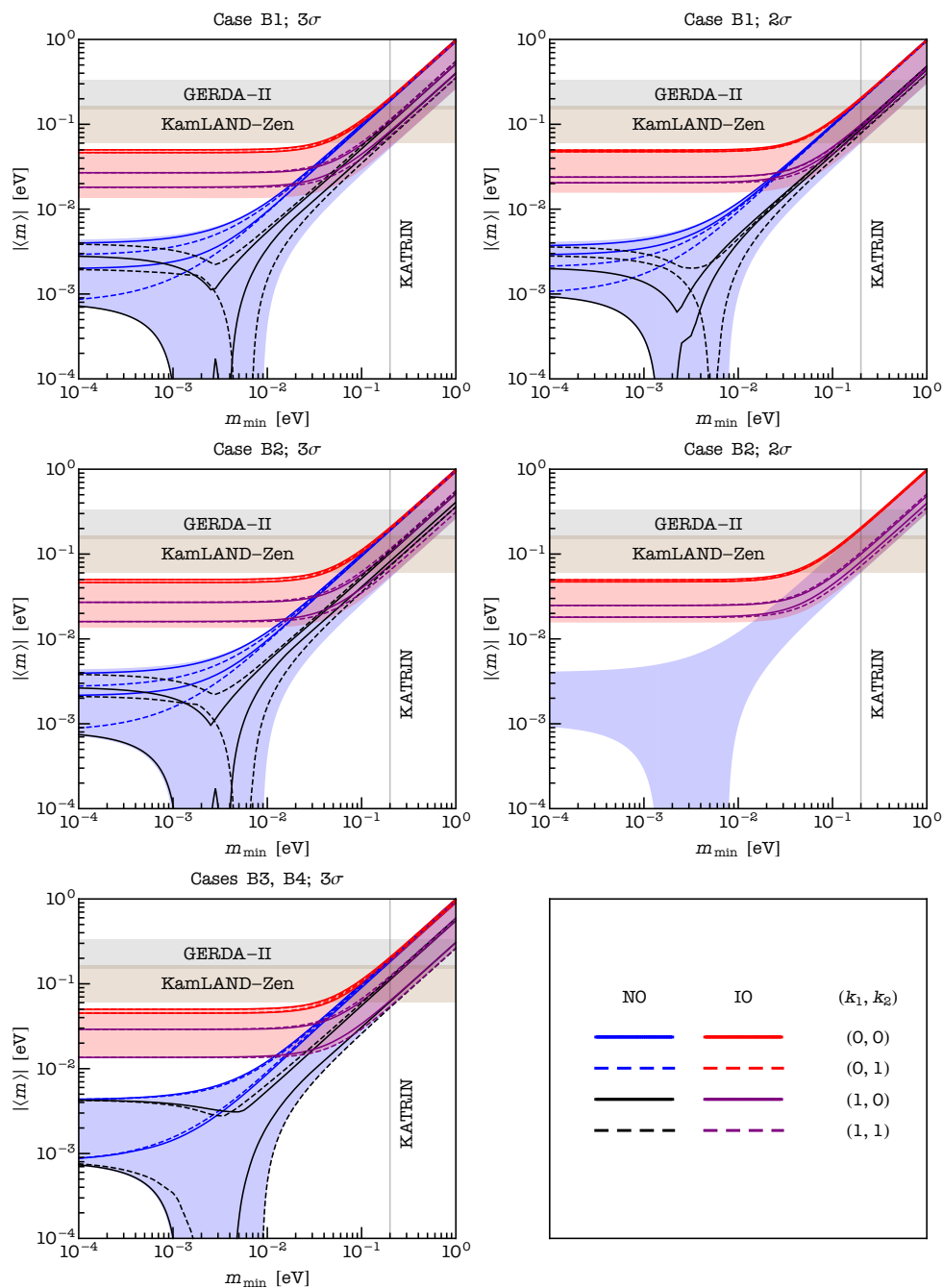


**Figure 13.** The magnitude of the effective Majorana mass  $|\langle m \rangle|$  versus the lightest neutrino mass  $m_{\min}$ . The *lines* limit the allowed regions of  $|\langle m \rangle|$  calculated using the predictions for the relevant mixing angles and the CPV phases obtained in cases B1–B4 and compatible with the  $3\sigma$  (*left panels*) and  $2\sigma$  (*right panels*) ranges of all the three mixing angles. The *light-blue* (*light-red*) areas are obtained varying the neutrino oscillation parameters  $\theta_{12}$ ,  $\theta_{13}$ ,  $\Delta m_{21}^2$  and  $\Delta m_{31(23)}^2$  for NO (IO) in their allowed  $3\sigma$  and  $2\sigma$  ranges in the left and right panels, respectively, and the phases  $\alpha_{21}$  and  $(\alpha_{31} - 2\delta)$  in the interval  $[0, 2\pi)$ . The *horizontal brown* and *grey bands* indicate the current upper bounds on  $|\langle m \rangle|$  quoted in eq. (4.1) set by KamLAND-Zen [54] and GERDA Phase II [55], respectively. The *vertical grey line* represents the prospective upper limit on  $m_{\min} \lesssim 0.2$  eV from KATRIN [61]. Cases B3 and B4 are compatible with the  $3\sigma$  ranges of the mixing angles, but not with their  $2\sigma$  ranges.

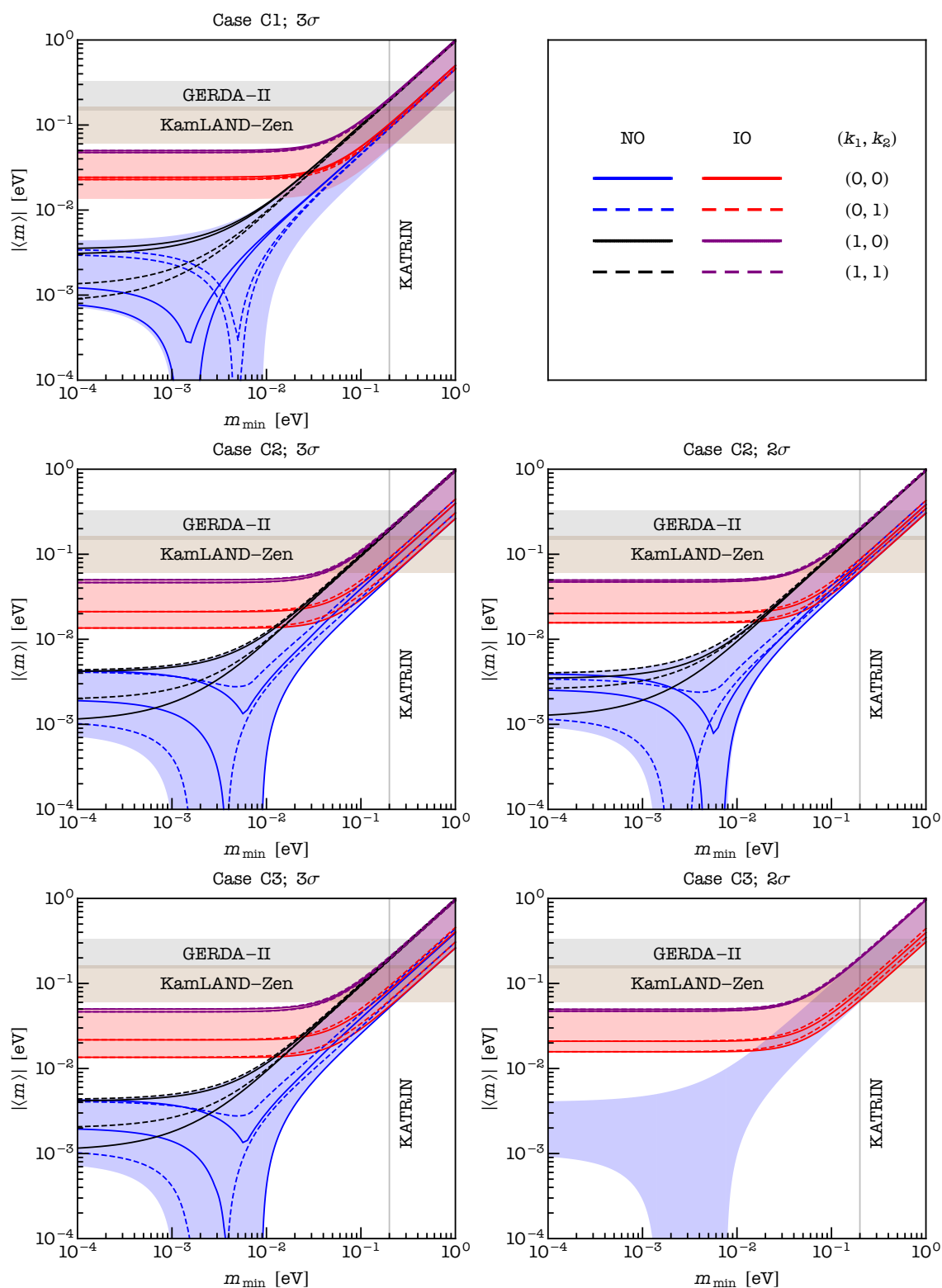


**Figure 14.** The same as in figure 13, but for cases C1–C3. Case C1 is compatible with the  $3\sigma$  ranges of the mixing angles, but not with their  $2\sigma$  ranges.

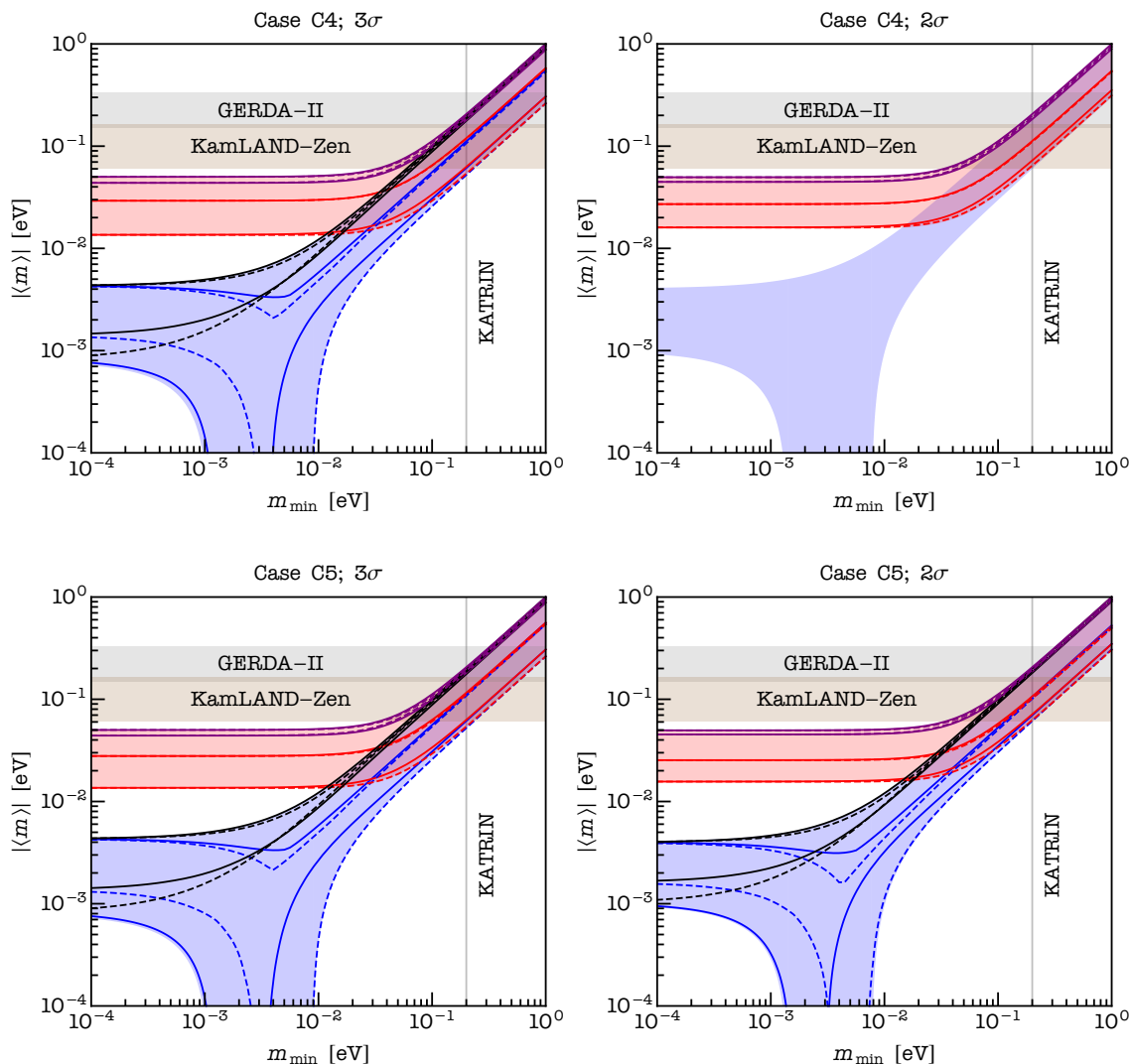


**Figure 15.** The same as in figure 13, but for cases C4 and C5.

residual  $Z_2^{g_e}$  and  $Z_2^{g_\nu} \times H_{\text{CP}}^\nu$  symmetries in the charged lepton and neutrino sectors, respectively, where  $Z_2^{g_e} = \{1, g_e\}$ ,  $Z_2^{g_\nu} = \{1, g_\nu\}$  and  $H_{\text{CP}}^\nu = \{X_\nu\}$ , 1 being the unit element of  $S_4$ . The massive neutrinos are assumed to be Majorana particles with their masses generated by the neutrino Majorana mass term of the left-handed (LH) flavour neutrino fields  $\nu_{lL}(x)$ ,  $l = e, \mu, \tau$ . We show that in this class of models the three neutrino mixing angles,  $\theta_{12}$ ,  $\theta_{23}$  and  $\theta_{13}$ , the Dirac and the two Majorana CP violation (CPV) phases,  $\delta$  and  $\alpha_{21}$ ,  $\alpha_{31}$ , are functions of altogether three parameters — two mixing angles and a phase,  $\theta^e$ ,  $\theta^\nu$  and  $\delta^e$ .

The  $S_4$  group has 9 different  $Z_2$  subgroups. Assuming that the LH flavour neutrino and charged lepton fields,  $\nu_{lL}(x)$  and  $l_L(x)$ ,  $l = e, \mu, \tau$ , transform under a triplet irreducible unitary representation of  $S_4$ , we prove that there are only 3 pairs of subgroups  $Z_2^{g_e}$  and  $Z_2^{g_\nu}$  which can lead to different viable (i.e., compatible with the current data) predictions for the lepton mixing. For these three pairs,  $\{g_e, g_\nu\} = \{S, TU\}$ ,  $\{TU, S\}$  and  $\{TU, U\}$ , where  $S$ ,  $T$  and  $U$  are the generators of  $S_4$  (see eq. (3.1)) taken here in the triplet repre-

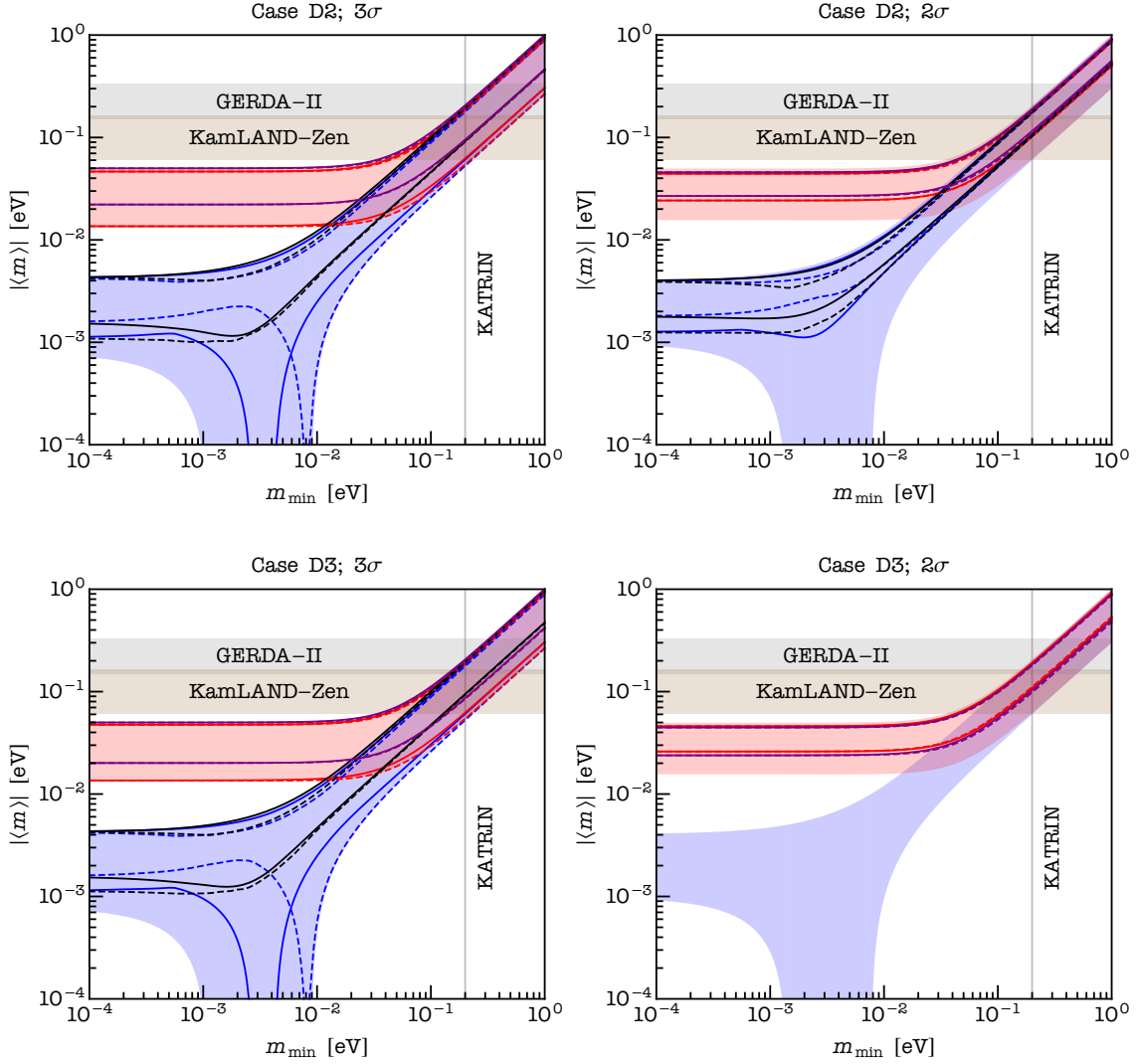


**Figure 16.** The same as in figure 13, but for cases D2 and D3.

sentation of  $S_4$  (eq. (3.12)). In what concerns the residual GCP symmetry in the neutrino sector,  $H_{\text{CP}}^\nu = \{X_\nu\}$ , we show that the constraints on  $X_\nu$  (following from the conditions of consistency between  $Z_2^{g_\nu}$  and  $H_{\text{CP}}^\nu$  and of having non-degenerate neutrino mass spectrum,  $X_\nu = X_\nu^T$ ) are satisfied in the following cases:

- i) for  $g_\nu = S$ , if  $H_{\text{CP}}^\nu = \{1, S\}$ ,  $\{U, SU\}$  or  $\{TST^2U, T^2STU\}$ ;
- ii) for  $g_\nu = U$ , if  $H_{\text{CP}}^\nu = \{1, U\}$  or  $\{S, SU\}$ ;
- iii) for  $g_\nu = TU$ , if  $H_{\text{CP}}^\nu = \{U, T\}$  or  $\{STS, T^2STU\}$ .

However,  $H_{\text{CP}}^\nu = \{U, SU\}$  and  $H_{\text{CP}}^\nu = \{TST^2U, T^2STU\}$  in the case of  $g_\nu = S$ , and  $H_{\text{CP}}^\nu = \{U, T\}$  and  $H_{\text{CP}}^\nu = \{STS, T^2STU\}$  in the case of  $g_\nu = TU$ , are shown to lead to the same predictions for the PMNS neutrino mixing matrix. Thus, we have found that effectively there are 4 distinct groups of cases to be considered. We have analysed

them case by case and have classified all phenomenologically viable mixing patterns they lead to. In all four groups of cases the PMNS neutrino mixing matrix is predicted to contain one constant element which does not depend on the three basic parameters,  $\theta^e$ ,  $\theta^\nu$  and  $\delta^e$ . The magnitude of this element is equal to  $1/\sqrt{2}$  in the “Group A” cases of  $\{G_e, G_\nu\} = \{Z_2^{TU}, Z_2^S \times H_{\text{CP}}^\nu\}$  with  $H_{\text{CP}}^\nu = \{1, S\}$ , and in the “Group B” cases of  $\{G_e, G_\nu\} = \{Z_2^{TU}, Z_2^S \times H_{\text{CP}}^\nu\}$  with  $H_{\text{CP}}^\nu = \{U, SU\}$ ; and it is equal to  $1/2$  in the “Group C” cases of  $\{G_e, G_\nu\} = \{Z_2^{TU}, Z_2^U \times H_{\text{CP}}^\nu\}$  with  $H_{\text{CP}}^\nu = \{1, U\}$ , and in the “Group D” cases of  $\{G_e, G_\nu\} = \{Z_2^{TU}, Z_2^U \times H_{\text{CP}}^\nu\}$  with  $H_{\text{CP}}^\nu = \{S, SU\}$ . In the approach to the neutrino mixing based on  $S_4$  flavour and GCP symmetries employed by us, the PMNS matrix is determined up to permutations of columns and rows. This implies that theoretically any of the elements of the PMNS matrix can be equal by absolute value to  $1/\sqrt{2}$  in the Group A and Group B cases, and to  $1/2$  in the Group C and Group D cases. However, the data on the neutrino mixing angles and the Dirac phase  $\delta$  imply that, taking into account the currently allowed  $3\sigma$  ranges of the PMNS matrix elements (see eqs. (3.10) and (3.11)), only 4 elements, namely,  $(U_{\text{PMNS}})_{\mu 2}$ ,  $(U_{\text{PMNS}})_{\mu 3}$ ,  $(U_{\text{PMNS}})_{\tau 2}$  or  $(U_{\text{PMNS}})_{\tau 3}$ , can have an absolute value equal to  $1/\sqrt{2} \approx 0.707$ , and only 5 elements, namely,  $(U_{\text{PMNS}})_{e 2}$ ,  $(U_{\text{PMNS}})_{\mu 1}$ ,  $(U_{\text{PMNS}})_{\tau 1}$ ,  $(U_{\text{PMNS}})_{\mu 2}$  or  $(U_{\text{PMNS}})_{\tau 2}$ , can have an absolute value equal to  $1/2$ . It should be added that i)  $|(U_{\text{PMNS}})_{\tau 2}| = 0.707$  lies outside the respective currently allowed  $3\sigma$  range in the case of NO neutrino mass spectrum, ii)  $|(U_{\text{PMNS}})_{\mu 2}| = 0.707$  is slightly outside the  $3\sigma$  allowed range for the IO spectrum, and that iii) the value of  $|(U_{\text{PMNS}})_{\mu 2}| = 1/2$  is allowed at  $3\sigma$  only for the IO spectrum.

We have derived predictions for the six parameters of the PMNS matrix,  $\theta_{12}$ ,  $\theta_{23}$  and  $\theta_{13}$ ,  $\delta$ ,  $\alpha_{21}$  and  $\alpha_{31}$ , in the potentially viable cases of Groups A–D. This was done for both NO and IO neutrino mass spectra in the cases compatible at  $3\sigma$  with the existing data. We have performed also a statistical analysis of the predictions for the neutrino mixing angles and CPV phases for each of these cases. We have found that in certain cases the predicted values of the neutrino mixing angles are ruled out, or are strongly disfavoured, by the existing data (see subsection 3.4 for details). These are:

- i) in Group A, the cases of  $|(U_{\text{PMNS}})_{\mu 3}| = 1/\sqrt{2}$  (strongly disfavoured), and  $|(U_{\text{PMNS}})_{\tau 3}| = 1/\sqrt{2}$  (strongly disfavoured);
- ii) in Group D, the cases of  $|(U_{\text{PMNS}})_{e 2}| = 1/2$  (ruled out),  $|(U_{\text{PMNS}})_{\mu 2}| = 1/2$  (strongly disfavoured), and  $|(U_{\text{PMNS}})_{\tau 2}| = 1/2$  (strongly disfavoured).

The results of the statistical analysis in the viable cases are presented graphically in figures 1–11. The predicted ranges of the neutrino mixing parameters and the their corresponding best fit values are summarised in tables 3–6.

Given the difference in the currently allowed  $2\sigma$  ranges of  $\sin^2 \theta_{23}$  (see table 1), the prediction for the allowed values of  $\sin^2 \theta_{23}$  in certain phenomenologically viable cases makes the IO (NO) spectrum statistically somewhat more favourable than the NO (IO) spectrum. At the same time, we have found that in a large number of viable cases the results we have obtained for the NO and IO spectra are very similar.

As a consequence of the fact that, in the class of models we consider, the six PMNS matrix parameters,  $\theta_{12}$ ,  $\theta_{23}$ ,  $\theta_{13}$ ,  $\delta$ ,  $\alpha_{21}$  and  $\alpha_{31}$ , are fitted with the three basic parameters,



$\theta^e$ ,  $\theta^\nu$  and  $\delta^e$ , it is not surprising that we have found that there are strong correlations i) between the values of the Dirac phase  $\delta$  and the values of the two Majorana phases  $\alpha_{21}$  and  $\alpha_{31}$ , which in turn are correlated between themselves (figures 1, 2, 6–9), and depending on the case ii) either between the values of  $\theta_{12}$  and  $\theta_{13}$  (figure 5), or between the values of  $\theta_{23}$  and  $\theta_{13}$  (figures 3 and 4) or else between the values of  $\theta_{12}$  and  $\theta_{23}$  (figures 1, 2, 6–11). In certain cases our results showed strong correlations between the predicted values of  $\theta_{23}$  and the Dirac phase  $\delta$  and/or the Majorana phases  $\alpha_{21,31}$  (figures 8–11).

In the cases of i) Group B with  $|(U_{\text{PMNS}})_{\mu 2}| = 1/\sqrt{2}$ , or  $|(U_{\text{PMNS}})_{\tau 2}| = 1/\sqrt{2}$ , ii) Group C with  $|(U_{\text{PMNS}})_{\mu 1}| = 1/2$ , or  $|(U_{\text{PMNS}})_{\tau 1}| = 1/2$ , or  $|(U_{\text{PMNS}})_{\mu 2}| = 1/2$ , or  $|(U_{\text{PMNS}})_{\tau 2}| = 1/2$ , and iii) Group D with  $|(U_{\text{PMNS}})_{\mu 1}| = 1/2$ , or  $|(U_{\text{PMNS}})_{\tau 1}| = 1/2$ , the cosine of the Dirac phase  $\delta$  satisfies a sum rule by which it is expressed in terms of the three neutrino mixing angles  $\theta_{12}$ ,  $\theta_{23}$  and  $\theta_{13}$ . Taking into account the ranges and correlations of the predicted values of the three neutrino mixing angles,  $\delta$  is predicted to lie in certain, in most of the discussed cases rather narrow, intervals (subsection 3.4). In the remaining viable cases of Groups B and C,  $\cos \delta$  was shown to satisfy sum rules which depend explicitly, in addition to  $\theta_{12}$ ,  $\theta_{23}$  and  $\theta_{13}$ , on one of the three basic parameters of the class of models considered,  $\theta^e$  or  $\theta^\nu$ . In these cases, as we have shown,  $\cos \delta$  can take any value.

We have derived also predictions for the Majorana CPV phases  $\alpha_{21}$  and  $\alpha_{31}$  in all viable cases of Groups B, C and D (subsection 3.4). With one exception — the case of  $|(U_{\text{PMNS}})_{e 2}| = 1/2$  of Group C — the values of  $\alpha_{21}$  and  $\alpha_{31}$ , as we have indicated earlier, are strongly correlated between themselves. In case C1 there is a strong linear correlation between  $\alpha_{31}$  and  $\delta$ .

Using the predictions for the Dirac and Majorana CPV phases allowed us to derive predictions for the magnitude of the neutrinoless double beta decay effective Majorana mass,  $|\langle m \rangle|$ , as a function of the lightest neutrino mass for all the viable cases belonging to Groups B, C and D. They are presented graphically in figures 13–16.

All viable cases in the class of  $S_4$  models investigated in the present article have distinct predictions for the set of observables  $\sin^2 \theta_{12}$ ,  $\sin^2 \theta_{23}$ ,  $\sin^2 \theta_{13}$ , the Dirac phase  $\delta$  and the absolute value of one element of the PMNS neutrino mixing matrix. Using future more precise data on  $\sin^2 \theta_{12}$ ,  $\sin^2 \theta_{23}$ ,  $\sin^2 \theta_{13}$  and the Dirac phase  $\delta$ , which will allow also to determine the absolute values of the elements of the PMNS matrix with a better precision, will make it possible to test and discriminate between the predictions of all the cases found by us to be compatible with the current data on the neutrino mixing parameters.

Future data will show whether Nature followed the  $S_4 \times H_{\text{CP}}$  flavour + GCP symmetry “three-parameter path” for fixing the values of the three neutrino mixing angles and of the Dirac (and Majorana) CP violation phases of the PMNS neutrino mixing matrix. We are looking forward to these data.

## Acknowledgments

We would like to thank F. Capozzi, E. Lisi, A. Marrone, D. Montanino and A. Palazzo for kindly sharing with us the data files for one-dimensional  $\chi^2$  projections. This work was supported in part by the INFN program on Theoretical Astroparticle Physics (TASP),

by the research grant 2012CPPYP7 under the program PRIN 2012 funded by the Italian Ministry of Education, University and Research (MIUR), by the European Union Horizon 2020 research and innovation programme under the Marie Skłodowska-Curie grants 674896 and 690575, and by the World Premier International Research Center Initiative (WPI Initiative), MEXT, Japan (S.T.P.).

## A Symmetry of $X_\nu$

If the neutrino sector respects a residual GCP symmetry  $H_{\text{CP}}^\nu = \{X_\nu\}$ , the neutrino mass matrix satisfies eq. (2.12), namely,

$$X_\nu^T M_\nu X_\nu = M_\nu^* . \tag{A.1}$$

The GCP transformation matrices  $X_\nu$  must be unitary due to the GCP invariance of the neutrino kinetic term. In what follows we show that these matrices are additionally constrained to be symmetric if the neutrino mass spectrum is non-degenerate, as is known to be the case.

Expressing  $M_\nu$  from eq. (2.14) and substituting it in eq. (A.1) yields

$$d_\nu \tilde{X} = \tilde{X}^* d_\nu , \tag{A.2}$$

where  $d_\nu \equiv \text{diag}(m_1, m_2, m_3)$  and  $\tilde{X} \equiv U_\nu^\dagger X_\nu U_\nu^*$  is unitary.

Being  $3 \times 3$  unitary,  $\tilde{X}$  can be parametrised as the product of three complex rotations  $U_{ij}$  and a diagonal matrix of phases  $\Psi$  as follows:

$$\tilde{X} = \Psi U_{23}(\vartheta_{23}, \delta_{23}) U_{13}(\vartheta_{13}, \delta_{13}) U_{12}(\vartheta_{12}, \delta_{12}) , \tag{A.3}$$

where  $\Psi = \text{diag}(e^{i\psi_1}, e^{i\psi_2}, e^{i\psi_3})$  and the  $U_{ij}(\vartheta_{ij}, \delta_{ij})$  are complex rotations in the  $i$ - $j$  plane. Explicitly,

$$U_{23}(\vartheta_{23}, \delta_{23}) = \begin{pmatrix} 1 & 0 & 0 \\ 0 & \cos \vartheta_{23} & \sin \vartheta_{23} e^{-i\delta_{23}} \\ 0 & -\sin \vartheta_{23} e^{i\delta_{23}} & \cos \vartheta_{23} \end{pmatrix} , \tag{A.4}$$

with a straightforward generalisation to  $(ij) = (12), (13)$ .

Imposing eq. (A.2) produces the following relations:

$$e^{i(\psi_1 - \delta_{13})} m_1 \sin \vartheta_{13} = e^{-i(\psi_1 - \delta_{13})} m_3 \sin \vartheta_{13} , \tag{A.5}$$

$$e^{i(\psi_2 - \delta_{23})} m_2 \cos \vartheta_{13} \sin \vartheta_{23} = e^{-i(\psi_2 - \delta_{23})} m_3 \cos \vartheta_{13} \sin \vartheta_{23} , \tag{A.6}$$

$$e^{i(\psi_1 - \delta_{12})} m_1 \cos \vartheta_{13} \sin \vartheta_{12} = e^{-i(\psi_1 - \delta_{12})} m_2 \cos \vartheta_{13} \sin \vartheta_{12} . \tag{A.7}$$

From the non-degeneracy of the neutrino mass spectrum it follows that  $\sin \vartheta_{13} = \sin \vartheta_{23} = \sin \vartheta_{12} = 0$ . Thus,  $\tilde{X}$  is constrained to be diagonal and hence symmetric,  $\tilde{X}^T = \tilde{X}$ . This finally implies that also  $X_\nu^T = X_\nu$ , i.e., a phenomenologically relevant  $X_\nu$  must be symmetric.

## B Conjugate pairs of $S_4$ elements

As detailed in subsection 2.2, residual flavour symmetries  $Z_2^{g_e}$  and  $Z_2^{g_\nu}$  which are conjugate to each other lead to the same form of the PMNS matrix. For  $G_f = S_4$ , there are nine group elements of order two, given in eqs. (3.2) and (3.3), which generate  $Z_2$  subgroups. The resulting 81 pairs of elements  $\{g_e, g_\nu\}$  can themselves be partitioned, under the conjugacy relation of eq. (2.25), into the following nine equivalence classes:

- **$\{S, S\}$** ,  $\{TST^2, TST^2\}$ ,  $\{T^2ST, T^2ST\}$ ;
- **$\{U, U\}$** ,  $\{SU, SU\}$ ,  $\{T^2U, T^2U\}$ ,  $\{TU, TU\}$ ,  $\{ST^2SU, ST^2SU\}$ ,  $\{STSU, STSU\}$ ;
- **$\{T^2ST, S\}$** ,  $\{TST^2, S\}$ ,  $\{T^2ST, TST^2\}$ ,  $\{S, T^2ST\}$ ,  $\{S, TST^2\}$ ,  $\{TST^2, T^2ST\}$ ;
- **$\{S, U\}$** ,  $\{S, SU\}$ ,  $\{TST^2, T^2U\}$ ,  $\{T^2ST, TU\}$ ,  $\{TST^2, ST^2SU\}$ ,  $\{T^2ST, STSU\}$ ;
- **$\{U, S\}$** ,  $\{SU, S\}$ ,  $\{T^2U, TST^2\}$ ,  $\{TU, T^2ST\}$ ,  $\{ST^2SU, TST^2\}$ ,  $\{STSU, T^2ST\}$ ;
- **$\{SU, U\}$** ,  $\{U, SU\}$ ,  $\{ST^2SU, T^2U\}$ ,  $\{STSU, TU\}$ ,  $\{T^2U, ST^2SU\}$ ,  $\{TU, STSU\}$ ;
- **$\{S, TU\}$** ,  $\{S, STSU\}$ ,  $\{S, T^2U\}$ ,  $\{TST^2, TU\}$ ,  $\{S, ST^2SU\}$ ,  $\{T^2ST, U\}$ ,  $\{T^2ST, SU\}$ ,  $\{TST^2, U\}$ ,  $\{T^2ST, T^2U\}$ ,  $\{TST^2, SU\}$ ,  $\{T^2ST, ST^2SU\}$ ,  $\{TST^2, STSU\}$ ;
- **$\{TU, S\}$** ,  $\{STSU, S\}$ ,  $\{T^2U, S\}$ ,  $\{TU, TST^2\}$ ,  $\{ST^2SU, S\}$ ,  $\{U, T^2ST\}$ ,  $\{SU, T^2ST\}$ ,  $\{U, TST^2\}$ ,  $\{T^2U, T^2ST\}$ ,  $\{SU, TST^2\}$ ,  $\{ST^2SU, T^2ST\}$ ,  $\{STSU, TST^2\}$ ;
- **$\{TU, U\}$** ,  $\{STSU, U\}$ ,  $\{STSU, SU\}$ ,  $\{TU, SU\}$ ,  $\{T^2U, U\}$ ,  $\{TU, T^2U\}$ ,  $\{ST^2SU, U\}$ ,  $\{U, TU\}$ ,  $\{TU, ST^2SU\}$ ,  $\{SU, STSU\}$ ,  $\{U, T^2U\}$ ,  $\{T^2U, TU\}$ ,  $\{U, ST^2SU\}$ ,  $\{SU, T^2U\}$ ,  $\{SU, ST^2SU\}$ ,  $\{T^2U, STSU\}$ ,  $\{ST^2SU, STSU\}$ ,  $\{ST^2SU, TU\}$ ,  $\{STSU, ST^2SU\}$ ,  $\{STSU, T^2U\}$ ,  $\{SU, TU\}$ ,  $\{ST^2SU, SU\}$ ,  $\{T^2U, SU\}$ ,  $\{U, STSU\}$ ;

where in boldface we have identified a representative pair of elements for each class, matching the choice made in eqs. (3.4) and (3.5).

## C Equivalent cases

A necessary condition for two matrices  $U_{\text{PMNS}}$  and  $U'_{\text{PMNS}}$  to be equivalent is the same magnitude of the fixed element. Indeed, in the four cases under consideration the absolute value of one element is  $1/\sqrt{2}$ . For  $P_e = P'_e$  and  $P_\nu = P'_\nu$ , the two matrices  $U_{\text{PMNS}}$  and  $U'_{\text{PMNS}}$  would be equivalent, if the products  $\Omega_e^\dagger \Omega_\nu$  and  $\Omega_e'^\dagger \Omega'_\nu$  could be related in the following way:

$$\Omega_e^\dagger \Omega_\nu = \text{diag}(e^{i\phi_1}, e^{i\phi_2}, e^{i\phi_3}) U_{23}(\theta_\circ^e, \delta_\circ^e) \Omega_e'^\dagger \Omega'_\nu R_{23}(\theta_\circ^\nu) \text{diag}(1, i^k, i^k), \quad (\text{C.1})$$

with  $\phi_i$ ,  $\delta_\circ^e$  and  $\theta_\circ^e$ ,  $\theta_\circ^\nu$  being fixed phases and angles, respectively, and  $k$  is allowed to be 0, 1, 2 or 3. Indeed, if this relation holds, from eq. (2.24) we have

$$\begin{aligned} U_{\text{PMNS}} &= P_e U_{23}(\theta^e, \delta^e) \text{diag}(e^{i\phi_1}, e^{i\phi_2}, e^{i\phi_3}) U_{23}(\theta_\circ^e, \delta_\circ^e) \Omega_e'^\dagger \Omega'_\nu R_{23}(\theta_\circ^\nu) \text{diag}(1, i^k, i^k) R_{23}(\theta^\nu) P_\nu Q_\nu \\ &= P_e \text{diag}(e^{i\phi_1}, e^{i\phi_2}, e^{i\phi_3}) U_{23}(\theta^e, \tilde{\delta}^e) U_{23}(\theta_\circ^e, \delta_\circ^e) \Omega_e'^\dagger \Omega'_\nu R_{23}(\hat{\theta}^\nu) P_\nu \hat{Q}_\nu, \end{aligned} \quad (\text{C.2})$$

$g_e$	$g_\nu$	$H_{\text{CP}}^\nu$	$S$	$TU$	$\{U, T\}$	$S$	$TU$	$\{STS, T^2STU\}$	$TU$	$S$	$\{TST^2U, T^2STU\}$
$\phi_1$					$\pi/6$			$-\pi/3$			$-\pi/2$
$\phi_2$					$-\arctan \sqrt{1 + 2\sqrt{2}/3}$			$-\arctan(\sqrt{2} + \sqrt{3})$			$\text{arccot}(2)$
$\phi_3$					$\arctan(3\sqrt{3} + 2\sqrt{6})$			$\text{arccot}(2\sqrt{2} + \sqrt{3})$			$\arctan(2)$
$\delta_\circ^e$					$\text{arccot}(5/\sqrt{3})$			$\pi/3$			$\arctan((5\sqrt{3} - 6)/13)$
$\theta_\circ^e$					$\arctan \sqrt{(11 - 6\sqrt{2})/7}$			$\arctan(\sqrt{2} + \sqrt{3})$			$\pi - \arctan(2/\sqrt{5})$
$\theta_\nu^e$					$\pi - \arctan(3 - 2\sqrt{2})$			$\pi/4$			$\pi/4$
$k$					$0$			$1$			$3$

**Table 8.** The values of the parameters  $\phi_i$ ,  $\delta_\circ^e$ ,  $\theta_\circ^e$ ,  $\theta_\nu^e$  and  $k$  for which eq. (C.1), proving the equivalence of the PMNS matrix in a given case to the PMNS matrix in the reference case of  $\{G_e, G_\nu\} = \{Z_2^{TU}, Z_2^S \times H_{\text{CP}}^\nu\}$  with  $H_{\text{CP}}^\nu = \{U, SU\}$ , holds.

with

$$\tilde{\delta}^e = \delta^e + \phi_2 - \phi_3, \quad \hat{\theta}^\nu = \theta_\nu^e + \theta^\nu \quad \text{and} \quad \hat{Q}_\nu = P_\nu^T \text{diag}(1, i^k, i^k) P_\nu Q_\nu. \quad (\text{C.3})$$

Now, using

$$U_{23}(\theta^e, \tilde{\delta}^e) U_{23}(\theta_\circ^e, \delta_\circ^e) = \text{diag}(1, e^{i\alpha}, e^{-i\alpha}) U_{23}(\hat{\theta}^e, \hat{\delta}^e), \quad (\text{C.4})$$

where (see appendix B in [7])

$$\begin{aligned} \alpha &= \arg \left\{ \cos \theta^e \cos \theta_\circ^e - \sin \theta^e \sin \theta_\circ^e e^{i(\delta_\circ^e - \tilde{\delta}^e)} \right\}, & \beta &= \arg \left\{ \sin \theta^e \cos \theta_\circ^e e^{-i\tilde{\delta}^e} + \cos \theta^e \sin \theta_\circ^e e^{-i\delta_\circ^e} \right\}, \\ \cos \hat{\theta}^e &= \left| \cos \theta^e \cos \theta_\circ^e - \sin \theta^e \sin \theta_\circ^e e^{i(\delta_\circ^e - \tilde{\delta}^e)} \right|, & \sin \hat{\theta}^e &= \left| \sin \theta^e \cos \theta_\circ^e e^{-i\tilde{\delta}^e} + \cos \theta^e \sin \theta_\circ^e e^{-i\delta_\circ^e} \right| \\ & & \text{and} & \hat{\delta}^e = \alpha - \beta, \end{aligned}$$

we obtain

$$U_{\text{PMNS}} = Q_e P_e U_{23}(\hat{\theta}^e, \hat{\delta}^e) \Omega_e^\dagger \Omega_\nu' R_{23}(\hat{\theta}^\nu) P_\nu \hat{Q}_\nu, \quad (\text{C.5})$$

with

$$Q_e = P_e \text{diag} \left( e^{i\phi_1}, e^{i(\phi_2 + \alpha)}, e^{i(\phi_3 - \alpha)} \right) P_e^T \quad (\text{C.6})$$

being the matrix of unphysical phases. Thus, up to this matrix,  $U_{\text{PMNS}}$  and  $U'_{\text{PMNS}}$  are the same.

Taking  $\{G_e, G_\nu\} = \{Z_2^{TU}, Z_2^S \times H_{\text{CP}}^\nu\}$  with  $H_{\text{CP}}^\nu = \{U, SU\}$  as a reference case and denoting the corresponding diagonalising matrices as  $\Omega_e'$  and  $\Omega_\nu'$ , we find the values of  $\phi_i$ ,  $\delta_\circ^e$ ,  $\theta_\circ^e$ ,  $\theta_\nu^e$  and  $k$  for which eq. (C.1) holds, if  $\Omega_e$  and  $\Omega_\nu$  are the diagonalising matrices in one of the three remaining cases under consideration. We summarise these values in table 8.

## D Correspondence with earlier results

The sum rules for  $\cos \delta$  or  $\sin^2 \theta_{23}$  ( $\sin^2 \theta_{12}$  in case C1) can formally be obtained from the corresponding sum rules derived in [7]. In certain cases, this requires an additional input which is provided by the residual GCP symmetry  $H_{\text{CP}}^\nu$  considered in the present article.

Below we provide the correspondence between the phenomenologically viable cases of the present study and the cases considered in [7].

- i) Cases B1, C4 and D4 of the present study correspond to case C8 in [7], since for all these cases  $(U_{\text{PMNS}})_{\mu 2}$  is fixed. The sum rule for  $\cos \delta$  in case B1, eq. (3.46), follows from that of case C8 in [7] (see table 4 therein) for  $\sin^2 \theta_{23}^{\circ} = 1/2$ , while the sum rule in eq. (3.57), valid in cases C4 and D4, can be obtained from the same sum rule found in [7], but for  $\sin^2 \theta_{23}^{\circ} = 3/4$ . As should be, these two values of  $\sin^2 \theta_{23}^{\circ}$  follow from  $G_f = S_4$ , when it is broken to two different non-equivalent specific pairs of residual  $\{Z_2^{g_e}, Z_2^{g_\nu}\}$  flavour symmetries (see table 10 in [7]).
- ii) Cases B2, C5 and D5 correspond to case C1 in [7], since for all of them  $(U_{\text{PMNS}})_{\tau 2}$  is fixed. The sum rule for  $\cos \delta$  in case B2, eq. (3.47), follows from that of case C1 in [7] (see table 4 therein) for  $\sin^2 \theta_{23}^{\circ} = 1/2$ , while the sum rule in eq. (3.58), valid in cases C5 and D5, can be obtained from the same sum rule found in [7], but for  $\sin^2 \theta_{23}^{\circ} = 1/4$ . Again, these values of  $\sin^2 \theta_{23}^{\circ}$  are fixed uniquely by  $G_f = S_4$  and the specific choice of the residual symmetries considered in the present article.<sup>16</sup>
- iii) Cases A1 and B3 of the present study correspond to case C2 in [7], since for these cases  $(U_{\text{PMNS}})_{\mu 3}$  is fixed. The expression for  $\sin^2 \theta_{23}$  in eq. (3.35) follows from the corresponding expression for case C2 in table 6 of [7] with  $\sin^2 \theta_{23}^{\circ} = 1/2$ . This value is in agreement with table 10 of [7]. Moreover, the sum rule for  $\cos \delta$  in eq. (3.37) in case A1 can be obtained from the sum rule for case C2<sup>17</sup> in table 4 of [7] with  $\sin^2 \theta_{23}^{\circ} = 1/2$  and  $\sin^2 \hat{\theta}_{12}^{\nu} = 1/2$ . The value of  $\sin^2 \hat{\theta}_{12}^{\nu}$ , which was an arbitrary free parameter in [7], is fixed by the GCP symmetry employed in the present study. Finally, we note that the expression for  $\cos \delta$  in eq. (3.49) valid in case B3 can formally be obtained from the corresponding expression in case C2 of table 4 in [7] setting  $\hat{\theta}_{12}^{\nu} = \theta^{\nu} - \pi/4$ .
- iv) Analogously, cases A2 and B4 correspond to case C7 in [7]. Equation (3.38) can be obtained from the corresponding formula in table 6 of [7] for  $\sin^2 \theta_{23}^{\circ} = 1/2$ , which agrees with the result in table 10 therein. The sum rule in eq. (3.40) follows from that in case C7 in table 4 of [7] with  $\sin^2 \theta_{23}^{\circ} = 1/2$  and  $\sin^2 \hat{\theta}_{12}^{\nu} = 1/2$ , where again the value of  $\sin^2 \hat{\theta}_{12}^{\nu}$ , which in [7] is a free parameter, here is fixed by the GCP symmetry. Similarly to the previous clause, eq. (3.51) can formally be derived from the corresponding expression in case C7 of table 4 in [7] setting  $\hat{\theta}_{12}^{\nu} = \theta^{\nu} - \pi/4$ .
- v) Case C1 corresponds to case C5 in [7], in which all possible residual flavour symmetries  $G_e = Z_2$  and  $G_\nu = Z_2$  have been considered. The expression for  $\sin^2 \theta_{12}$  in eq. (3.53) follows from that of case C5 in table 6 in [7] with  $\sin^2 \theta_{12}^{\circ} = 1/4$ . This value of  $\sin^2 \theta_{12}^{\circ}$

<sup>16</sup>Note that the value of  $\sin^2 \theta_{23}^{\circ} = 1/2$  is not present in table 10 of [7], since in this reference the best fit values of the mixing angles for the NO spectrum quoted in eqs. (6)–(8) therein have been used, and employing them, one obtains  $\cos \delta \approx 2.76$ .

<sup>17</sup>We would like to point out a typo in eq. (85) in [7]:  $\cos^2 \theta_{23}^{\circ}$  should read  $\cos \theta_{23}^{\circ}$ . This typo, however, does not affect the corresponding sum rule for  $\cos \delta$  in eq. (86) and in table 4 of [7].

is found for  $G_f = S_4$  and the specific choice of the residual symmetries (see table 10 in [7]). Moreover, eq. (3.56) for  $\cos \delta$  can formally be obtained from the corresponding formula in case C5 of table 4 in [7] setting  $\sin^2 \hat{\theta}_{23}^e = \sin^2 \theta^e$ .

- vi) Cases C2 and D2 correspond to case C4 of [7]. The sum rule for  $\cos \delta$  in eq. (3.37), valid in cases C2 and D2, follows from that of case C4 in [7] (see table 4 therein) for  $\sin^2 \theta_{12}^\circ = 1/4$ , which is in agreement with table 10 in [7].
- vii) Cases C3 and D3 correspond to case C3 in [7]. Equation (3.40) for  $\cos \delta$ , which holds in these cases, can be obtained from the corresponding sum rule for case C3 from table 4 in [7] with  $\sin^2 \theta_{13}^\circ = 1/4$ . As it should be, we find this value in table 10 of [7].

**Open Access.** This article is distributed under the terms of the Creative Commons Attribution License ([CC-BY 4.0](https://creativecommons.org/licenses/by/4.0/)), which permits any use, distribution and reproduction in any medium, provided the original author(s) and source are credited.

## References

- [1] K. Nakamura and S.T. Petcov, *Neutrino Mass, Mixing and Oscillations*, in PARTICLE DATA GROUP collaboration, C. Patrignani et al., *Review of Particle Physics*, *Chin. Phys. C* **40** (2016) 100001 [[INSPIRE](#)].
- [2] G. Altarelli and F. Feruglio, *Discrete Flavor Symmetries and Models of Neutrino Mixing*, *Rev. Mod. Phys.* **82** (2010) 2701 [[arXiv:1002.0211](#)] [[INSPIRE](#)].
- [3] H. Ishimori, T. Kobayashi, H. Ohki, Y. Shimizu, H. Okada and M. Tanimoto, *Non-Abelian Discrete Symmetries in Particle Physics*, *Prog. Theor. Phys. Suppl.* **183** (2010) 1 [[arXiv:1003.3552](#)] [[INSPIRE](#)].
- [4] S.F. King, A. Merle, S. Morisi, Y. Shimizu and M. Tanimoto, *Neutrino Mass and Mixing: from Theory to Experiment*, *New J. Phys.* **16** (2014) 045018 [[arXiv:1402.4271](#)] [[INSPIRE](#)].
- [5] S.T. Petcov, *Predicting the values of the leptonic CP-violation phases in theories with discrete flavour symmetries*, *Nucl. Phys. B* **892** (2015) 400 [[arXiv:1405.6006](#)] [[INSPIRE](#)].
- [6] I. Girardi, S.T. Petcov and A.V. Titov, *Predictions for the Leptonic Dirac CP-violation Phase: a Systematic Phenomenological Analysis*, *Eur. Phys. J. C* **75** (2015) 345 [[arXiv:1504.00658](#)] [[INSPIRE](#)].
- [7] I. Girardi, S.T. Petcov, A.J. Stuart and A.V. Titov, *Leptonic Dirac CP-violation Predictions from Residual Discrete Symmetries*, *Nucl. Phys. B* **902** (2016) 1 [[arXiv:1509.02502](#)] [[INSPIRE](#)].
- [8] D. Marzocca, S.T. Petcov, A. Romanino and M.C. Sevilla, *Nonzero  $|U_{e3}|$  from Charged Lepton Corrections and the Atmospheric Neutrino Mixing Angle*, *JHEP* **05** (2013) 073 [[arXiv:1302.0423](#)] [[INSPIRE](#)].
- [9] M. Tanimoto, *Neutrinos and flavor symmetries*, *AIP Conf. Proc.* **1666** (2015) 120002 [[INSPIRE](#)].
- [10] P. Ballett, S.F. King, C. Luhn, S. Pascoli and M.A. Schmidt, *Testing atmospheric mixing sum rules at precision neutrino facilities*, *Phys. Rev. D* **89** (2014) 016016 [[arXiv:1308.4314](#)] [[INSPIRE](#)].

- [11] S.-F. Ge, D.A. Dicus and W.W. Repko, *Residual Symmetries for Neutrino Mixing with a Large  $\theta_{13}$  and Nearly Maximal  $\delta_D$* , *Phys. Rev. Lett.* **108** (2012) 041801 [[arXiv:1108.0964](#)] [[INSPIRE](#)].
- [12] S.-F. Ge, D.A. Dicus and W.W. Repko,  *$Z_2$  Symmetry Prediction for the Leptonic Dirac CP Phase*, *Phys. Lett. B* **702** (2011) 220 [[arXiv:1104.0602](#)] [[INSPIRE](#)].
- [13] S. Antusch, S.F. King, C. Luhn and M. Spinrath, *Trimaximal mixing with predicted  $\theta_{13}$  from a new type of constrained sequential dominance*, *Nucl. Phys. B* **856** (2012) 328 [[arXiv:1108.4278](#)] [[INSPIRE](#)].
- [14] A.D. Hanlon, S.-F. Ge and W.W. Repko, *Phenomenological consequences of residual  $\mathbb{Z}_2^s$  and  $\overline{\mathbb{Z}}_2^s$  symmetries*, *Phys. Lett. B* **729** (2014) 185 [[arXiv:1308.6522](#)] [[INSPIRE](#)].
- [15] I. Girardi, S.T. Petcov and A.V. Titov, *Determining the Dirac CP-violation Phase in the Neutrino Mixing Matrix from Sum Rules*, *Nucl. Phys. B* **894** (2015) 733 [[arXiv:1410.8056](#)] [[INSPIRE](#)].
- [16] I. Girardi, S.T. Petcov and A.V. Titov, *Predictions for the Dirac CP-violation Phase in the Neutrino Mixing Matrix*, *Int. J. Mod. Phys. A* **30** (2015) 1530035 [[arXiv:1504.02402](#)] [[INSPIRE](#)].
- [17] S.M. Bilenky, J. Hosek and S.T. Petcov, *On Oscillations of Neutrinos with Dirac and Majorana Masses*, *Phys. Lett. B* **94** (1980) 495 [[INSPIRE](#)].
- [18] G.C. Branco, L. Lavoura and M.N. Rebelo, *Majorana Neutrinos and CP Violation in the Leptonic Sector*, *Phys. Lett. B* **180** (1986) 264 [[INSPIRE](#)].
- [19] F. Feruglio, C. Hagedorn and R. Ziegler, *Lepton Mixing Parameters from Discrete and CP Symmetries*, *JHEP* **07** (2013) 027 [[arXiv:1211.5560](#)] [[INSPIRE](#)].
- [20] M. Holthausen, M. Lindner and M.A. Schmidt, *CP and Discrete Flavour Symmetries*, *JHEP* **04** (2013) 122 [[arXiv:1211.6953](#)] [[INSPIRE](#)].
- [21] G.-J. Ding, S.F. King, C. Luhn and A.J. Stuart, *Spontaneous CP-violation from vacuum alignment in  $S_4$  models of leptons*, *JHEP* **05** (2013) 084 [[arXiv:1303.6180](#)] [[INSPIRE](#)].
- [22] G.-J. Ding, S.F. King and A.J. Stuart, *Generalised CP and  $A_4$  Family Symmetry*, *JHEP* **12** (2013) 006 [[arXiv:1307.4212](#)] [[INSPIRE](#)].
- [23] C.-C. Li and G.-J. Ding, *Lepton Mixing in  $A_5$  Family Symmetry and Generalized CP*, *JHEP* **05** (2015) 100 [[arXiv:1503.03711](#)] [[INSPIRE](#)].
- [24] A. Di Iura, C. Hagedorn and D. Meloni, *Lepton mixing from the interplay of the alternating group  $A_5$  and CP*, *JHEP* **08** (2015) 037 [[arXiv:1503.04140](#)] [[INSPIRE](#)].
- [25] P. Ballett, S. Pascoli and J. Turner, *Mixing angle and phase correlations from  $A_5$  with generalized CP and their prospects for discovery*, *Phys. Rev. D* **92** (2015) 093008 [[arXiv:1503.07543](#)] [[INSPIRE](#)].
- [26] F. Capozzi, E. Di Valentino, E. Lisi, A. Marrone, A. Melchiorri and A. Palazzo, *Global constraints on absolute neutrino masses and their ordering*, *Phys. Rev. D* **95** (2017) 096014 [[arXiv:1703.04471](#)] [[INSPIRE](#)].
- [27] I. Esteban, M.C. Gonzalez-Garcia, M. Maltoni, I. Martinez-Soler and T. Schwetz, *Updated fit to three neutrino mixing: exploring the accelerator-reactor complementarity*, *JHEP* **01** (2017) 087 [[arXiv:1611.01514](#)] [[INSPIRE](#)].

- [28] C.-Y. Yao and G.-J. Ding, *CP Symmetry and Lepton Mixing from a Scan of Finite Discrete Groups*, *Phys. Rev. D* **94** (2016) 073006 [[arXiv:1606.05610](#)] [[INSPIRE](#)].
- [29] I. Girardi, A. Meroni, S.T. Petcov and M. Spinrath, *Generalised geometrical CP-violation in a  $T'$  lepton flavour model*, *JHEP* **02** (2014) 050 [[arXiv:1312.1966](#)] [[INSPIRE](#)].
- [30] J. Turner, *Predictions for leptonic mixing angle correlations and nontrivial Dirac CP-violation from  $A_5$  with generalized CP symmetry*, *Phys. Rev. D* **92** (2015) 116007 [[arXiv:1507.06224](#)] [[INSPIRE](#)].
- [31] I. Girardi, S.T. Petcov and A.V. Titov, *Predictions for the Majorana CP-violation Phases in the Neutrino Mixing Matrix and Neutrinoless Double Beta Decay*, *Nucl. Phys. B* **911** (2016) 754 [[arXiv:1605.04172](#)] [[INSPIRE](#)].
- [32] J.-N. Lu and G.-J. Ding, *Alternative Schemes of Predicting Lepton Mixing Parameters from Discrete Flavor and CP Symmetry*, *Phys. Rev. D* **95** (2017) 015012 [[arXiv:1610.05682](#)] [[INSPIRE](#)].
- [33] C. Hagedorn, S.F. King and C. Luhn, *A SUSY GUT of Flavour with  $S_4 \times SU(5)$  to NLO*, *JHEP* **06** (2010) 048 [[arXiv:1003.4249](#)] [[INSPIRE](#)].
- [34] C.-C. Li and G.-J. Ding, *Deviation from bimaximal mixing and leptonic CP phases in  $S_4$  family symmetry and generalized CP*, *JHEP* **08** (2015) 017 [[arXiv:1408.0785](#)] [[INSPIRE](#)].
- [35] F. Capozzi, private communication.
- [36] S.F. King and C. Luhn, *A New family symmetry for  $SO(10)$  GUTs*, *Nucl. Phys. B* **820** (2009) 269 [[arXiv:0905.1686](#)] [[INSPIRE](#)].
- [37] P.I. Krastev and S.T. Petcov, *Resonance Amplification and  $T$  Violation Effects in Three Neutrino Oscillations in the Earth*, *Phys. Lett. B* **205** (1988) 84 [[INSPIRE](#)].
- [38] S.M. Bilenky, S. Pascoli and S.T. Petcov, *Majorana neutrinos, neutrino mass spectrum, CP-violation and neutrinoless double beta decay. 1. The Three neutrino mixing case*, *Phys. Rev. D* **64** (2001) 053010 [[hep-ph/0102265](#)] [[INSPIRE](#)].
- [39] J.F. Nieves and P.B. Pal, *Minimal Rephasing Invariant CP Violating Parameters With Dirac and Majorana Fermions*, *Phys. Rev. D* **36** (1987) 315 [[INSPIRE](#)].
- [40] J.A. Aguilar-Saavedra and G.C. Branco, *Unitarity triangles and geometrical description of CP-violation with Majorana neutrinos*, *Phys. Rev. D* **62** (2000) 096009 [[hep-ph/0007025](#)] [[INSPIRE](#)].
- [41] J.F. Nieves and P.B. Pal, *Rephasing invariant CP-violating parameters with Majorana neutrinos*, *Phys. Rev. D* **64** (2001) 076005 [[hep-ph/0105305](#)] [[INSPIRE](#)].
- [42] S.M. Bilenky and S.T. Petcov, *Massive Neutrinos and Neutrino Oscillations*, *Rev. Mod. Phys.* **59** (1987) 671 [*Erratum ibid.* **60** (1988) 575] [*Erratum ibid.* **61** (1989) 169] [[INSPIRE](#)].
- [43] W. Rodejohann, *Neutrino-less Double Beta Decay and Particle Physics*, *Int. J. Mod. Phys. E* **20** (2011) 1833 [[arXiv:1106.1334](#)] [[INSPIRE](#)].
- [44] S.T. Petcov, *The Nature of Massive Neutrinos*, *Adv. High Energy Phys.* **2013** (2013) 852987 [[arXiv:1303.5819](#)] [[INSPIRE](#)].
- [45] J. Ling, *Precision Measurement of  $\sin^2(2\theta_{13})$  and  $|\Delta m_{ee}^2|$  from Daya Bay*, *PoS(ICHEP2016)467* [[INSPIRE](#)].
- [46] JUNO collaboration, F. An et al., *Neutrino Physics with JUNO*, *J. Phys. G* **43** (2016) 030401 [[arXiv:1507.05613](#)] [[INSPIRE](#)].



- [47] Y.-F. Li, *Overview of the Jiangmen Underground Neutrino Observatory (JUNO)*, *Int. J. Mod. Phys. Conf. Ser.* **31** (2014) 1460300 [[arXiv:1402.6143](#)] [[INSPIRE](#)].
- [48] T2K collaboration, K. Abe et al., *Neutrino oscillation physics potential of the T2K experiment*, *PTEP* **2015** (2015) 043C01 [[arXiv:1409.7469](#)] [[INSPIRE](#)].
- [49] K. Abe et al., *Proposal for an Extended Run of T2K to  $20 \times 10^{21}$  POT*, [arXiv:1609.04111](#) [[INSPIRE](#)].
- [50] HYPER-KAMIOKANDE proto-collaboration, K. Abe et al., *Physics potential of a long-baseline neutrino oscillation experiment using a J-PARC neutrino beam and Hyper-Kamiokande*, *PTEP* **2015** (2015) 053C02 [[arXiv:1502.05199](#)] [[INSPIRE](#)].
- [51] DUNE collaboration, R. Acciarri et al., *Long-Baseline Neutrino Facility (LBNF) and Deep Underground Neutrino Experiment (DUNE) Conceptual Design Report Volume 2: The Physics Program for DUNE at LBNF*, [arXiv:1512.06148](#) [[INSPIRE](#)].
- [52] DUNE collaboration, R. Acciarri et al., *Long-Baseline Neutrino Facility (LBNF) and Deep Underground Neutrino Experiment (DUNE) Conceptual Design Report Volume 1: The LBNF and DUNE Projects*, [arXiv:1601.05471](#) [[INSPIRE](#)].
- [53] DUNE collaboration, R. Acciarri et al., *Long-Baseline Neutrino Facility (LBNF) and Deep Underground Neutrino Experiment (DUNE) Conceptual Design Report Volume 4 The DUNE Detectors at LBNF*, [arXiv:1601.02984](#) [[INSPIRE](#)].
- [54] KAMLAND-ZEN collaboration, A. Gando et al., *Search for Majorana Neutrinos near the Inverted Mass Hierarchy Region with KamLAND-Zen*, *Phys. Rev. Lett.* **117** (2016) 082503 [*Addendum ibid.* **117** (2016) 109903] [[arXiv:1605.02889](#)] [[INSPIRE](#)].
- [55] GERDA collaboration, M. Agostini et al., *Background-free search for neutrinoless double- $\beta$  decay of  $^{76}\text{Ge}$  with GERDA*, *Nature* **544** (2017) 47 [[arXiv:1703.00570](#)] [[INSPIRE](#)].
- [56] J.D. Vergados, H. Ejiri and F. Šimkovic, *Neutrinoless double beta decay and neutrino mass*, *Int. J. Mod. Phys. E* **25** (2016) 1630007 [[arXiv:1612.02924](#)] [[INSPIRE](#)].
- [57] S. Pascoli and S.T. Petcov, *The SNO solar neutrino data, neutrinoless double beta decay and neutrino mass spectrum*, *Phys. Lett. B* **544** (2002) 239 [[hep-ph/0205022](#)] [[INSPIRE](#)].
- [58] S. Pascoli and S.T. Petcov, *The SNO solar neutrino data, neutrinoless double beta decay and neutrino mass spectrum: Addendum*, *Phys. Lett. B* **580** (2004) 280 [[hep-ph/0310003](#)] [[INSPIRE](#)].
- [59] S. Dell’Oro, S. Marcocci, M. Viel and F. Vissani, *Neutrinoless double beta decay: 2015 review*, *Adv. High Energy Phys.* **2016** (2016) 2162659 [[arXiv:1601.07512](#)] [[INSPIRE](#)].
- [60] S.T. Petcov, *Theory prospective on leptonic CP-violation*, *Nucl. Phys. B* **908** (2016) 279 [[INSPIRE](#)].
- [61] K. Eitel, *Direct neutrino mass experiments*, *Nucl. Phys. Proc. Suppl.* **143** (2005) 197 [[INSPIRE](#)].